COMPLEX NANOSCOPIC OBJECTS FROM WELL-DEFINED POLYMERS THAT CONTAIN FUNCTIONAL UNITS

A Dissertation

by

ANG LI

Submitted to the Office of Graduate Studies of
Texas A&M University
in partial fulfillment of the requirements for the degree of

DOCTOR OF PHILOSOPHY

Approved by:

Chair of Committee,	Karen L. Wooley
Committee Members,	David E. Bergbreiter
	Jiong Yang
	Elizabeth M. Cosgriff-Hernández
Head of Department,	David H. Russell

December 2012

Major Subject: Chemistry

ABSTRACT

The construction of nanoscale polymeric objects with complex, well-defined structures and regiochemical functionalities is of great importance, because it enables the fabrication of soft materials with tunable properties. Direct polymerization of macromonomers through covalent bond formation and self-assembly of block copolymers *via* non-covalent interactions are two typical strategies to afford nanoscopic structures. Molecular brush polymers are composed of densely-grafted side chains along a polymeric backbone. Due to the significant steric repulsion from the side chains, they tend to adopt bottle-brush like conformations, as opposed to linear polymers. "Grafting through" synthesis of molecular brush polymers can provide precise control over the dimensions and functionalities of brush polymers. Shell crosslinked knedel-like nanoparticles (SCKs) are constructed by assembling from amphiphilic block copolymers into micelles, followed by covalent shell crosslinking to further stabilize the nanoparticles and introduce additional functional moieties. SCKs are attractive nanocarriers because of their variable morphologies, compositions and functionalities, which allow for the development of platforms for therapeutic or diagnostic purposes.

By utilizing the orthogonal reactivity of the norbornene group and methacrylate group, two distinctly different reactive well-defined linear polymers, and a facile, one-pot synthesis of well-defined molecular brush polymers were studied by selective, orthogonal controlled radical polymerizations (CRPs) and ring-opening metathesis polymerization (ROMP). The living and high efficient characteristics of "grafting-

through" strategy were further investigated for the preparation of topology-controlled brush polymers with tunable dimensions of both backbone and side chain lengths. Apart from the fundamental investigation of molecular brush polymers, a series of poly(carboxybetaine) (PCB)- and poly(ethylene glycol) (PEG)-grafted degradable SCKs were developed to evaluate their *in vivo* pharmacokinetics and biodistributions, aiming to achieve novel therapeutic and diagnostic platforms that may surpass the performance of the conventional PEGylated analogs.

DEDICATION

To my parents and Liu

ACKNOWLEDGEMENTS

I would like to thank my advisor, Dr. Karen L. Wooley, for her great guidance, support and patient, during my graduate study at both Washington University in Saint Louis and Texas A&M University. What I have learnt from her are not only cutting-edge knowledge and techniques, but also the enthusiasm, curiosity and detail-oriented research attitude, which will be invaluable for my future career development. It is her faith and trust in me that enables me to complete this tough journey. Her concern of me and my career is forever remembered, and she will always be a great mentor and friend.

I also want to thank my committee members, Dr. David E. Bergbreiter, Dr. Jiong Yang and Dr. Elizabeth M. Cosgriff-Hernández, for providing helpful and critical suggestions, and advices for solidifying fundamental knowledge while conducting in-depth research in specific research areas.

Special recognition must also be given to Dr. Michael J. Welch, a prominent professor and research chemist in radiology at Washington University in Saint Louis, who passed away on May 6th, 2012. His insightful and constructive advices, as well as great personalities made our collaboration productive and enjoyable.

I would like to thank my collaborator, Dr. Yongjian Liu and Mrs. Hannah P. Luehmann, for their helpful discussion with the research plans and their efforts in *in vivo/in vitro* evaluation experiments. I also want to thank many other brilliant scientists, including Dr. Richard B. Dorshow, Mr. Amolkumar Karwa, Dr. James G. Kostelc, Dr. Gary E. Cantrell and Dr. Raghavan Rajagopalan from Covidien Pharmaceutics; Dr. Peter

Trefonas and Dr. James W. Thackeray from Dow Electronic Materials, for their unique perspectives and enlightening suggestions during the collaborative projects.

I would like to acknowledge many past and present Wooley group members, Dr. Jun Ma, Dr. Zhou Li, Dr. Guorong Sun, Dr. Nam Lee, Dr. Ke Zhang, Dr. Yali Li, Dr. Zicheng Li, Dr. Jeremy W. Bartels, Dr. Yun Lin, Dr. Philip M. Imbesi, Ms. Ritu Shrestha, Mr. Shiyi Zhang, Ms. Sandani Samarajeewa, Dr. Jiong Zou, Dr. Jeffery Raymond, Dr. Mahmoud Elsabahy, Mr. Fuwu Zhang, Mr. Sangho Cho, Ms. Danielle M. Policarpio, Ms. Corrie Clark, for their contributions to this work through either direct collaboration or helpful discussion. It's a privilege of mine to work with these excellent individuals and benefit from their expertise. I express my gratitude to all Wooley group members, who have created an enjoyable laboratory environment.

I would also like to thank the staff members who were very helpful and patient during my transfer process from the Washington University in Saint Louis to Texas A&M University. They are Mrs. Norma Taylor, Mrs. Phyllis Noelken, Dr. Ed Hiss, Mrs. Martha L. Turner from Washington University in Saint Louis; and Mrs. Sandy Manning, Mrs. Julie Zercher from Texas A&M University. Special thanks should also be given to Mrs. Judy Taylor for her excellent administrative assistance.

I would like to thank my mother and father for their encouragement and my girlfriend Liu Xiao for her patience and love.

Finally, I would like to thank the National Science Foundation, the Department of Energy, the Welch Foundation through the W. T. Doherty-Welch Chair in Chemistry,

and the National Institutes of Health as a Program of Excellence in Nanotechnology for their financial support for the research works in this dissertation.

NOMENCLATURE

ACEM	Active chain end mechanism
AFM	Atomic force microscopy
AIBN	*2,2'*-azobis(isobutyronitrile)
AMM	Activated monomer mechanism
ARGET	Activators regenerated by electron transfer
ATRA	Atom transfer radical addition
ATRP	Atom transfer radical polymerization
BSA	Bovine serum albumin
CMC	Critical micelle concentration
CTA	Chain transfer agent
CRP	Controlled radical polymerization
DBU	*1,8*-Diazabicyclo[5.4.0]-undec-7-ene
DCM	Dichloromethane
DLS	Dynamic light scattering
DMF	*N*,*N*-dimethylformamide
DMSO	Dimethyl sulfoxide
DNA	Deoxyribonucleic acid
DOTA	*1,4,7,10*-tetraazacyclododecane-1,4,7,10-tetraacetic acid
DP	Degree of polymerization
DSC	Differential scanning calorimetry

dSCK	Degradable shell crosslinked knedel-like nanoparticle
DT	Degenerative transfer
DTB	Dithiobenzoate
eATRP	Electrochemical atom transfer radical polymerization
EBiB	Ethyl 2-bromoisobutyrate
EDCI	1-[*3'*-(dimethylamino)propyl]-3-ethylcarbodiimide methiodide
EDDA	*2,2'*-(ethylenedioxy) bis(ethylamine)
EDTA	Ethylene diamine tetraacetic acid
EVE	Ethyl vinyl ether
FT-IR	Fourier transform infrared spectroscopy
GPC	Gel permeation chromatography
HMTETA	*1,1,4,7,10,10*-hexamethyltriethylenetetramine
HPLC	High performance liquid chromatography
ICAR	Initiators for continuous activator regeneration
LA	Lactide
MMA	Methyl methacrylate
M_n	Number-average molecular weight
MW	Molecular weight
MWCO	Molecular weight cut off
MWD	Molecular weight distribution
MPS	Mononuclear phagocyte system
NB	Norbornene

NMP	Nitroxide-mediated radical polymerization
NMR	Nuclear magnetic resonance
PAA	Poly(acrylic acid)
PCB	Poly(carboxybetaine)
PCEVE	Poly(chloroethyl vinyl ethyl)
PDI	Polydispersity index
PEG	Poly(ethylene glycol)
PET	Positron emission tomography
PLA	Poly(lactide)
PMANb	Methacrylate-functionalized poly(norbornene)
PMDETA	*N*,*N*,*N*',*N*'',*N*''-pentamethyldiethylenetriamine
PMMA	Poly(methyl methacrylate)
PNB	Poly(norbornene)
PNbMA	Norbornene-functionalized poly(methacrylate)
PnBA	Poly(n-butyl acrylate)
PS	Poly(styrene)
P*t*BA	Poly(*tert*-butyl acrylate)
RAFT	Reversible addition-fragmentation chain transfer
RB	Round bottom
REO	Robust, efficient and orthogonal
RI	Refractive index
ROMP	Ring-opening metathesis polymerization

ROP	Ring-opening polymerization
SEC	Size exclusion chromatography
SCK	Shell crosslinked knedel-like nanoparticles
TEM	Transmission electron microscopy
TFA	Trifluoroacetic acid
T_g	Glass transition temperature
TGA	Thermogravimetric analysis
THF	Tetrahydrofuran
TMEDA	*N*,*N*,*N*',*N*'-tetramethylethylenediamine
TU	Thiourea

TABLE OF CONTENTS

Page

LIST OF FIGURES

LIST OF TABLES

CHAPTER I

INTRODUCTION

1.1. Nanotechnology

Nanotechnology, the manipulation of matter on an atomic and molecular scale, has drawn great interest from various disciplines over the past decades, due to its potential capability to change the current technology with innovations that have never been considered.[1,2] The emergence of the nanotechnology concept in 1980s originated from both the inspirations from K. Eric Drexler and his book *Engines of Creation: The Coming Era of Nanotechnology*, and experimental progress, such as the discover of fullerenes[3] and the invention of scanning tunneling microscopy[4]. Nanometer ($^{-9}$ meter) scale is 1000 times smaller than microscale, which was traditionally associated with electronic industry. Given the fact that a typical red blood cell has 2000 nm in height, 7000 nm in width; common cold virus are about 25 nm; the width of a DNA molecule is *ca.* 2 nm and sp^3 carbon-carbon bond length is 0.154 nm, the nanoscopic material has the size and properties very close to macromolecules and basic biological structures. Thanks to rigorous scientific researches, there have been significant progresses of both fundamental studies and their applications that greatly impact our lives, such as high-performance nanoelectronics,[5-8] multifunctional nanoparticles for therapeutic or diagnostic purposes,[9-11] increasing the energy production efficiency and reducing energy consumption,[12-15] *etc.* It's estimated that, by 2015, 50% of new technology products and 15% of the global manufactured goods will incorporate nanotechnology.

The nanoscopic structures can be constructed by two ways: "top down" and "bottom up". "Top down" approach generates nanoscale objects from larger devices, such as the fabrication of microprocessors with sub-100 nm patterns,[16-18] while "bottom up" method involves the manipulation of individual molecules into more complex assemblies, including the formation of macromolecules by covalent bonds, or self-assembled structures through non-covalent interactions, such as van der Waals force, hydrogen bonding, electrostatic force *etc.*[19-24] Nature has provided examples of constructing complex structures from simple building blocks in a "bottom up" manner. For instance, proteins are assembled from polypeptides, polymers of amino acids connected by peptide bonds; deoxyribonucleic acids (DNA) are composed of two polymers of nucleotides; lipids, having a hydrophilic head and hydrophobic tail, form the cell bilayer membranes with embedded proteins. Inspired by the great complexity from nature, scientists have long sought to precisely control the macromolecular structure and function to mimic some biological processes or functions. Due to the remarkable advances in controlled/living polymerizations, well-defined block copolymers can be synthesized to afford complex nanoscopic structures through sophisticated assembly processes by non-covalent interactions.[25-31] Moreover, using modern synthetic polymer chemistry, well-controlled discrete objects with unique structures and properties can also be afforded from polymerization of monomeric units through the formation of covalent bonds.[32-36] The structures and properties of nanoscale objects from self-assembly in the bulk or solution can be tuned by control the block copolymer composition and the assembly process, while the discrete macromolecular

objects can be controlled by selecting monomers as well as polymerization techniques. Moreover, the objects can undergo further hierarchy supermolecular assembly.

1.2. Living/Controlled Polymerizations

Uncontrolled polymerizations give ill-defined polymers with significant chain terminations and chain transfer reactions, while living polymerization, a form of addition polymerization, enables more constant chain growth rate with greatly decreased chain termination, moreover, block copolymers can be achieved by switching the monomer while keeping the chain end active. Among all the living polymerization techniques, controlled radical polymerization (CRP), such as nitroxide-mediated radical polymerization (NMP),[37] atom transfer radical polymerization (ATRP)[38] and reversible addition-fragmentation chain transfer (RAFT),[39] have attracted tremendous attention over the past two decades, due to the exceptional functional group tolerance and good control over the polymer architectures. Distinguished from termination-free polymerizations, such as living anionic polymerization, CRP has reversible activation process, during which most of the dormant species (P-X) are in deactivated form and upon certain stimuli (thermal, photo, chemical), they are activated into radical form ($P^{\bullet}$) which undergo chain propagation, as shown in figure 1.1. An ideal CRP system usually has $[P\text{-}X]/[P^{\bullet}] \geq 10^5$.

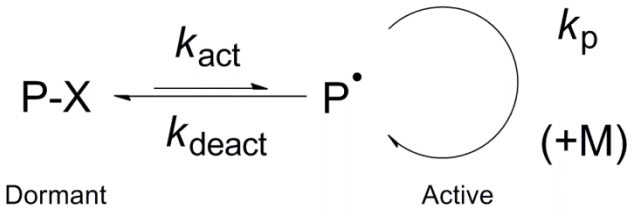

Figure 1.1. General scheme of the reversible activation process.

In NMP, alkoxyamines work as the initiating species with nitroxides being persistent radicals.[40] Bulky nitroxide is needed to reduce the bond dissociation energy of C-O bonds formed during propagation step, which enables the controlled polymerization of various monomers other than styrene. The repeated and reversible capping of nitroxide to the growing polymer chain ends prevents the coupling of two active radicals. ATRP (or transition-metal mediated radical polymerization),[41,42] mechanistically related to transition-metal mediated atom transfer radical addition (ATRA), was independently discovered by Sawamoto *et al.*[43] and Matyjaszewski *et al.*[44] In ATRP, the alkyl halogen bond from dormant species (P-X) undergo hemolytic cleavage, which generates an organic radical ($P^{\bullet}$) and a high oxidation state complex (Mt^{n+1}/L) by reacting with the transition metal complex (Mt^{n}/L), as shown in figure 1.2. Since the dormant polymer is vastly preferred in this equilibrium ($k_{deact} \geq k_{act}$), side reactions from radical species are largely avoided. Copper-based ATRP is mostly wide studied due to its easy experimental setup, inexpensive copper catalysts, and commercially-available ligands and initiators.[42] Later, more advanced techniques were developed with significantly reduced amount of copper catalyst, such as activators

regenerated by electron transfer (ARGET) ATRP,[45,46] initiators for continuous activator regeneration (ICAR) ATRP[47,48] and electrochemical ATRP (eATRP).[49,50]

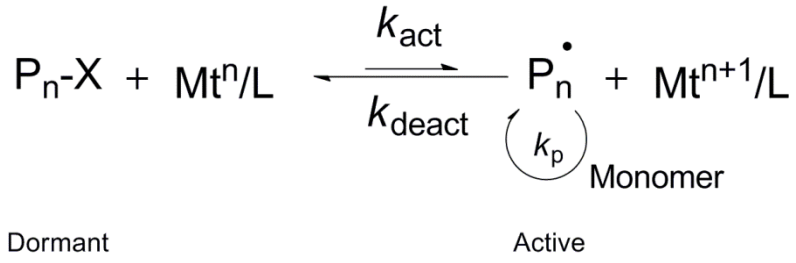

Figure 1.2. Representative scheme of the ATRP equilibrium.

Unlike the living chain end reversible capping/uncapping mechanism of NMP and ATRP, RAFT polymerization bases on degenerative transfer (DT) chain transfer to establish the equilibrium between dormant and active species. The controlled process is realized by the careful selection of RAFT chain transfer agent (CTA) (dithioesters, trithiocarbonates, xanthates, *etc*.), which reacts with propagating radicals to form radical adduct that can undergo either the formation back to reactant or release another macro(radical) with an optimum equilibrium between dormant and active species. The general mechanism of RAFT polymerization is shown in figure 1.3.[51,52]

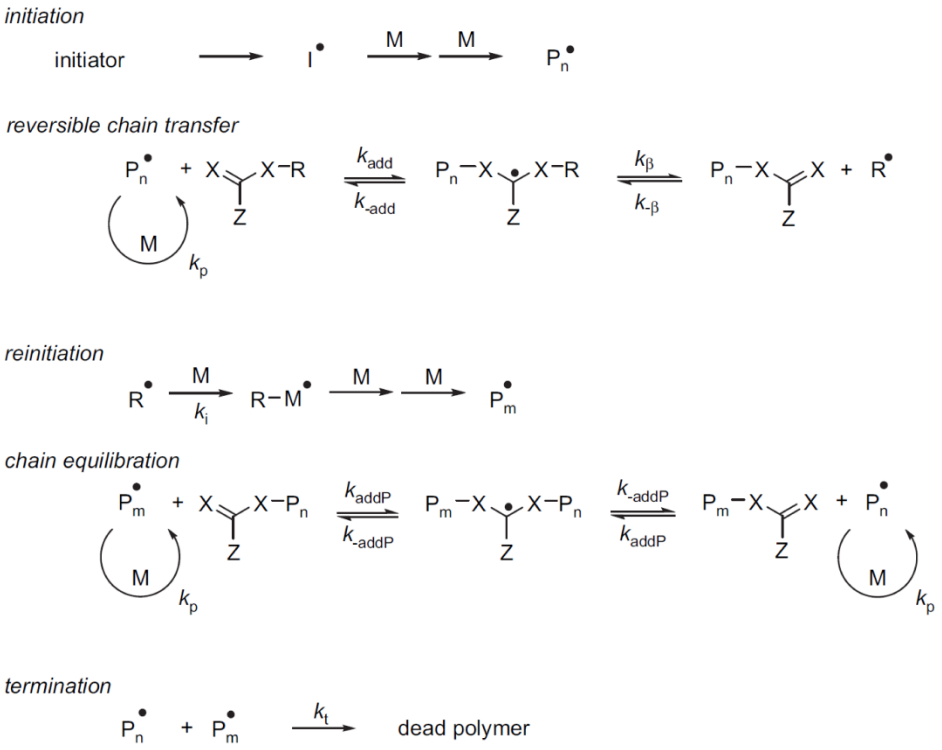

Figure 1.3. General mechanism of RAFT polymerization.[52]

Other than controlled radical polymerizations that afford vinyl polymers, living ring-opening polymerizations (ROP), driven by the release of the ring strains from the cyclic compounds (monomers), generate well-defined polymers bearing heteroatoms or carbon-carbon double bonds along the polymer backbone. The latter technique is specifically defined as ring-opening metathesis polymerization (ROMP), with ROP often stands for the polymerization of heterocyclic monomers. The general mechanism of ROMP is shown in figure 1.4. It's the pioneer work from Calderon,[53,54] who first realized both ROMP and acyclic metathesis of olefins by the same catalyst; Katz,[55,56] who first applied well-defined Fisher-type carbenes as initiator to achieve the

polymerization of cyclic olefins and Fred Tebbe,[57] who demonstrated that the metathesis exchange of terminal olefins with titanocene methylene complex, that lead the later development of tungsten, molybdenum and ruthenium catalysts. With the development of several generations of ruthenium-based Grubbs' catalyst, the fast-initiating modified 2nd generation Grubbs' catalyst $(H_2IMes)(pyr)_2(Cl)_2RuCHPh$ was utilized to prepare a wide variety of well-defined polymers.[58,59] Although the *meta*-bromopyridine analog has very rapid initiation rate, the slower initiating pyridine complex is preferred for ROMP due to the improved stability and comparable control over the polymerization.[60] Moreover, by "grafting through" strategy, the high efficiency of ROMP also allows for the preparation of molecular brush polymers by polymerizing macromonomers having polymerizable end groups, in most cases norbornenes (NB) groups, with high conversions of macromonomers and good control over the polymer structures (low polydispersity index (PDI)).[61,62]

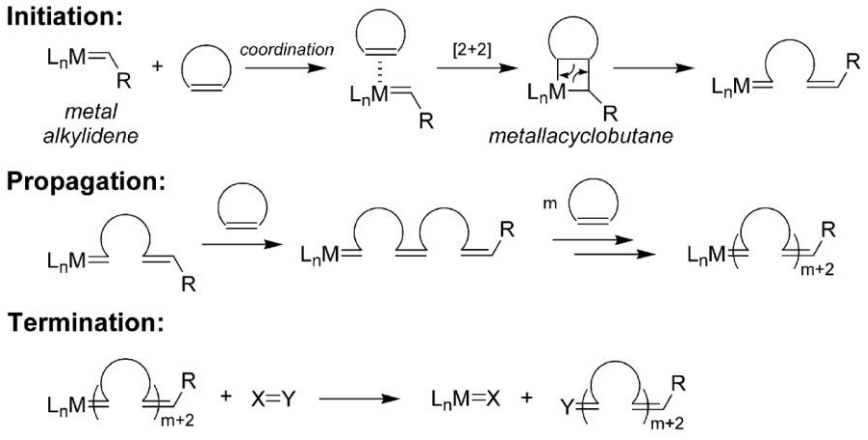

Figure 1.4. General mechanism of ROMP reaction.[58]

Living ROP of heterocyclic monomers can generate a variety of well-define polymers, such as polyesters, polycarbonates, poly(ethylene glycol)s, polypeptide, polyoxazolines, *etc*. In contrast to metal-based catalysis, which may cause environmental problem and hazards of polymers for biomedical, food packaging and microelectronic applications, organocatalyzed ROP has attracted great interest since the first reports in 2001 by Hedrick (IBM) and Waymouth (Stanford) using dialkylaminopyridines as catalysts.[63] A series of organocatalysts, such as 4-(dialkylamino)pyridines,[64-66] guanidines and amidines,[67-71] thiourea (TU)-amino derivatives,[67,72,73] phosphorus-based catalyst,[74] and *N*-heterocyclic carbenes,[69,75,76] have been developed to synthesize well-defined polymers from the living ROP of lactides, lactones, and cyclic carbonates. It's still unclear about the polymerization mechanism of organocatalyzed ROP, but in general the reaction proceed with either "activated monomer mechanism" (AMM) or "active chain end mechanism" (ACEM) or both mechanisms cooperatively.[77]

The great functional group tolerance of living/controlled polymerizations (ATRP, RAFT polymerization, ROMP, ROP) also allows for the preparation of well-defined reactive polymers by direct polymerizing bifunctional monomers with a polymerizable group and a functional group.[27,78-80] The introduction of multiple reactive groups onto the polymer backbone can tune the polymer physicochemical properties for various applications, such as drug delivery carriers, photoresists, sensors, adhesive, functional membranes *etc*. Compared to post-polymerization modification strategy, direct polymerization of functional polymers is preferred due to its high atom efficient nature

and the ability to incorporate high densities of reactive groups.[81] By taking advantage of orthogonal reactivities of different functional groups and polymerization groups, a variety of well-defined reactive (co)polymers having pendent reactive groups, such as activated ester,[82,83] isocyanate,[84,85] alkene,[86-88] alkyne,[89,90] azide,[91,92] epoxide,[93-95] ketone,[96] aldehyde,[97,98] have been achieved.

1.3. Molecular Brush Polymers

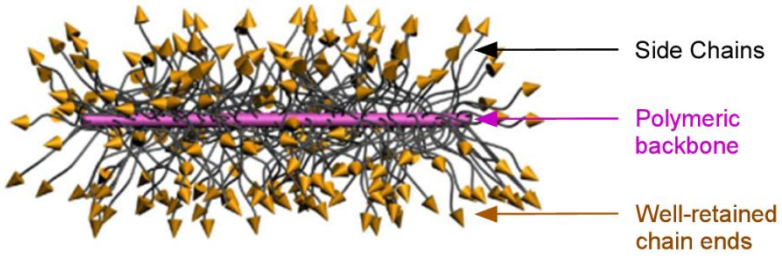

Figure 1.5. Illustration of a molecular brush polymer composed of densely-grafted side chains along a polymeric backbone. The reactive side chain ends can be applied for chain extensions or chain end modifications.

Inspired by the unique bottlebrush-like structure of aggrecan, which acts as a critical component for cartilage structure and the function of joints, scientists have great interest in developing synthetic methodologies and investigating properties of molecular brush polymers.[99,100] As shown in figure 1.5, due to the unique structure of molecular brush polymers, having densely-grafted side chains along a linear long polymer backbone, they tend to adopt characteristic cylindrical or worm-like conformation as a result of strong intramolecular repulsion from side chains.[101,102] Unlike cylindrical structures that originated from the self-assemble of block copolymers,[103-105] the side

chains are connected *via* covalent bond, thus robust and efficient chemistries are required to achieve the dimensionally gigantic structures. Modern imaging techniques, such as atomic force microscopy (AFM) or transmission electron microscopy (TEM) can be applied to visualize the polymers with size range from 10 nm to several hundreds of nm.[106,107] Due to the unique properties, synthetic challenges and potential applications as supersoft elastomer,[108-110] photonic materials,[111-115] template for inorganic nanowire,[116-119] nanocarrier for drug delivery,[120-125] three different synthetic strategies have been developed to construct molecular brush polymers: "grafting onto" (the attachment of pre-established side chains onto a polymer back bone), "grafting from" (the polymerization of monomers from a polyinitiator backbone) and "grafting through" (the end-group polymerization of macromonomers), as shown in figure 1.6.

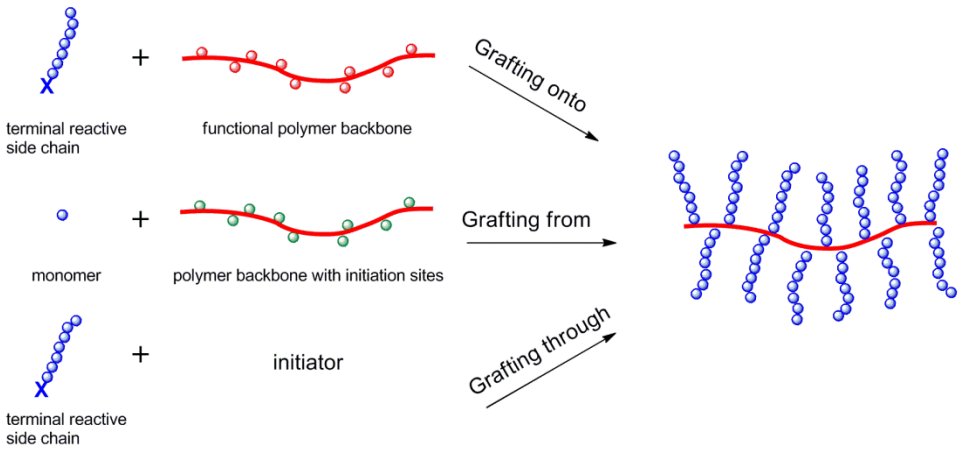

Figure 1.6. Three different strategies for the preparation of molecular brush polymers: "grafting onto", "grafting from" and "grafting through".

In the "grafting onto" strategy, both side chains and backbones are prepared independently, followed by the coupling reaction to form molecular brush polymers. The "grafting onto" method allows for the good control and characterization of both polymers before the brush synthesis step. However with the increase of side chain grafting density, the reaction will become both thermodynamically and kinetically unfavorable, due to the dramatic increase of the steric hindrance of the side chain reactive site. Thus highly efficiently coupling reaction and excess of side chain polymer are required to achieve high grafting densities. To date, both the nucleophilic substitution and "click" chemistry have yielded molecular brush polymers with relatively high density of side chains. For example, Gauthier and Möller, as well as Deffieux and Schaooacher have reported the successful synthesis of high grafting density brush polymers by the reaction between polystyryllithium as the side chain and poly(chloroethyl vinyl ethyl) (PCEVE) as the backbone;[126,127] Gao and Matyjaszewski applied copper(I)-catalyzed azide-alkyne coupling reaction between side chains with terminal azido group and backbone with alkynes along the backbone with highest efficiency close to 90%.[128] However, the purification of unreacted side chain polymers and the MW limitation of side chains should be considered.

In the "grafting from" strategy, the brush polymer side chains are synthesized by polymerizing monomers from a polyinitiator back bone, which resembles the process of forming brush polymers from initiator-modified surfaces or particles. Several polymerization techniques have been involved in the "grafting from" approach, and ATRP is currently the most widely used polymerization due to the excellent functional

group tolerance, good control over the polymerization process and the facile setup.[129-132] By designing the morphology and composition of polyinitiatior backbones, cylindrical, star-like[133] brush polymers with homo-, block type,[134] gradient type,[135] as well as alternating type[136,137] brush polymers have been prepared. However, initiation efficiency and the loss of living side chain end may cause low grafting density and the difficulty of efficient preparation side chain block copolymers. Moreover, backbone diblock or multiblock brush polymers are very challenging by "grafting from", since orthogonal polymerization methods or complicated protection/deprotection are required.[138]

"Grafting through" is the construction of end-polymerizable macromonomers and the later polymerization "through" the terminal functionalities. The most attractive feature of "grafting through" is the full grafting density of side chains, which provide excellent templates to understand their unique properties. Although several polymerization methods, such as free radical polymerization,[139-141] CRP,[142] have been employed to synthesize well-defined brush polymers, ROMP of macromonomers with norbornene chain end was proved to be the most effective method to synthesize brush polymer with high macromonomer conversion, low polydispersity (PDI), long polymer back bone and tunable side chain compositions.[61,62] The release of ring strain of norbornene functionality and the relative larger spacing between adjacent side chains to vinyl type polymer backbone (5 C-C bonds *vs.* 2 C-C bonds) make the ROMP "grafting through" strategy thermodynamically and kinetically favorable. Due to the different reactivity toward CRP, such as ATRP and RAFT, macromonomers with terminal norbornene groups can be synthesized directly by selective radical polymerization of

various monomers (acrylate, methacrylate, styrene), to afford macromonomers with well retained norbornene chain end,[143,144] moreover, polyester macromonomers can also be simple obtained by ROP from alcohol initiator with a norbornene group.[111,145] Other than direct polymerization from norbornene-containing bifunctional initiator or chain transfer agent (CTA), the NB group with alkyne functionality can also be installed onto the polymer chain end with an azido group, generated from substitution reaction of NaN_3 with a bromo chain end from ATRP, by "click" chemistry.[62,111,146] However, this strategy may be problematic with poly(methacrylate)s, whose chain end displacement efficient is not as high as those of poly(acrylate)s and poly(styrene)s.[147]

The living characteristic and high efficiency of ROMP allows for facile preparation of backbone block brush polymers by sequential addition of each macromonomer in a one-pot method. Moreover, the dimensions of the brush polymer can be precisely controlled by tuning the lengths of the side chains and backbones. Two backbone block-type polynorbornene (PNB) brush polymers with poly(*tert*-butyl acrylate) and poly(styrene) side chains, P(NB-*g*-P*t*BA)-*b*-P(NB-*g*-PS);[61] and PNB brush polymers with poly(lactide) and poly(n-butyl acrylate) side chains, P(NB-*g*-PLA)-*b*-P(NB-*g*-PnBA)[111], were synthesized by sequential polymerizations of two macromonomers in a one-pot way, and they displayed unique hierarchical nanoassembly behaviors in aqueous medium or in the bulk.

1.4. Nanomedicine

Biomedical application is one of the most important topics of nanotechnology.[148-152] In contrast to the nanoscopic objects, such as molecular brush polymers that were

obtained from covalent linkage between macromonomers, polymeric nanoparticles, assembled from amphiphilic block copolymers are most widely used as carriers in nanomedicine research.[11,26,148,153-157] The hydrophobic blocks form the core domain to minimize the exposure to aqueous medium, while the hydrophilic blocks form the shell to stabilize the core. The core-shell architecture enables the nanoparticles to incorporate hydrophobic guest molecules into the core domain, that provide increased solubility and stability for the hydrophobic guest molecules, while the shell domain can be functionalized with various moieties, such as targeting ligands, polymer grafts, imaging sites, *etc*., to control their pharmacokinetics as well as functions. However, due to highly dilution after *in vivo* administration of core-shell nanoparticles, they may lose the structural integrities when below the critical micelle concentration (CMC), which results in uncontrolled release of guest molecules and poor biodistributions. To overcome this potential issue, shell crosslinked knedel-like nanoparticles (SCK)s have been developed with stabilizing crosslinkers throughout the hydrophilic shell domain.[158-163] Moreover, by employing functional crosslinkers, extra properties could be introduced to increase the versatility of the SCKs.[164-167] Rapid clearance of nanoparticles from circulatory system by the mononuclear phagocyte system (MPS) is one of the major issues that prevent their clinical applications.[168-172] Tremendous efforts have been made to develop "stealth" nanoparticles with optimized pharmacokinetics and biodistributions, and till now poly(ethylene glycol) (PEG) is the most widely used material for modifying nanoparticles to reach long circulation time.[173-176] Despite the wide applications of PEG, its disadvantages, such as the lack of functionalizable groups, accelerated clearance after

second dose, the decrease of biological activity of PEG conjugated proteins,[177-181] direct scientists to develop novel nanocarrier platforms which may outperform the PEG-modified platforms.

1.5. Scope of the Thesis

This dissertation is focused on the fundamental studies on the development of complex nanoscopic objects from well-defined polymers that contain functional units, by combinations of living polymerization techniques, such as ATRP, RAFT polymerization, ROP, ROMP, as well as the assembly techniques.

Chapter II is focused on the preparation of two distinct, reactive linear (co)polymers that have pendent norbornene groups and methacrylate groups, from one bifunctional monomer by selective ATRP and ROMP. The orthogonal reactivities of methacrylate and norbornene groups toward CRP and ROMP were utilized to achieve selective polymerization to construct reactive polymers by direct polymerizing functional monomers. Block copolymers were also prepared to demonstrate the living characteristic. The functional groups embedded along the well-defined polymer backbone can be further employed as reactive sites for crosslinking, conjugation to achieve desired physicochemical properties.

In Chapter III, the orthogonal reactivities of methacrylate and norbornene groups were applied to develop an efficient one-pot, "grafting through" synthesis of molecular brush polymers with polynorbornene as the backbone and poly(methyl methacrylate) (PMMA) as the side chains. Due to the high reactivity and functional group tolerance of the modified 2nd Grubbs' catalyst, the well-defined brush polymers with tunable

dimensions, were afforded without intermediate steps of isolation or purification, which significantly simplified the process of preparation of well-defined brush polymers. AFM characterization was also applied to confirm the bottlebrush-like architectures, as well as the precisely controlled sizes.

In Chapter IV, we demonstrated the further application of ROMP, as a highly efficient polymerization technique, to create triblock brush polymers with controllable architectures and sizes. Dumbbell-shaped triblock brush polymers, which are difficult to be obtained by other living/controlled polymerizations, were synthesized by sequential addition of norbornene-terminated poly(lactide)s (NB-PLA) with different molecular weights. Confirmed by AFM, the sizes of the "bar" and "ball" of dumbbell-shaped triblock brush polymers can be tuned by controlling the lengths of PLA side chains and PNB backbones, which demonstrated the possibility of achieving more complicated morphologies by varying the side chain compositions, addition sequences and post-modifications.

Besides nanoscopic objects synthesized by covalently connecting monomeric units, aqueous self-assembly of amphiphilic block copolymers were also investigated. In Chapter V, to develop nanomedicine platforms that may surpass the performance of current PEGylated platforms, two sets of degradable PLA-core SCKs (dSCK) with PEG grafts and poly(carboxybetaine) (PCB) grafts, as well as sites (1,4,7,10-tetraazacyclododecane-1,4,7,10-tetraacetic acid (DOTA) and tyramine) for radiolabeling, were prepared by the "pre-grafting" strategy, to compare their *in vivo* pharmacokinetics and biodistributions. The dSCKs were synthesized by self-assembly

of polymer grafts in water, followed by shell crosslinking. The PCB polymer is chosen as an alternative material to PEG due to the recent studies that demonstrated its superior resistance to non-specific protein binding, and its capability to stabilize proteins while maintaining the protein bioactivity, making the PCB a promising material to create "stealth" nanoparticles with improved targeting efficiency than its PEG-functionalized analogs.

CHAPTER II

TWO DISTINCT, REACTIVE POLYMERS DERIVED FROM A SINGLE NORBORNENYL-METHACRYLOYL BIFUNCTIONAL MONOMER BY SELECTIVE ATRP OR ROMP*

2.1. Introduction

The synthesis of well-defined polymers bearing reactive functionalities has great importance because of their potential capabilities as building blocks for the construction of smart materials and advanced macromolecular architectures. Decoration of functionalities along a polymer backbone, which can be achieved by the direct polymerization of functional monomers, can incorporate high densities of groups for ultimate utility in modification of polymer compositions, structures and properties. Direct polymerization of functional monomers also provides for an atom efficient route toward complex materials, relative to post-polymerization modification reactions or protection-deprotection strategies. In this work, we were interested in the production of two distinctly different polymers, in terms of their backbone structures and side chain functionalities, by direct, selective, orthogonal polymerizations of a single bifunctional monomer.

---

*Part of this work is reprinted with permission from "Two distinct, reactive polymers derived from a single norbornenyl-methacryloyl bifunctional monomer by selective ATRP or ROMP" by Ang Li, Jun Ma and Karen L. Wooley, 2009. *Macromolecules*, 42, 5433-5436. Copyright [2009] by the American Chemical Society.

Recently, both controlled radical polymerization (CRP) and ring-opening (metathesis) polymerization (RO(M)P) have been shown to be effective methods to synthesize functional polymers bearing terminal alkenyl,[87,88,182,183] cycloalkenyl,[184,185] norbornenyl,[186,187] alkynyl,[161,188-190] and methacryloyl[191-195] pendant groups. Moreover, these two polymerization mechanisms can proceed orthogonally. Therefore, a bifunctional monomer of this study was designed as a single monomer bearing both a CRP-reactive and a ROMP-reactive unit, to allow for either CRP or ROMP to be performed. Specifically, conditions were optimized to achieve selective atom transfer radical polymerization (ATRP) and ROMP of 5-norbornene-2-methylene methacrylate (**1**), a bifunctional monomer having both a methacryloyl (MA) unit (ATRP reactive) and a norbornenyl (Nb) unit (ROMP reactive). In addition to interesting aspects of selective polymerizations of this monomer, the resulting polymers from one single monomer possess different types of backbone structures, functional side chain units and properties (figure 2.1). For instance, while this work was under review, Li and coworkers reported reversible addition-fragmentation chain transfer (RAFT) polymerization of this bifunctional monomer, aiming to obtain unique norbornenyl-functionalized hyperbranched structures;[196] in our study, however, we were interested in the preparation of well-defined functional linear polymers.

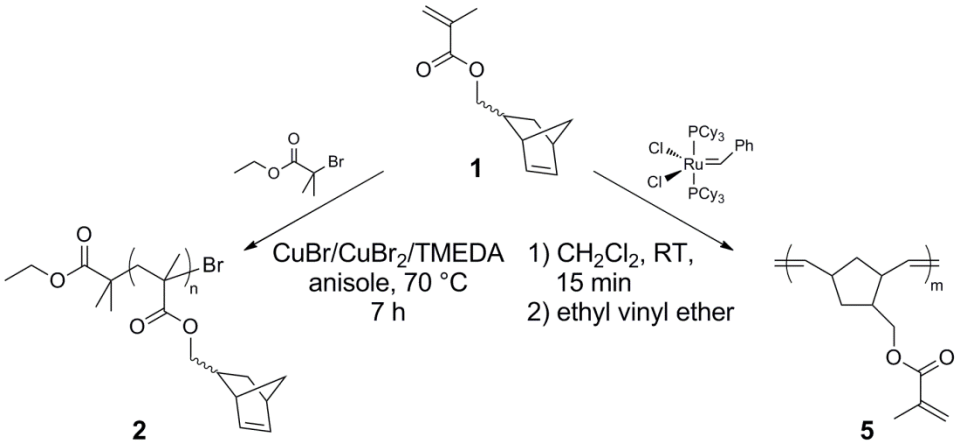

Figure 2.1. Selective polymerization of **1** by either ATRP or ROMP to afford two distinctly different reactive polymers.

The radical polymerization of the methacrylate head group, uniquely, in the presence of the norbornenyl group was investigated initially. Since the bifunctional monomer **1** has a MA group and a Nb functionality, radical polymerization of **1** could be considered as copolymerization of two types of unsaturations. Quantitative analysis using Alfrey-Price equations[197] and the *Q* and *e* values (MA $Q_1 = 0.78$, $e_1 = 0.45$; Nb $Q_2 = 0.02$, $e_2 = -1.00$) gave estimated reactivity ratios of $r_1 \approx 20$ and $r_2 \approx 0.006$. These values indicate that the MA groups have significantly higher reactivities than do the Nb groups and further suggest that the radical polymerization of **1** is essentially a homopolymerization of the substituted MA groups.

2.2. Results and Discussion

Selective atom transfer radical homopolymerization of **1** was investigated by using ethyl 2-bromoisobutyrate (EBiB) as initiator, CuBr/$CuBr_2$/*N*,*N*,*N*',*N*'',*N*''-pentamethyldiethylenetriamine (PMDETA) or *N*,*N*,*N*',*N*'-tetramethylethylenediamine

(TMEDA) as the catalyst, anisole (67 vol%) as the solvent at 65-80 ℃. ^{1}H NMR spectroscopy was used to determine the monomer conversions and number-averaged molecular weights (M_n). Gel permeation chromatography (GPC) was used to analyze the molecular weights and polydispersities (PDI). As shown in table 2.1, less control of polymerization with relatively high PDIs was observed for the ATRP of **1** without $CuBr_2$ as a deactivator (entry 1), with highly active PMDETA as the ligand (entries 1 and 2),[198] at high monomer conversions (> 45%, entries 2 and 3) or at high temperature (80 ℃, entry 4). Among all the entries, selective ATRP of **1** at 70 ℃ with a feed ratio of [**1**]:[EBiB]:[CuBr]:[$CuBr_2$]:[TMEDA] = 100:1:1:0.1:2 (entry 5), quenched at 7.0 h when conversion of **1** had reached 42%, resulted in Nb-functionalized poly(methacrylate), PNbMA, **2**, with a mono-modal molecular weight distribution and a PDI of 1.14.

Table 2.1. ATRP of 5-norbornene-2-methylene methacrylate, **1**.[a]

entry	L	[**1**]:[*I*]:[CuBr]:[$CuBr_2$]:[L]	*T* (℃)	*t* (h)	Conv. (%)	$M_n^{theo.}$ (Da)	M_n^{GPC} (Da)	PDI
1	P	100:1:1:0:2	70	0.5	60	12 840	13 000	1.36
2	P	100:1:1:0.1:2	65	1.2	60	12 840	22 000	1.26
3	T	44:1:1:0.1:2	70	7.4	55	5 250	7 900	1.24
4	T	100:1:1:0.1:2	80	4.8	46	9 880	8 880	1.61
5	T	100:1:1:0.1:2	70	7.0	42	9 110	8 270	1.14

[a] L = ligand; *I* = initiator (ethyl 2-bromoisobutyrate); P = PMDETA; T = TMEDA; *T* = temperature; *t* = time; Conv. = monomer conversion, measured by ^{1}H NMR spectroscopy; $M_n^{theo.}$ = calculated number-average molecular weight based on monomer conversions measured by ^{1}H NMR spectroscopy; M_n^{GPC} = number-average molecular weight measured by GPC, relative to polystyrene standards; PDI = polydispersity index measured by GPC.

The well-defined structure of **2** was also verified by both ^{1}H NMR spectroscopy and GPC. As shown in figure 2.2a, the ratio of the resonance intensities of the two norbornenyl protons *vs.* methylene protons (-OC$\boldsymbol{H}_2$-) in **2** was 1.99:2.00, indicating, essentially, an absence of side reactions on the pendant Nb groups. The molecular weight determined by GPC (M_n^{GPC}) was measured to be 8270 Da, in good agreement with the theoretical value ($M_n^{theo.}$ = 9110 Da), calculated from the monomer conversion as determined by ^{1}H NMR spectroscopy.

To further identify the controlled characteristics of the ATRP of **1**, the relationships of monomer conversions *vs.* M_n and PDI values of the resulting polymers, and the polymerization kinetics were also investigated. As shown in figure 2.3a, ATRP of **1** ([**1**]:[EBiB]:[CuBr]:[$CuBr_2$]:[PMDETA] = 100:1:1:0.2:2, 67 vol% anisole, at 65 ℃) followed linear first-order kinetics, showing a constant concentration of active species for up to 3.0 h. These conditions were applied in order to reach control over the polymerization process, employing increased levels of deactivator ($CuBr_2$) to reduce the polymerization rate[42], as compared with entry 2, table 2.1. Below 48% monomer conversion, excellent linear agreement between M_ns and monomer conversions were obtained, and the resulting polymers also maintained narrow molecular weight distributions (PDI = 1.12-1.18) (figure 2.3b). Such results verified the controlled characteristics of the selective ATRP of **1**. However, it was noticed that after the monomer conversion reached 50% at 3.5 h, a high MW shoulder on the GPC profile (figure 2.3c) was observed, suggesting a minor occurrence of reactions of the Nb,

presumably, due to the increased molar ratio of the Nb groups to the remaining MA vinyl groups.

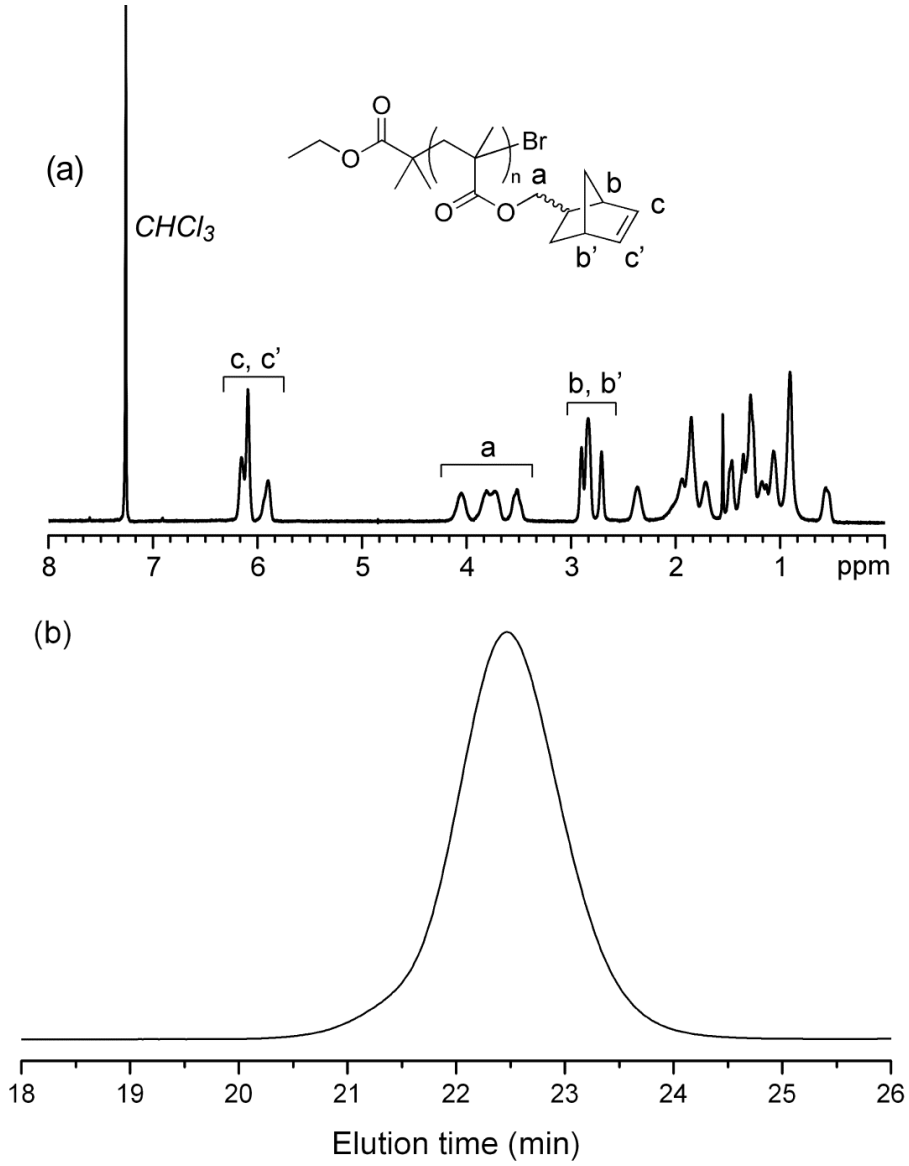

Figure 2.2. Atom transfer radical homopolymerization of 5-norbornene-2-methylene methacrylate, **1**: (a) ^{1}H NMR spectrum of **2** (300 MHz, $CDCl_3$; table 1, entry 5); (b) GPC profile of **2** (THF eluent; table 1, entry 5).

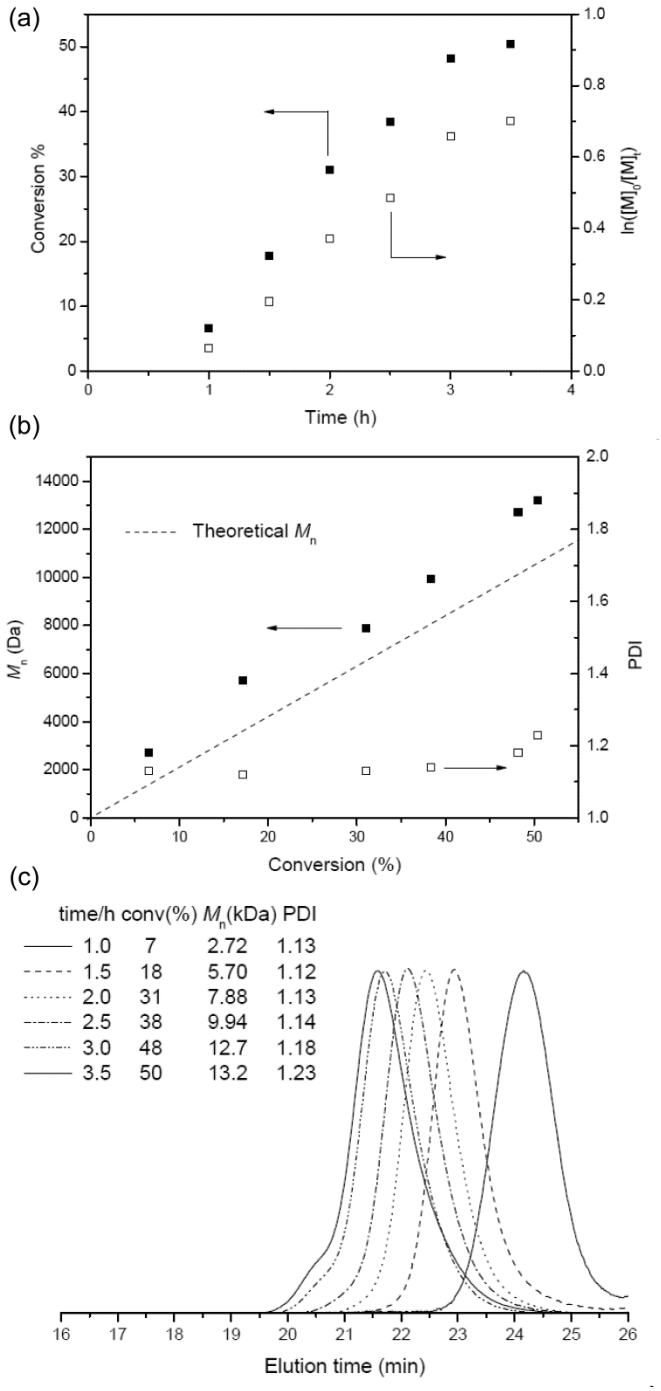

Figure 2.3. Kinetic plots for the ATRP of **1**: (a) time dependence of monomer conversions and $\ln([M]_0:[M]_t)$ (polymerization conditions: [**1**]:[EBiB]:[CuBr]:[$CuBr_2$]:[PMDETA] = 100:1:1:0.2:2, vol 67 % anisole, at 65 ℃); (b) dependence of M_n^{GPC} and PDI relative to monomer conversions; (c) evolution of GPC traces during ATRP of **1**.

The controlled characteristics of ATRP allow ready preparation of a broad range of block copolymers. Therefore, we investigated chain extension polymerizations of **1** from a poly(methyl methacrylate) (PMMA) macroinitiator and polymerizations of methyl methacrylate (MMA) from a Nb-functionalized macroinitiator **2** *via* ATRP, for the preparation of Nb-side chain functionalized diblock copolymers (figure 2.4). Using PMMA (M_n^{GPC} = 10100 Da, PDI = 1.06) as the macroinitiator, chain extension ATRP of **1** ([**1**]:[PMMA]:[CuBr]:[$CuBr_2$]:[PMDETA] = 189:1:3.0:0.1:6, at 70 ℃, in 86 vol% of anisole as the solvent) resulted in well-defined diblock polymer PMMA-*b*-PNbMA, **3**, after 7.0 h and a conversion of **1** of 11%. Chain extension of **2** (M_n^{GPC} = 8270 Da, PDI = 1.14) with MMA ([MMA]:[**2**]:[CuBr]:[$CuBr_2$]:[PMDETA] = 200:1:1.5:0.2:3, at 70 ℃, in 79 vol% of anisole as solvent) quenched at 7.0 h with 12% conversion of MMA afforded diblock copolymer PNbMA-*b*-PMMA, **4**. As shown in figure 2.5, the formation of diblock copolymers **3** (M_n^{GPC} = 12800 kDa, $M_n^{theo.}$ = 14300 kDa, PDI = 1.16) and **4** (M_n^{GPC} = 11300 kDa, $M_n^{theo.}$ = 10800 kDa, PDI = 1.11) were verified by the shifts of the GPC profiles of the resulting diblock structures to shorter retention times compared with those of their macroinitiator precursors. Moreover, the good agreement between the experimental and theoretical molecular weights and the mono-modal molecular weight distributions of both diblock copolymers illustrated the quantitative initiation efficiency and tunability of the length of Nb-functionalized blocks.

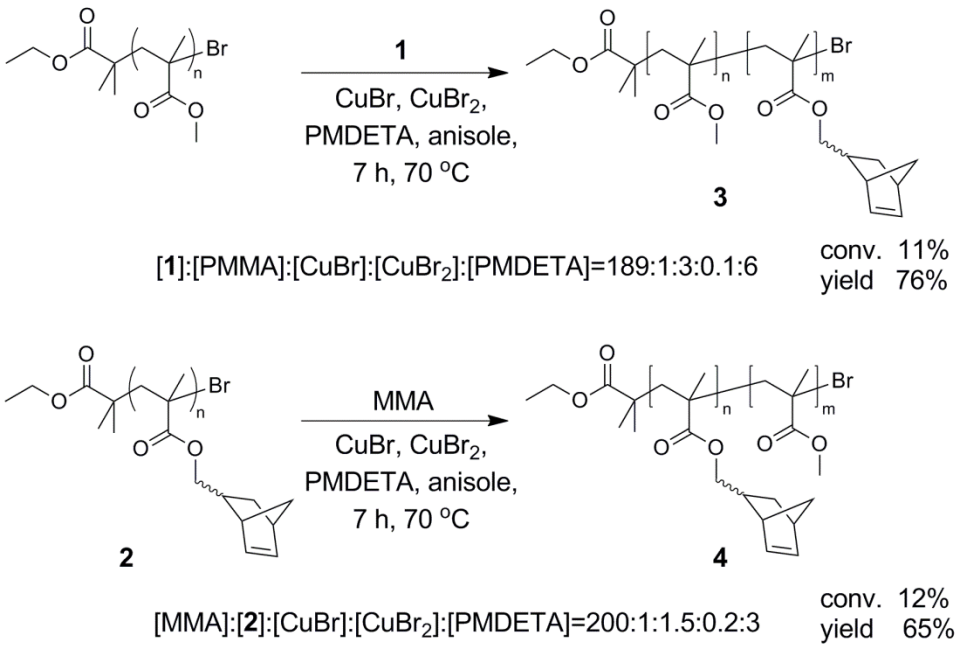

Figure 2.4. Regio-functionalized diblock copolymers **3** and **4** prepared by atom transfer radical block copolymerizations of **1** from PMMA macroinitiator or ATRP of MMA from macroinitiator **2**.

Because the MA group and Nb group in monomer **1** also have different reactivities toward alkene metathesis reaction, selective ROMP homopolymerization of **1** was studied by using Grubbs' catalyst (1st generation) $RuCl_2(CHC_6H_5)[P(C_6H_{11})_3]_2$ under diluted condition using CH_2Cl_2 as solvent ([**1**]:[Ru] = 100:1, concentration of **1** = 0.025 g/mL, in CH_2Cl_2). As measured by ^{1}H NMR spectroscopy, nearly complete conversion of **1** was observed after 15 min at room temperature, by the disappearance of ^{1}H NMR resonances of Nb alkenyl protons (5.8-6.2 ppm). After termination with ethyl vinyl ether followed by purification, the resulting methacrylate-functionalized polynorbornene (PMANb, **5**) was found to have a M_n^{GPC} of 34600 Da and mono-modal MW distribution with a PDI of 1.18 (figure 2.6b). The successful incorporation of

pendant MA units on the side chain was supported by ^{1}H NMR spectroscopy (figure 2.6a), with the appearance of the MA vinyl protons and methylene protons, having an integration area ratio of 1.97:2.00, which further confirmed the good selectivity of ROMP for the norbornenyl unit with little to no cross metathesis of the methacryloyl units.

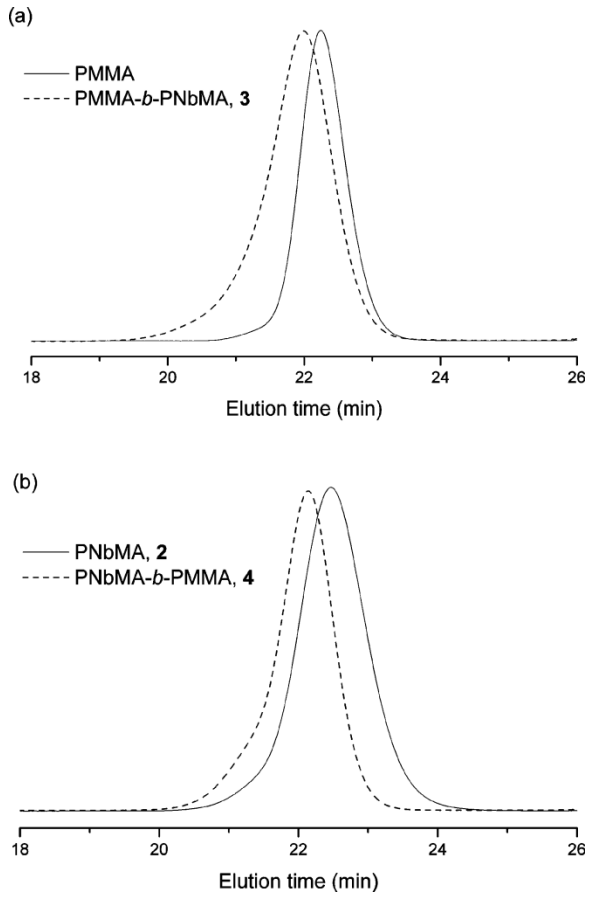

Figure 2.5. Overlaid GPC profiles of (a) PMMA and PMMA-*b*-PNbMA, **3** and (b) PNbMA, **2** and PNbMA-*b*-PMMA, **4**.

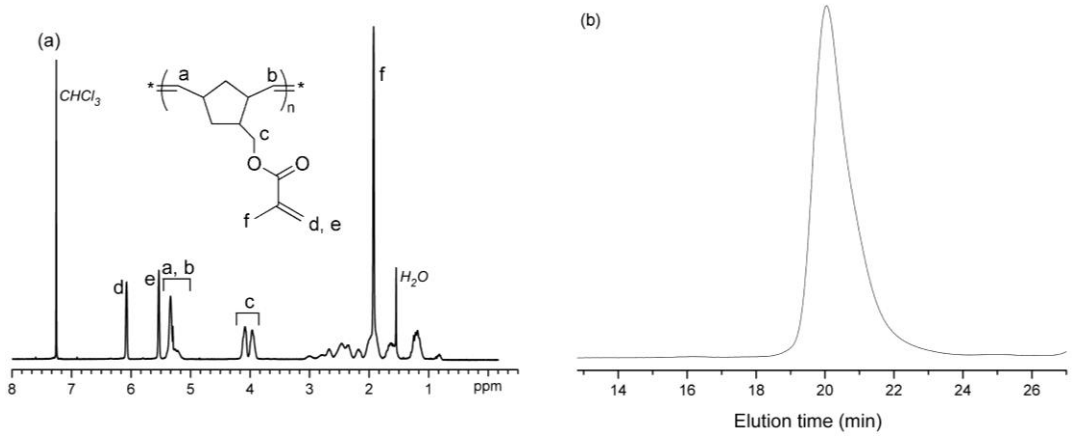

Figure 2.6. (a) ^{1}H NMR spectrum of **5** (300 MHz, $CDCl_3$). (b) GPC (THF eluent) profile of **5**.

2.3. Experimental Section

2.3.1. Materials

All Chemicals and reagents were purchased from Aldrich Chemical Co. and used as received, unless otherwise noted. Methyl methacrylate was passed through a neutral alumina column to remove the inhibitor before use. Dichloromethane (CH_2Cl_2) was distilled over CaH_2 and stored under N_2 before use. The bifunctional monomer 5-norbornene-2-methylene methacrylate **1** was synthesized according to the literature[191] and stored at 0 ℃.

2.3.2. Characterization methods

IR spectra were recorded on a Perkin-Elmer Spectrum BX FT-IR system as thin films on NaCl disks and were analyzed using FT-IR Spectrum v2.00 software (Perkin-Elmer Corp., Beaconsfield, Bucks, England). ^{1}H NMR spectra were recorded at 300

MHz on solutions in $CDCl_3$ on a Varian Mercury 300 spectrometer, with the solvent proton signal as standard. ^{13}C NMR spectra were recorded at 75 MHz on at Varian Mercury 300 spectrometer with the solvent carbon signal as standard. Gel permeation chromatography (GPC) was conducted on a Waters 1515 HPLC (Waters Chromatography, Inc.), equipped with a Waters 2414 differential refractometer and a three-column series PL gel 5 μm Mixed C, 500 Å, and 10^4 Å, 300×7.5 mm columns (Polymer Laboratories, Inc.). The system was equilibrated at 35 ℃ in THF, which served as the polymer solvent and eluent with a flow rate of 1.0 mL/min. Polymer solutions were prepared at a known concentration (*ca*. 3 mg/mL), and an injection volume of 200 μL was used. Data collection and analysis were performed, respectively, with Precision Acquire software and Discovery 32 software (Precision Detectors, Inc.). Molecular weight and molecular weight distributions were determined, based on calibration of the GPC system with polystyrene standards. Thermogravimetric analysis (TGA) was performed on a TGA/SDTA851e instrument (Mettler-Toledo, Inc.) measuring the total mass loss on approximately 6 mg samples from 25 to 550 ℃ at a heating rate of 10 ℃/min in a nitrogen flow of 50 mL/min. Glass transition temperature (T_g) determinations were measured by differential scanning calorimetry (DSC) on a DSC822^e instrument (Mettler-Toledo, Inc.) in a temperature range of -50 to 200 ℃ with a heating rate of 10 ℃/min under nitrogen. For both TGA and DSC, data were acquired and analyzed with STAR^e software (Mettler-Toledo, Inc.). The T_g values were taken at the midpoint of the inflection tangent upon the third heating scans.

2.3.3. General procedure for the ATRP

To a 10 mL Schlenk flask equipped with a magnetic stir bar was added sequentially the monomer, ethyl 2-bromoisobutyrate as the initiator, CuBr as the catalyst, $CuBr_2$ as the deactivator, PMDETA or TMEDA as the ligand, and anisole as the solvent. The reaction flask was sealed, degassed by three cycles of freeze-pump-thaw, backfilled with Ar, and then placed in an oil bath at 65-80 ℃. The polymerization was quenched by immersing the reaction flask into liquid N_2 and opening the flask to the air. The polymer solution was further diluted by CH_2Cl_2, passed through a short column packed with neutral alumina to remove the metal catalyst, and then precipitated into a large amount of pentane.

2.3.4. Procedure for the kinetic study on the selective ATRP of 1

To a 10 mL Schlenk flask equipped with a magnetic stir bar was added sequentially **1** (0.410 g, 1.90 mmol), ethyl 2-bromoisobutyrate (3.7 mg, 0.019 mmol), CuBr (2.7 mg, 0.019 mmol), $CuBr_2$ (0.4 mg, 0.002 mmol), PMDETA (0.010 mL, 0.048 mmol), and anisole (0.80 mL). The reaction flask was sealed, degassed by three cycles of freeze-pump-thaw, backfilled with Ar, and then was placed in an oil bath at 65 ℃. During polymerization, small aliquots (~0.1 mL) of polymerization solution were withdrawn with syringe and were analyzed by ^1H NMR spectroscopy and GPC for determinations of conversions of **1** and molecular weights of the polymers formed. The polymerization was quenched after 3.5 h when conversion of **1** reached 50%. The polymer solution was further diluted by CH_2Cl_2 (3.0 mL), passed through a small column packed with neutral alumina to remove the metal catalyst, and then precipitated

into pentane twice (20 mL × 2). The precipitants were collected, and dried under vacuum to afford the **2** (85.4 mg, 43%) as white powder. $M_n^{theo.}$ = 10.6 kDa, M_n^{GPC} = 13.2 kDa, M_w/M_n = 1.23. IR (NaCl, cm^{-1}): 3060-2850, 2255, 1728, 1639, 1570, 1483, 1447, 1389, 1336, 1324, 1268, 1240, 1176, 990, 905, 913, 828, 731, 648. ^{1}H NMR (300 MHz, $CDCl_3$, ppm) δ 0.65-1.48 (br, -C***H***$_3$ of polymer backbone, -C***H***$_2$CHCH$_2$O- of Nb group, and -OCH$_2$C***H***$_3$ of the initiator), 1.60-2.42 (br, -C***H***$_2$ of polymer backbone, >CHC***H***$_2$CH< and >C***H***CH$_2$O- of Nb group, and -C***H***$_3$ of the initiator), 2.85-2.98 (m, -C***H***CH=CHC***H***-), 3.42-4.05 (m, -C***H***$_2$O-), 6.85-6.11 (m, -C***H***=C***H***-). ^{13}C NMR (75 MHz, $CDCl_3$, ppm) δ 16.4, 18.3, 29.2, 30.0, 37.6, 41.8, 42.4, 44.2, 45.1, 49.7, 68.5, 69.4, 136.4, 137.1, 138.0, 180.2.

2.3.5. Synthesis of 2

PNbMA, **2**, was prepared from the mixture of **1** (1.20 g, 5.69 mmol), ethyl 2-bromoisobutyrate (11.1 mg, 0.0569 mmol), CuBr (8.3 mg, 0.058 mmol), $CuBr_2$ (1.3 mg, 0.0058 mmol), TMEDA (0.018 mL, 0.15 mmol), and anisole (2.40 mL) at 70 ℃. The polymerization was quenched after 7.0 h when the conversion of **1** reached 42%. The isolated yield of **2** was 300 mg (58%, based on the 42% conversion of **1**). $M_n^{theo.}$ = 9.10 kDa, M_n^{GPC} = 8.27 kDa, M_w/M_n = 1.14. T_g = 102 ℃. TGA in N_2: 245-335 ℃, 76% mass loss; 335-450 ℃, 24% mass loss.

2.3.6. Synthesis of PMMA macroinitiator

PMMA was prepared from the polymerization mixture of methyl methacrylate (MMA, 5.05 g, 50.5 mmol), ethyl 2-bromoisobutyrate (97.5 mg, 0.500 mmol), CuBr (71.5 mg, 0.500mmol), $CuBr_2$ (11.0 mg, 0.0500 mmol), TMEDA (0.210 mL, 100

mmol), and anisole (10.0 mL) at 70 ℃. The polymerization was quenched after 5.0 h when conversion of MMA reached 82%. The isolated yield of PMMA was 3.50 g (83%, based on the conversion of MMA). $M_n^{theo.}$ = 8.40 kDa, M_n^{GPC} = 10.1 kDa M_w/M_n = 1.06. ^{1}H NMR (300 MHz, $CDCl_3$, ppm) δ 0.80-1.10 (br, -C***H***$_3$ of polymer backbone), 1.20-1.30 (br, -C***H***$_2$- of polymer backbone, -C***H***$_3$ of the initiator), 3.50-3.68 (br, C***H***$_3$O-, -CH_3C***H***$_2$- of the initiator). ^{13}C NMR (75 MHz, $CDCl_3$, ppm) δ 16.7, 18.9, 44.8, 45.1, 52.5, 54.4, 54.7, 117.2 178.0, 178.3. T_g = 109 ℃. TGA in N_2: 270-310 ℃, 11% mass loss; 310-420 ℃, 89% mass loss.

2.3.7. Synthesis of 3

PMMA-*b*-PNbMA, **3**, was prepared from the mixture of **1** (0.403 g, 0.191 mmol), PMMA macroinitiator (0.100 g, 0.00100 mmol), CuBr (4.3 mg, 0.030 mmol), $CuBr_2$ (0.3 mg, 0.001 mmol), PMDETA (0.013 mL, 0.062 mmol), and anisole (1.50 mL) at 70 ℃. The polymerization was quenched after 7.0 h when conversion of **1** reached 11%. The isolated yield of **3** was 0.144 g (75%, based on the 11% conversion of **1**). $M_n^{theo.}$ = 14.3 kDa, M_n^{GPC} = 12.8 kDa, M_w/M_n = 1.16. IR (NaCl, cm^{-1}): 3100-2860, 1883, 1715, 1637, 1453, 1403, 1376, 1339, 1318, 1295, 1165, 1012, 971, 939, 814, 699, 658, 649, 595. ^{1}H NMR (300 MHz, $CDCl_3$, ppm) δ 0.65-1.48 (br, -C***H***$_3$ of polymer backbone, -C***H***$_2$CHCH_2O, -OCH_2C***H***$_3$), 1.60-2.42 (br, -C***H***$_2$- of polymer backbone, -C***H***$_2$CHCH=CH- of Nb group, >CHC***H***$_2$CH< and >C***H***CH_2O- of Nb group, -C***H***$_3$ of the initiator), 2.85-2.98 (m, >C***H***CH=CHC***H***<), 3.42-4.05 (br, C***H***$_3$O-, CH_3C***H***$_2$- of the initiator), 6.85-6.11 (m, -C***H***=C***H***-). ^{13}C NMR (75 MHz, $CDCl_3$, ppm) δ 16.7, 18.9, 29.3, 36.9, 37.7, 41.8, 42.4, 44.8, 45.1, 49.7, 52.0, 54.6, 53.1, 137.0, 177.1, 178.0, 178.3.

$(T_g)_1$ = 98 ℃, $(T_g)_2$ = 118 ℃. TGA in N_2: 235-345 ℃, 73% mass loss; 345-430 ℃, 27% mass loss.

2.3.8. Synthesis of 4

PNbMA-*b*-PMMA, **4**, was prepared from the polymerization the mixture of MMA (0.121 g, 1.21 mmol), PNbMA macroinitiator **2** (50.4 mg, 0.00610 mmol), CuBr (1.3 mg, 0.0091 mmol), $CuBr_2$ (0.3 mg, 0.001 mmol), PMDETA (0.004 mL, 0.02 mmol), and anisole (1.50 mL) at 70 ℃. The polymerization was quenched after 7.0 h when conversion of MMA reached 12% and the isolated yield of **4** was 42.0 mg (65%, based on the 12% conversion of MMA). $M_n^{theo.}$ = 10.8 kDa, M_n^{GPC} = 11.3 kDa, M_w/M_n = 1.11. T_g = 113 ℃. TGA in N_2: 260-340 ℃, 74% mass loss; 340-450 ℃, 26% mass loss.

2.3.9. Synthesis of 5

To a 10 mL Schlenk flask was placed in 5-norbornene-2-methylene methacrylate **1** (0.125 g, 0.590 mmol) and CH_2Cl_2 (5.0 mL). This monomer solution was allowed to stir for 10 min, degassed by three cycles of freeze-pump-thaw, and backfilled with Ar. To another 10 mL Schlenk flask equipped with a magnetic stir bar was added Grubbs' catalyst (1^{st} generation, 3.9 mg, 0.0047 mmol) and CH_2Cl_2 (3.00 mL). This catalyst solution was stirred for 10 min, degassed by three cycles of freeze-pump-thaw, and backfilled with Ar. A portion of the monomer solution (4.00 mL, containing 0.472 mmol of **1**) was transferred into the catalyst solution by a degassed syringe. The ROMP was allowed to proceed under Ar at room temperature for 15 min and then terminated by addition of ethyl vinyl ether (~100 μL). The polymer solution was concentrated and

precipitated into a large amount of methanol to yield **5** (78.8 mg, 79%, based on the 100% conversion of monomer **1**). $M_n^{theo.}$ = 21.1 kDa, M_n^{GPC} = 34.7 kDa, M_w/M_n = 1.18. IR (NaCl, cm^{-1}): 3100-2800, 1884, 1715, 1636, 1452, 1380, 1318, 1296, 1164, 1012, 971, 940, 814, 736, 653, 595. ^{1}H NMR (300 MHz, $CDCl_3$, ppm) δ 1.10-1.65 (br, -C***H***$_2$- of polymer backbone), 1.80-2.22 (s, -C***H***$_3$), 2.10-3.10 (br, >C***H***CH_2O- and >C***H***CH=CHC***H***< of polymer backbone), 3.90-4.20 (br, -C***H***$_2$O-), 5.10-5.40 (br, -C***H***=C***H***- of polymer backbone), 5.48 (s, CH***H***=CCH_3), 6.10 (s, C***H***H=CCH_3). ^{13}C NMR (75 MHz, $CDCl_3$, ppm) δ 18.5, 36.0, 36.8, 41.6, 42.5, 43.9, 66.5, 67.5, 125.4, 125.5, 136.6, 136.7, 167.8. T_g = 83 ℃. TGA in N_2: 280-450 ℃, 65% mass loss; 450-550 ℃, 10% mass loss.

2.4. Conclusions

In summary, by taking advantage of the difference of reactivities of two unsaturated groups in bifunctional monomer 5-norbornene-2-methylene methacrylate (**1**), both selective ATRP and selective ROMP of **1** were successfully achieved to prepare two types of well-defined polymers with nearly quantitative installation of Nb groups pendant on polymethacrylate backbones or side chain MA groups pendant on polynorbornene backbones. Although ROMP could proceed to quantitative conversion without adverse effects, ATRP was limited to less than *ca*. 50% conversion of the MA units to avoid significant side reactions of the Nb units and obtain a linear polymer of uniform structure and narrow molecular weight distribution. Well-defined regio-functionalized diblock copolymers containing a PMMA segment and a PNbMA segment have also been synthesized by chain extension ATRP from both PMMA and PNbMA

macroinitiators. We believe that this direct route to versatile alkene-functionalized homopolymers and block copolymers is highly attractive, and further, that these functional materials can be used as building blocks for the construction of advanced macromolecular architectures. Moreover, the imbedded functional groups can also serve as reactive sites for further conjugation, modification or cross-linking by using robust, efficient and orthogonal (REO)[88,161,199] chemical reactions.

CHAPTER III

ONE-POT, FACILE SYNTHESIS OF WELL-DEFINED MOLECULAR BRUSH COPOLYMERS BY A TANDEM RAFT AND ROMP, "GRAFTING-THROUGH" STRATEGY*

3.1. Introduction

Over the past decade, molecular brush copolymers, as an important type of nanoscopic single macromolecule, have attracted significant interest because of their synthetic challenges,[32,35,41,101,102] unique properties,[200-202] and potential applications as organic-inorganic hybrid nanomaterials,[107,116,203] photonic materials,[111,112,114] and carriers for nanomedicine.[121-123,204-206] Composed of densely-grafted side chains along a polymeric backbone, brush copolymers can adopt spherical, cylindrical or worm-like structures by varying the composition and chain length of either backbone or side chains. "Grafting-from"[131,207-209] (polymerization of monomers from pre-synthesized backbones with multi-initiating sites), "grafting-onto"[41,126,128,210,211] (construction of functionalized backbone and side chains separately followed by coupling reactions), and "grafting-through"[61,62,142,212-214] (end-group polymerization of macromonomers) are three major synthetic methods for the preparation of molecular brush copolymers. Being the most

*Part of this work is reprinted with permission from "One-pot, facile synthesis of well-defined molecular brush copolymers by a tandem RAFT and ROMP, "grafting-through" strategy" by Ang Li, Jun Ma, Guorong Sun, Zhou Li, Sangho Cho, Corrie Clark and Karen L. Wooley, 2012. *J. Polym. Sci., Part A: Polym. Chem.*, 50, 1681-1688. Copyright [2012] by Wiley Periodicals, Inc., A Wiley Company.

explored method, the "grafting-from" has been employed to prepare a variety of well-defined brush copolymers with different backbone and side chain compositions, however, the initiation efficiency of the macroinitiator may be limited with the increased steric hindrance during side chain growth.[215,216] The "grafting-onto" method allows the fine tuning of the lengths and compositions of both backbone and side chain, although steric challenges limit sufficient incorporation of side chains and the removal of uncoupled side chains can cause complications. After the first report of ROMP of norbornenes by modified 2nd generation Grubbs' catalyst,[217] "grafting-through" by ring-opening metathesis polymerization (ROMP) of macromonomers bearing terminal norbornene groups (NB macromonomers) has been proven to be an efficient method to control both the backbone and side chains of brush copolymers. By the "grafting-through" method, well-defined homo-grafted,[61,62] hetero-grafted[111,218,219] as well as cyclic molecular brush polymers[146,220] were achieved with narrow molecular weight distributions (MWD), high molecular weights (MW) and high conversions of macromonomers. In addition, the reactivity and versatility of Grubbs' catalysts have been utilized in an interesting example of Ru-catalyzed metathesis cyclopolymerization of dendronized macromonomers to afford dendronized molecular brush polymers containing a semiconducting backbone and dendritic side chains as insulated molecular wires.[221]

Despite the efficacy of all three methods to prepare molecular brush copolymers, overcoming synthetic challenges remains as an important issue, since complicated and tedious procedures are required to synthesize and purify the intermediates for brush

copolymer synthesis. One of our interests is to develop facile synthetic routes to well-defined molecular brush copolymers with good control over both the backbones and the side chains, independently. One-pot synthesis of well-defined brush copolymers from small molecule reactants is attractive and challenging because it requires two tandem living polymerizations with orthogonality over the backbone and side chain formation steps without purification of intermediate products. To our knowledge, only few examples of "grafting-from" synthesis of brush copolymers were reported in a one-pot manner. Our group has demonstrated examples of one-pot "grafting-from" synthesis of homo-grafted brush copolymers having a polynorbornene backbone and poly(methyl methacrylate) side chains (PNB-*g*-PMMA)[222] and core-shell brush copolymers having a polynorbornene backbone grafted with block copolymer side chains of styrene-maleic anhydride alternating copolymer and styrene (PNB-*g*-poly(St-*stat*-MAn)-*b*-poly(St))[216] by tandem ROMP/ATRP (atom transfer radical polymerization) or ROMP/RAFT (reversible addition-fragmentation chain transfer), respectively. Cheng and coworkers reported a one-pot "grafting-from" synthesis of brush copolymers by combining ROMP and polymerization of amino acid *N*-carboxyanhydrides, however, when a "grafting-through" method was attempted, the polymerizations were uncontrolled and led to broad molecular weight distributions.[223] Inspired by recent studies of the direct synthesis of NB macromonomer by selective controlled radical polymerizations (RAFT and ATRP)[143,144,213,224,225] and the high efficacy of ROMP of NB-functionalized (macro)monomers by Grubbs' catalysts in the presence of methacrylate functional groups,[226,227] herein this Communication, we report advancement of synthetic

methodologies to accomplish the facile, one-pot tandem RAFT and ROMP, "grafting-through" preparation of well-defined brush copolymers with controllable dimensions.

3.2. Results and Discussion

The tandem RAFT and ROMP, "grafting-through" approach for the preparation of well-defined brush copolymers involved four sequential steps of RAFT polymerization, quenching, ROMP, and quenching, each performed in one pot without intermediate steps of isolation or purification. As shown in figure 3.1, by this method, the side chains of brush copolymers were constructed by selective RAFT polymerization of methacrylate monomers from the norbornenyl-functionalized dithiobenzoate chain transfer agent (NB-DTB, **1**), without the participation of norbornenyl groups, which are required for the second ROMP process. After cooling the reaction mixture to quench the RAFT polymerization, a predetermined amount of modified 2nd generation Grubbs' catalyst ($(H_2IMes)(pyr)_2(Cl)_2RuCHPh$) was directly added to initiate the ROMP to afford the backbone of the brush copolymer, without interference of the remaining methacrylate monomers. In this one-pot brush copolymer synthesis, the lengths of side chain and backbone could be effectively controlled by tuning the monomer conversion and the amount of Grubbs' catalyst added, respectively. Moreover, the synthetic methodology was significantly simplified compared to conventional brush copolymer synthesis.

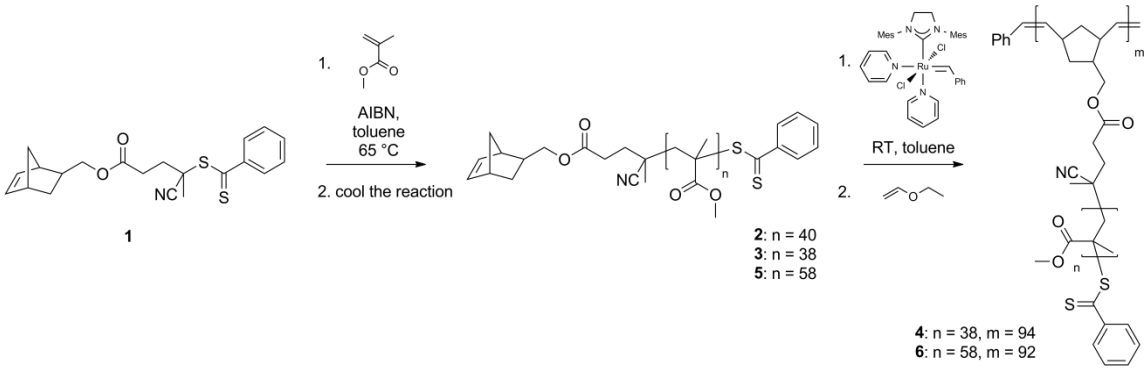

Figure 3.1. One-pot, "grafting-through" synthesis of molecular brush copolymers, PNB-*g*-PMMA.

The norbornenyl-functionalized dithiobenzoate chain transfer agent (NB-DTB, **1**) was synthesized by coupling an *exo*-norbornenyl (NB) group with a dithiobenzoate RAFT chain transfer agent (DTB) *via* esterification of *exo*-5-norbornene-2-methanol and 4-cyano-4-(phenylcarbonothioylthio)pentanoic acid. ^{1}H NMR spectroscopy of **1** showed a series of characteristic resonances, including those of aromatic protons of DTB at 7.90-7.41 ppm, norbornene alkenyl protons at 6.09 ppm, CH_2OC(O) at 4.17 and 3.99 ppm and CH_3 at 1.92 ppm, and the integration intensity ratios agreed with the theoretical values. A similar RAFT agent, containing *endo/exo* isomers of norbornenyl groups, was reported by Advincula and coworkers.[144] They demonstrated the synthesis of well-defined poly(methyl methacrylate) (PMMA) with terminal *endo/exo* NB groups, which could be polymerized with a degree of polymerization (DP) of 8 *via* ROMP with near-quantitative macromonomer conversion. In our study, we were interested in the preparation of densely-grafted bottle brush-like copolymers, therefore, the *exo*-

norbornenyl group was chosen, owing to its significantly higher ROMP reactivity compared with the *endo*-norbornenyl isomer.[228-231]

To identify the conditions under which well-defined NB-PMMA macromonomer could be synthesized, a series of polymerizations was performed with isolation and analysis of the polymer products. The NB-PMMA$_{40}$ macromonomer (**2**) was synthesized by selective RAFT polymerization of methyl methacrylate (MMA) using NB-DTB as the chain transfer agent, *2,2'*-azobis(isobutyronitrile) (AIBN) as the thermal radical initiator and toluene (50 vol %) as the solvent at 65 ℃, with the feed ratio $[MMA]_0$:$[NB\text{-}DTB]_0$ of 100:1. ^{1}H NMR spectroscopy was used to determine the monomer conversions and number-averaged molecular weights (M_n). Gel permeation chromatography (GPC) was used to analyze the molecular weights and polydispersities (PDIs). When higher amounts of AIBN were employed (20 mol % to [NB-DTB]), a high molecular weight shoulder was observed in the GPC traces once monomer conversion reached >40%, which suggested the participation of terminal norbornenyl groups during the RAFT polymerization. Whereas, when lower amounts of AIBN (10 mol % to [NB-DTB]) were applied, well-defined NB-PMMA macromonomer, **2**, was afforded after 4.3 h with a monomer conversion of 40%. The well-defined structure of NB-PMMA$_{40}$ was verified by both ^{1}H NMR and GPC analysis. As shown in figure 3.2, the integral ratio of phenyl protons of the DTB unit (7.88-7.37 ppm), alkenyl protons of the NB group (6.09 ppm) and the protons of the -OCH_3 group (3.7-3.5 ppm) of PMMA were measured to be *ca*. 5.2:2:121, indicating the nearly quantitative retention of both the norbornenyl and the dithiobenzoate functionalities, as well as good agreement of the

DP value to the theoretical value calculated by monomer conversion. As analyzed by GPC, the NB-PMMA$_{40}$ macromonomer, **2**, had a monomodal molecular weight distribution and a PDI of 1.12, and the molecular weight calculated by GPC (M_n^{GPC} = 4600 Da) was close to the theoretical value ($M_n^{theo.}$ = 4360 Da) from monomer conversion.

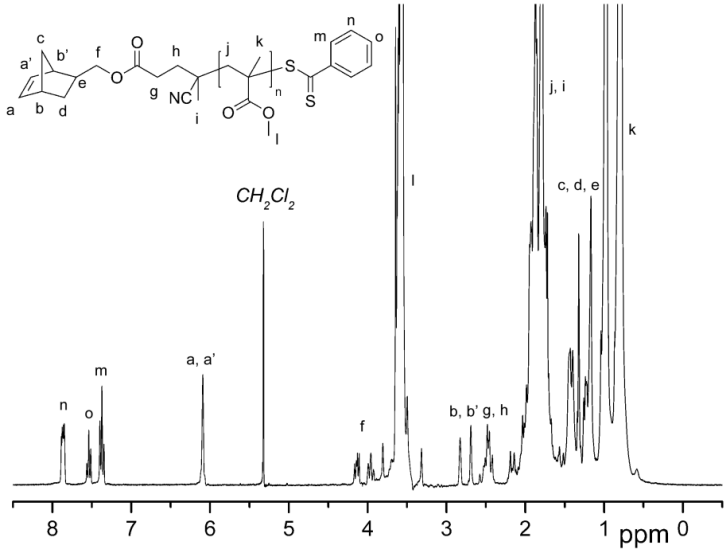

Figure 3.2. ^{1}H NMR (300 MHz, CD_2Cl_2) spectrum of NB-PMMA$_{40}$, **2**.

To precisely control the NB-PMMA lengths for tuning the brush copolymer sizes, a kinetic study of RAFT polymerization of MMA was then conducted, using [MMA]:[NB-DTB]:[AIBN] = 200:1:0.1, and 50 vol % toluene at 65 ℃. The feed ratio was selected to achieve well-controlled RAFT polymerization of MMA while maintaining the macromonomer concentration in the range of 50-300 mg/mL for the later ROMP. As shown in figure 3.3, the RAFT polymerization of MMA followed

linear first-order kinetics, and the PDIs remained low throughout the polymerization process. Linear relationships were obtained for M_n values *vs*. monomer conversions

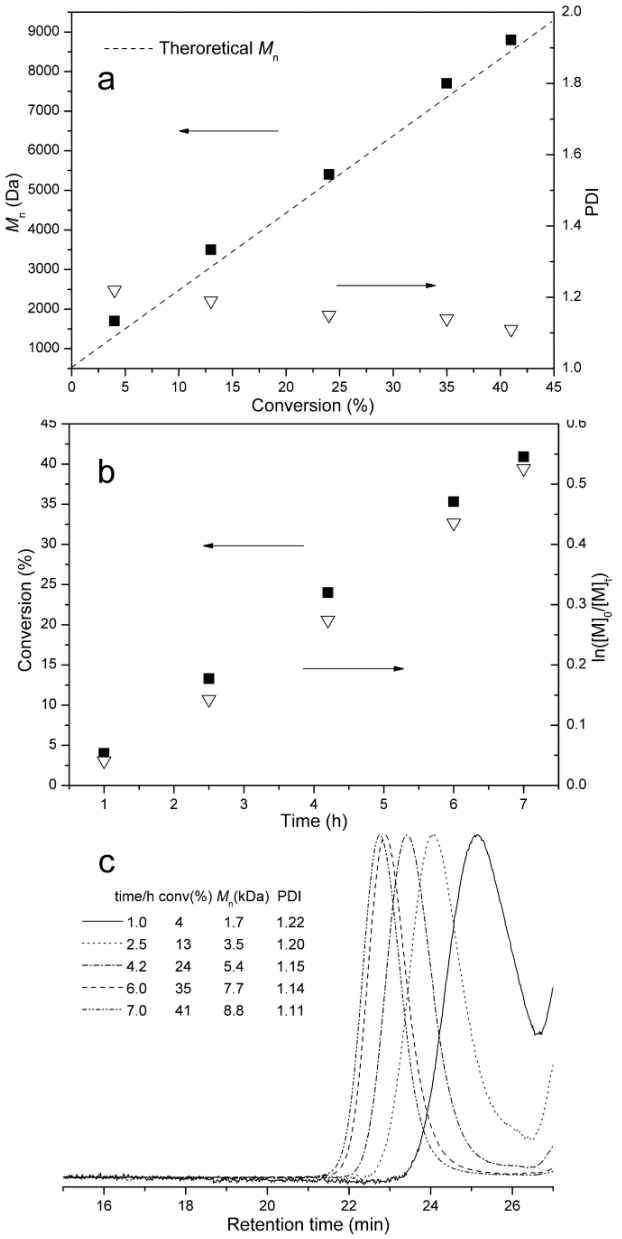

Figure 3.3. Kinetic study of RAFT polymerization of MMA: (a) dependence of M_n^{GPC} and PDI relative to monomer conversions; (b) time dependence of monomer conversions and $\ln([M]_0:[M]_t)$ from ^{1}H NMR measurements; (c) evolution of GPC traces during RAFT of **1**.

from GPC (figure 3.3a) and $\ln([M]_0/[M]_t)$ *vs*. time from ^{1}H NMR (figure 3.3b) measurements, which indicated precise control over the NB-PMMA structure. In addition, the monomer conversion *vs*. time was linear, due to the kinetic experiments being performed to limited overall conversions to avoid the incorporation of NB groups during RAFT polymerization.

Conditions under which ROMP of NB-PMMA macromonomers would proceed to high conversion and with control, even in the presence of residual methacrylate monomer, were then determined by a series of polymerization studies. We first investigated the ROMP of **2** with modified Grubbs' 2nd generation catalyst in toluene with MMA or methyl acrylate (MA) as the co-solvents at room temperature. To avoid changing solvent in the sequential RAFT and ROMP steps, toluene was selected as the solvent for ROMP. MMA and MA were chosen as the co-solvent to explore the efficiency ROMP of macromonomers in the presence of methacrylate or acrylate monomers to determine the feasibility of a one-pot synthesis of brush polymers by this "grafting-through" method. Comparisons of MMA *vs.* MA were made to confirm the lack of involvement of methacrylates during ROMP, whereas acrylates[232] competed with NB. The two ROMP experiments (run **1** and run **2**) were performed at room temperature with a feed ratio $[NB\text{-}PMMA_{40}]_0$:$[catalyst]_0$ of 100:1 and the macromonomer concentration of *ca.* 100 mg/mL in mixed solvents of toluene (60 vol%) and MMA (40 vol% for run **1**) or MA (40 vol % for run **2**). Small aliquots were withdrawn from the polymerization solution after 1 h and the macromonomer conversions were determined by GPC. As shown in figure 3.4, the ROMP of macromonomer in the toluene/MMA co-

solvent showed high conversion (91%) of the macromonomer, which suggested a highly efficient transformation of the NB terminal group in ROMP by modified 2nd generation Grubbs' catalyst. Moreover, the DTB functionality as well as the large excess of MMA (*ca.* 150000 eq. to catalyst) were both compatible with the Ru-catalyst during ROMP, which allowed for the one-pot, "grafting-through" brush copolymer synthesis. However, when MA was employed as the co-solvent, incomplete conversion (< 50%) of macromonomer was observed, and the conversion did not improve over longer reaction times, which was attributed to significant chain termination from the acrylate functionalities.[233]

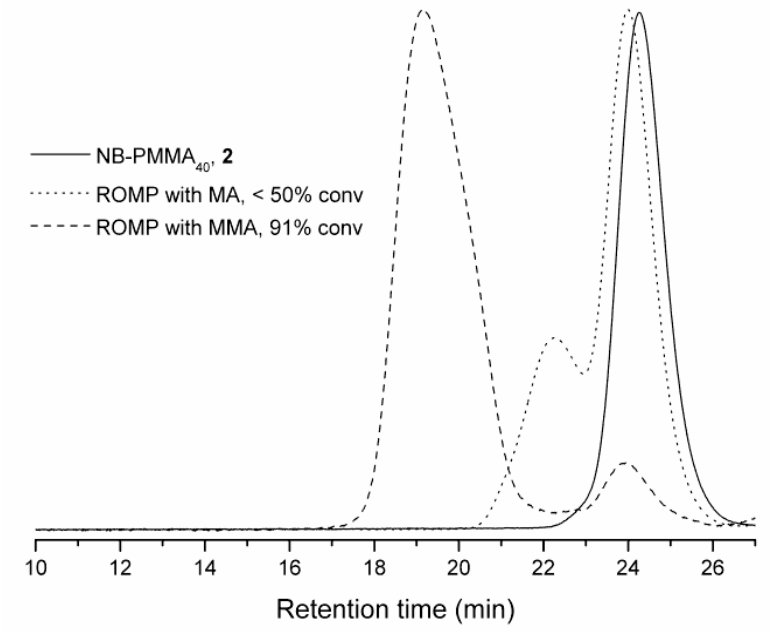

Figure 3.4. GPC traces of NB-PMMA$_{40}$, **2** and two control studies of ROMP of **2** with MMA or MA as co-solvent.

Two PMMA brush polymers were then synthesized by the sequential RAFT and ROMP "grafting-through" method in a one-pot manner, utilizing the conditions identified, to demonstrate control over the backbone and side chain lengths. The feed ratio of RAFT polymerization was employed as optimized by the kinetics study ([MMA]:[NB-DTB]:[AIBN] = 200:1:0.1, 50 vol % toluene, 65 ℃). The RAFT polymerizations were stopped at 3 h and 5 h, respectively, by immersing the Schlenk flasks into liquid nitrogen for 10 min, followed by stirring at room temperature in a water bath for 20 min. Aliquots were withdrawn for the purpose of characterization studies, giving NB-PMMA$_{38}$, **3**, (19% conversion of MMA, M_n^{GPC} = 4700 Da, M_w/M_n = 1.14) and NB-PMMA$_{58}$, **5**, (29% conversion of MMA, M_n^{GPC} = 6450 Da, M_w/M_n = 1.12), whose chain lengths agreed with predetermined molecular weights and narrow PDIs, as estimated from applying information from the kinetics studies. These macromonomer chain lengths were held, intentionally, to relatively low degrees of polymerization to allow for the preparation of fully extended molecular brushes with backbones significantly longer than the side chain lengths. In the next step, modified 2nd generation Grubbs' catalyst (0.01 eq.) in stock solution was added to the crude macromonomer solutions to initiate the ROMP reactions to construct the polynorbornene backbones. The polymerizations were quenched at 1 h by adding several drops of ethyl vinyl ether. As determined by GPC analyses (figure 3.5), the formation of well-defined brush copolymers was verified by the observation of the shifts of the GPC traces from retention times of the macromonomers (**3**, **5**) to the respective brush copolymers (**4**, **6**) with high conversions of the macromonomers (94% of **3** and 92% of **5**, respectively).

The residual unreacted macromonomers as well as the remaining MMA could be readily removed by precipitation of the crude brush polymers into methanol three times (figure 3.5). As summarized in table 3.1, the well-defined structure of the brush polymers synthesized by the one-pot, "grafting-through" method were confirmed by the good agreement between the M_ns calculated by macromonomer conversions and measured by GPC, as well as the monomodal molecular weight distributions and low PDIs.

Table 3.1. One-pot, "grafting through" syntheses of brush copolymers **4** and **6**.

	t[a]	Conv PMMA	$M_n^{theo.}$ PMMA	M_n^{GPC} PMMA[b]	PDI PMMA	Conv PMMA	$M_n^{theo.}$ brush	M_n^{GPC} brush[c]	PDI
4	3 h	19	4160 Da	4700 Da	1.14	94	391 kDa	414 kDa	1.22
6	5 h	29	6160 Da	6450 Da	1.12	92	566 kDa	607 kDa	1.27

[a] Polymerization time of RAFT. [b] Determined by ^{1}H-NMR. [c] Determined by refractive index (RI) detection with calibration using polystyrene standards. [d] The conversions of macromonomers (NB-PMMA) were determined by comparing the peak areas of brush copolymers and macromonomers from GPC measurements (RI detector) of crude products. [e] Determined by light scattering detection.

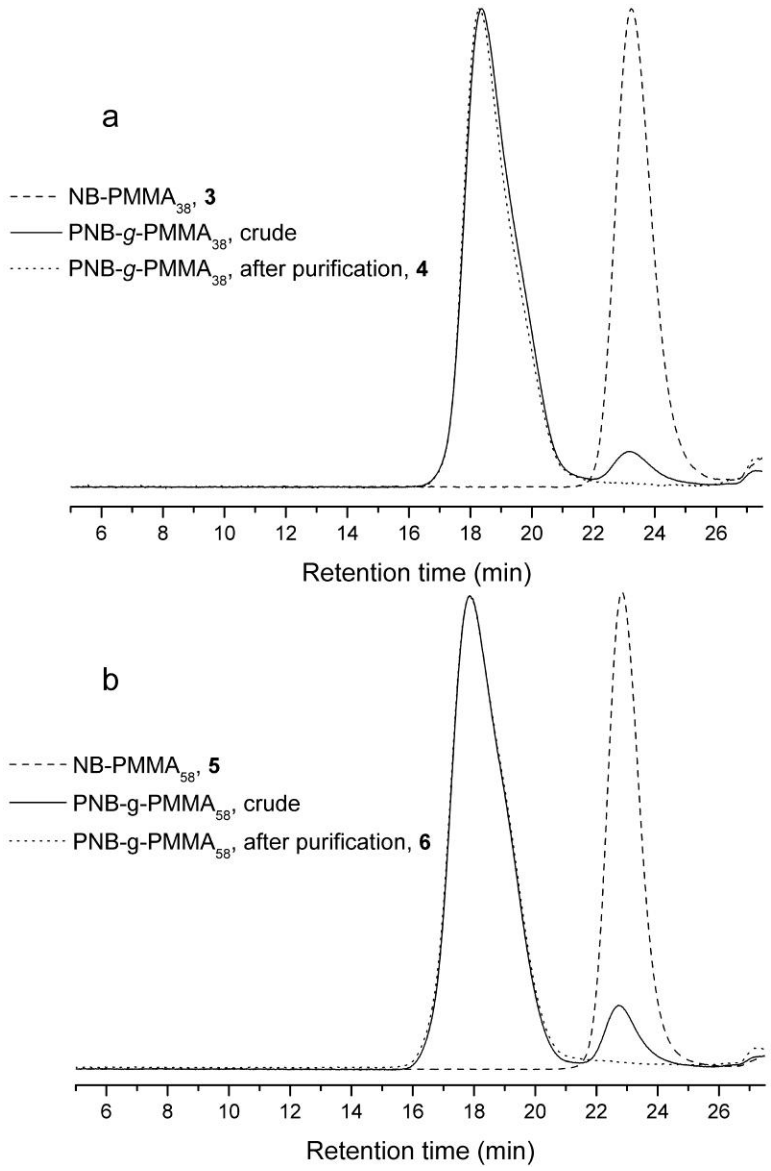

Figure 3.5. GPC traces of polymers **3**-**6**.

Atomic force microscopy (AFM, tapping-mode) was utilized to visualize individual brush copolymers, with the samples being prepared by spin-casting dilute polymer solutions (*ca.* 0.01 mg/mL in chloroform) onto freshly-cleaved mica surfaces. As shown in figure 3.6, AFM images of both PNB_{94}-*g*-$PMMA_{38}$ (**4**) and PNB_{92}-*g*-$PMMA_{58}$ (**6**) showed bottle brush-like morphologies with average contour lengths of 66 ± 13 nm and 68 ± 12 nm, respectively, which is in good agreement with degrees of polymerization of *ca*. 90 multiplied by the reported NB monomeric unit length (0.62 nm) of brush copolymers having PNB backbones.[62] These results also suggested full extension of the PNB backbones caused by repulsion between individual PMMA side chains densely-grafted to the PNB backbones. Due to the differences in side chain length, the average widths of **4** and **6** were measured to be 22 ± 2 nm and 32 ± 2 nm, respectively, which are close to the sizes calculated from the degrees of polymerization for a fully stretched MMA monomeric length of 0.25 nm, suggesting the brush polymer side chains are also fully extended due to the steric effects from the high grafting density and the large size of the macromonomers. However, the actual sizes of the brush copolymers may be slightly smaller than the values measured by AFM due to the broadening effect caused by AFM tip deconvolution (tip radius (Nom) = 2 nm in this study).

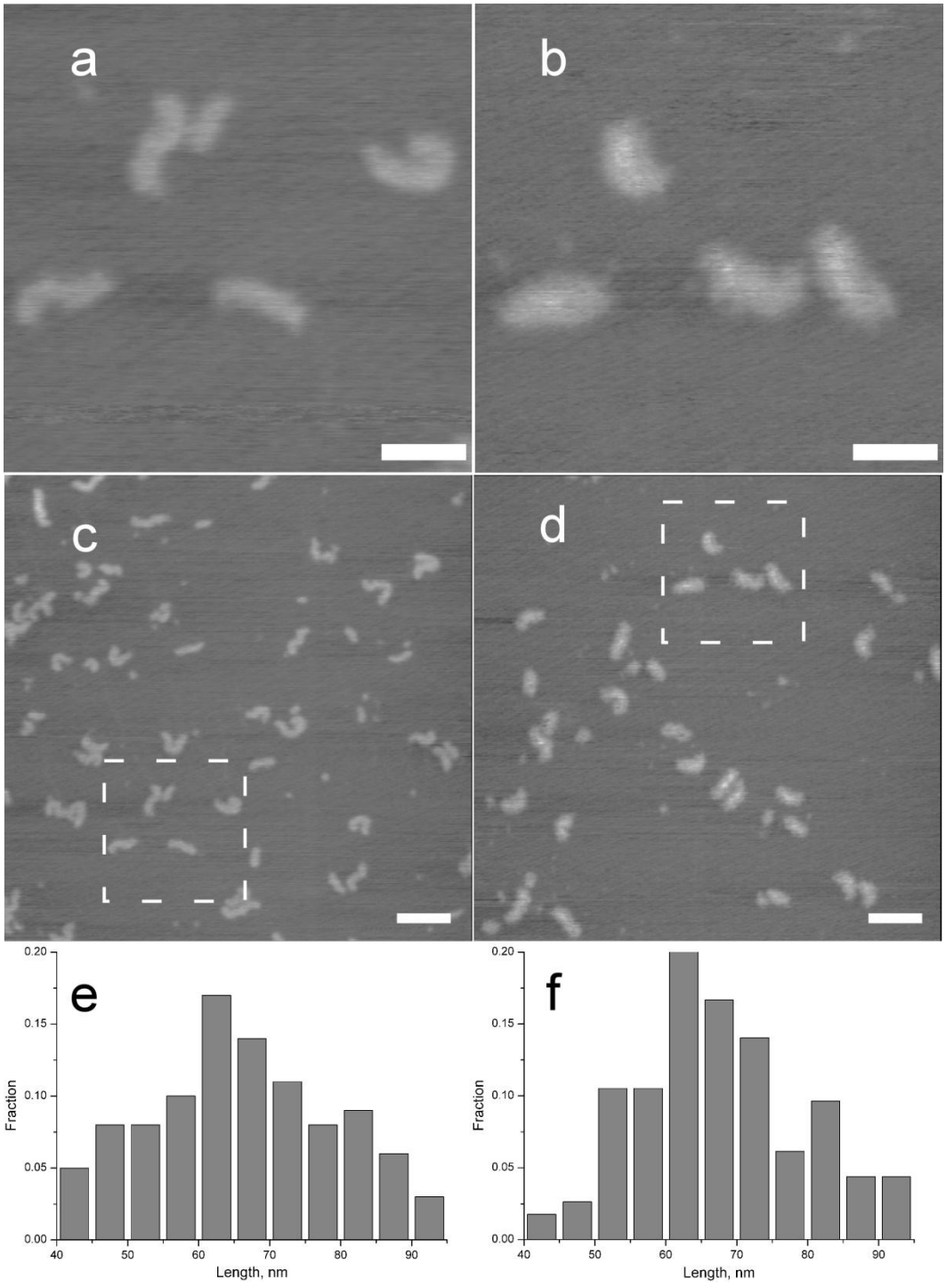

Figure 3.6. AFM height images of PNB_{94}-*g*-$PMMA_{38}$, **4** (selected area in c) (a) and PNB_{92}-*g*-$PMMA_{58}$, **6** (selected area in d) (b); large scale AFM height images of **4** (c) and **6** (d); scale bars = 50 nm (a and b), scale bars = 100 nm (c and d), z scale = 3 nm; distributions of **4** (e) and **6** (f).

3.3. Experimental Section

3.3.1. Instruments

^{1}H NMR and ^{13}C NMR spectra were recorded on Varian Inova 300 MHz or Varian Mercury 300 MHz spectrometers interfaced to a UNIX computer using VnmrJ software. Chemical shifts were referred to the solvent resonance signals. IR spectra were recorded on an IR Prestige 21 system (Shimadzu Corp., Japan) and analyzed using IRsolution v. 1.40 software. Gel permeation chromatography (GPC) was performed on a Waters Chromatography, Inc., 1515 isocratic HPLC pump equipped with an inline degasser, a model PD2020 dual angle (15 ° and 90 °), static light scattering detector (Precision Detectors, Inc.), a model 2414 differential refractometer (Waters, Inc.), and four PLgel polystyrene-*co*-divinylbenzene gel columns (Polymer Laboratories, Inc.) connected in series: 5 μm Guard (50 × 7.5 mm), 5 μm Mixed C (300 × 7.5 mm), 5 μm 10^4 (300 × 7.5 mm), and 5 μm 500 Å (300 × 7.5 mm) using the Breeze (version 3.30, Waters, Inc.) software. The instrument was operated at 35 ℃ with THF as eluent (flow rate set to 1.0 mL/min). Polymer solutions were prepared at a known concentration (*ca*. 3 mg/mL) and an injection volume of 200 μL was used. Data collection was performed with Precision Acquire 32 Acquisition program (Precision Detectors, Inc.) and analyses were carried out using Discovery32 software (Precision Detectors, Inc.) with a system calibration curve generated from plotting molecular weight as a function of retention time for a series of broad polydispersity poly(styrene) standards. Glass transition temperatures (*T*g) were measured by differential scanning calorimetry on a Mettler-Toledo DSC822^{e} (Mettler-Toledo, Inc., Columbus, OH), with a heating rate of 10 ℃

/min. Measurements were analyzed using Mettler-Toledo Star^{e} v. 10.00 software. The *T*g was taken as the midpoint of the inflection tangent, upon the third heating scan. Thermogravimetric analysis was performed under N_2 atmosphere using a Mettler-Toledo model TGA/DSC 1, with a heating rate of 5 ℃/min. Measurements were analyzed using Mettler-Toledo Star^{e} v. 10.00 software. Atomic force microscopy (AFM) imaging was performed using a MFP-3D system (Asylum Research, Santa Barbara, CA) in tapping mode using standard silicon tips (SCANASYST-AIR, from Bruker, 115 μM, spring constant 0.4 N m^{-1}, with tip radius (Nom) = 2 nm). Samples were prepared by spin casting dilute solutions (*ca.* 0.01 mg/mL) in chloroform onto freshly-cleaved mica at 2500 rpm.

3.3.2. Materials

All Chemicals and reagents were purchased from Aldrich Chemical Co. and used as received, unless otherwise noted. Methyl methacrylate and methyl acrylate were passed through a neutral alumina column to remove the inhibitor before use. *2,2'*-Azobis(isobutyronitrile) (AIBN) was recrystallized twice from methanol before use. Dichloromethane (CH_2Cl_2) was distilled over CaH_2 and stored under N_2 before use. The norbornenyl-functionalized dithiobenzoate chain transfer agent (NB-DTB, **1**) was synthesized according to the reported method[144] with modifications. Modified 2nd generation Grubbs' catalyst ($(H_2IMes)(pyr)_2(Cl)_2RuCHPh$) was prepared according to reported method.[59]

3.3.3. Synthesis of exo-norbornenyl 4-cyano-4-(phenylcarbonothioylthio)pentanoate (NB-CTA, 1)

To a 100 mL RB flask wrapped with aluminum foil and equipped with a stir bar was placed *exo*-5-norbornene-2-methanol (0.502 g, 4.11 mmol), 4-cyano-4-(phenylcarbonothioylthio)pentanoic acid (1.37 g, 4.92 mmol) and 4-(dimethylamino)pyridine (0.103 g, 0.844 mmol). Dry CH_2Cl_2 (10 mL) was then added into the flask to dissolve all reagents followed by dropwise addition of a solution of *N,N′*-dicyclohexylcarbodiimide (1.02 g, 4.98 mmol) in CH_2Cl_2. The reaction mixture was allowed to stir at room temperature for 10 h. The solid was removed by filtration, and the filtrate was concentrated under vacuum and purified by silica gel flash chromatography eluting with ethyl acetate/hexanes (1:10). The product was afforded as a red oil. Yield: 77%. IR (cm^{-1}): 3132-2792, 2229, 1728, 1442, 1388, 1280, 1180, 1049, 964, 864, 702. ^{1}H NMR (300 MHz, CD_2Cl_2, δ, ppm) 7.91-7.40 (m, 4H, Ar*H*), 6.09 (s, 2H, norbornenyl alkenyl protons), 4.19 (dd, J = 7 and 11 Hz, 1H, CH_2OC(O)), 4.01 (dd, J = 9 and 11 Hz, 1H, CH_2OC(O)), 2.82 (s, 1H, allylic proton of norbornenyl group), 2.69 (s, 1H, allylic proton of norbornenyl group), 2.67-2.40 (m, 4H, -CH_2CH_2C(O)-), 1.92 (s, 3H, -CH_3), 1.69 (m, 1H, >C*H*CH_2O-), 1.31-1.11 (m, 4H, >CHCH_2CH<). ^{13}C NMR (75 MHz, CD_2Cl_2, δ, ppm) 223.7, 172.0, 145.2, 137.5, 136.7, 133.6, 129.1, 127.2, 119.0, 69.6, 46.4, 45.4, 44.2, 42.1, 38.5, 33.9, 30.3, 30.0, 24.5. HRMS (m/z): calcd for $C_{21}H_{23}NO_2S_2$, 385.1170; found, 386.1250 $[M + H]^+$.

3.3.4. Synthesis of NB-PMMA$_{40}$, 2

A 25 mL Schlenk flask with a stir bar and sealed by a rubber septum was charged with MMA (5.61 g, 56.1mmol), NB-CTA (200 mg, 0.560 mmol), AIBN (9.18 mg, 0.0560 mmol, 10 mol %), and 6 mL of toluene as the solvent. After three cycles of freeze-pump-thaw, the flask was placed in an oil bath at 65 ℃. The polymerization was quenched after 4.3 h when the monomer conversion was measured to be 40% by ^{1}H NMR. The polymer solution was precipitated three times in hexanes. The product was collected and dried under vacuum for 24 h at room temperature to afford Nb-PMMA$_{40}$ as a pink solid. Yield: 1.51 g (67%, based on 40% conversion of MMA). $M_n^{theo.}$ = 4360 Da, M_n^{GPC} = 4600 Da, M_w/M_n = 1.12. IR (cm^{-1}): 3093-2808, 1728, 1442, 1388, 1242, 1149, 987, 840, 756. ^{1}H NMR (300 MHz, CD_2Cl_2, δ, ppm) 7.86-7.38 (m, Ar*H* of CTA), 6.09 (s, norbornenyl alkenyl protons), 4.14-3.96 (m, -C*H*$_2$OC(O)-) of Nb group), 3.64-3.53 (br, -OC*H*$_3$ of polymer backbone), 2.82 (s, 1H, allylic proton of Nb group), 2.69 (s, 1H, allylic proton of Nb group), 2.46-1.63 (br, -C*H*$_2$C*H*$_2$C(O)- of CTA, >C*H*CH$_2$O- of CTA, C*H*$_2$ of polymer backbone), 1.49-1.13 (m, -C*H*$_3$ and >CHC*H*$_2$CH< of Nb group), 1.10-0.80 (br, -C*H*$_3$ of polymer backbone). ^{13}C NMR (75 MHz, CD_2Cl_2, δ, ppm) 178.6, 178.3, 177.6, 177.4, 172.7, 145.5, 137.5, 136.8, 133.2, 129.0, 127.1, 69.3, 54.9, 52.2, 45.3, 45.0, 44.2, 42.2, 38.5, 30.0, 19.1, 16.1. T_g = 106 ℃, TGA in Ar: 170-205 ℃, 6% mass loss; 250-425 ℃, 79% mass loss.

3.3.5. General procedure for the kinetic study of the synthesis of Nb-PMMA by RAFT polymerizations

A 10 mL Schlenk flask with a stir bar was charged with Nb-CTA, MMA, AIBN, and toluene as the solvent, and then sealed with rubber septum. After three cycles of freeze-pump-thaw, the flask was placed into an oil bath at 65 ℃ to allow for polymerization. During polymerization, small aliquots (~0.1 mL) of polymerization solution were withdrawn with N_2-washed syringes and were analyzed by ^{1}H NMR spectroscopy and GPC for determinations of conversions of monomer and molecular weights of the polymers formed. The polymerizations were quenched at 7 to 9 h followed by precipitation three times in hexanes. The products were collected and dried under vacuum for 24 h at room temperature.

3.3.6. Synthesis of PNB_{94}-g-$PMMA_{38}$ (4) by one-pot RAFT and ROMP method

To a 10 mL Schlenk flask equipped with a stir bar was charged Nb-CTA (30.3 mg, 0.0848 mmol), MMA (1.68 g, 16.8 mmol), AIBN (1.38 mg, 0.00841 mmol, 10 mol %) and 2 mL toluene (50 vol %) as the solvent. After three cycles of freeze-pump-thaw, the flask was placed in an oil bath at 65 ℃. The polymerization was quenched at 3 h by immersing the reaction flask into liquid nitrogen when the monomer conversion was measure to be 19% by ^{1}H NMR. After the reaction mixture was allowed to warm to room temperature, modified Grubbs' catalyst solution (2.17 mg/mL, 0.280 mL, 0.834 μmol) was added *via* a N_2-washed syringe. The reaction was quenched at 1 h by adding several drops of ethyl vinyl ether. The final brush polymer was obtained after precipitation into methanol three times to remove toluene, MMA and any unreacted Nb-

PMMA macromonomer. The product was collected and dried under vacuum for 24 h at room temperature to afford 4 as a pink solid. Yield: 255 mg (80%, based on 19% monomer conversion). $M_n^{theo.}$ = 391 kDa, M_n^{GPC} = 414 kDa, M_w/M_n = 1.22. ^{1}H NMR (300 MHz, $CDCl_3$, δ, ppm) 7.86-7.38 (m, Ar*H* of CTA), 5.46-5.02 (s, alkenyl protons of PNB backbone), 4.16-4.00 (br, -C*H*$_2$OC(O)- of Nb group), 3.64-3.53 (br, -OC*H*$_3$ of polymer backbone), 3.10-1.58 (br, >C*H*CH$_2$O- and allylic protons of PNB, -C*H*$_2$C*H*$_2$C(O)- of CTA, >C*H*CH$_2$O- of CTA, C*H*$_2$ of polymer backbone), 1.49-1.20 (m, -C*H*$_3$ and >CHC*H*$_2$CH< of Nb group), 1.01-0.84 (br, -C*H*$_3$ of polymer backbone). ^{13}C NMR (75 MHz, CD_2Cl_2, δ, ppm) 178.6, 178.3, 177.6, 177.4, 133.0, 128.9, 127.1, 54.9, 52.0, 45.3, 45.0, 19.1, 16.9. T_g = 110 ℃, TGA in Ar: 185-210 ℃, 3% mass loss; 280-440 ℃, 74% mass loss.

3.3.7. Synthesis of PNB$_{92}$-g-PMMA$_{58}$ (6) by one-pot RAFT and ROMP method

The same procedure as for the synthesis of 4 was followed with quenching the RAFT polymerization at 5h, when the monomer conversion was measure to be 29% by ^{1}H NMR. Yield: 386 mg (78%, based on 29% monomer conversion). $M_n^{theo.}$ = 566 kDa, M_n^{GPC} = 607 kDa, M_w/M_n = 1.27. T_g = 110 ℃, TGA in Ar: 185-205 ℃, 3% mass loss; 280-440 ℃, 76% mass loss.

3.4. Conclusions

In summary, by taking advantage of the reactivity differences of methacryl *vs*. norbornenyl monomers between RAFT and ROMP polymerizations, facile "grafting-through" synthesis of molecular brush copolymers was achieved by tandem RAFT and ROMP in a one-pot manner. Following detailed kinetic studies to identify optimized

polymerization conditions, two well-defined PMMA brush copolymers with similar backbone length (DP ≈ 100) and different side chain lengths (DP = 38, 58) were synthesized without changing or adding solvent, or purification of the intermediate products between the RAFT (side chain formation) and ROMP (backbone formation) steps. The controlled dimensions of two brush copolymers were verified by GPC and AFM. By using this one-pot, "grafting-through" method, the brush copolymer synthesis procedures were significantly simplified. It is anticipated that more types of brush copolymers can be prepared by combining other controlled polymerizations, such as ATRP and/or ROP, with ROMP, based on the efficiency, robustness and orthogonality of the polymerization methods.

CHAPTER IV

SYNTHESIS AND DIRECT VISUALIZATION OF DUMBBELL-SHAPED MOLECULAR BRUSHES*

4.1. Introduction

The construction of nanoscale polymeric architectures with complex and well-defined structures is of great interest because it enables the fabrication of soft materials with tunable properties and functionalities.[32,34-36,41] Molecular brushes represent a unique class of densely-grafted polymers with control over the grafting densities, as well as the compositions and lengths of both the brush polymer backbone and the side chains, to affect their shapes and sizes from macromolecular to nanoscopic dimensions.[101,102] Due to their worm-like or cylindrical conformations caused by the steric repulsion among densely-distributed side chains, molecular brushes have been explored in various applications, such as photonic materials,[111,113,114] templates for inorganic nanowires,[107,119,203,234] supersoft elastomers[108] and nano-carriers for nanomedicine.[121,125,204,235] By employing various controlled/living polymerization methodologies, numerous molecular brush polymer architectures, such as cyclic,[126,146,220,236] tubular,[138,237] dumbbell-,[238] tadpole-,[239-241] and star-like,[133,242] have been synthesized and directly visualized by atomic force microscopy (AFM).

---

*Part of this work is reprinted with permission from "Synthesis and direct visualization of dumbbell-shaped molecular brushes" by Ang Li, Zhou Li, Shiyi Zhang, Guorong Sun, Danielle M. Policarpio and Karen L. Wooley, 2012. ACS *Macro Lett.*, 1, 241-245. Copyright [2012] by the American Chemical Society.

We are particularly interested in hetero-grafted block brush copolymers, having differential side chains distributed along the backbone, because such macromolecules with increased complexities and defined three-dimensional morphologies may better mimic some features of biomacromolecules, compared to their linear block copolymer counterparts, and lead to unusual hierarchical nanoassemblies in aqueous medium[218] and in the bulk.[111] The backbone-based block brush copolymers can be synthesized by three strategies: "grafting-onto", "grafting-from", and "grafting-through". The first two strategies include the preparation of long and well-defined block copolymer backbones, decorated with orthogonal functionalities, followed by coupling pre-synthesized side chains ("grafting onto"),[243,244] or by growing different side chains using orthogonal polymerizations[114,132,134,237,245] or selective protection/deprotection methodologies ("grafting from").[138] The "grafting-through" approach allows for variation in the side chain composition and structure in a straightforward manner that involves sequential polymerizations of macromonomers, and is analogous to the standard procedures for the growth of typical linear block copolymers. Steric effects and relatively low concentration of the polymerizable functionality can pose challenges for "grafting-through" polymerizations, however, ring-opening metathesis polymerization (ROMP) has been proven to be an effective chemistry to polymerize norbornene groups in macromolecules to form molecular brush polymers.[61,62,213] Moreover, due to the high activity of Ru-based olefin metathesis catalysts, high tolerance of the catalyst to functional groups, and the living characteristics,[58] ROMP displays advantages and conveniences toward preparing block brush copolymers. It allows fast polymerization

with high macromonomer conversion, facile incorporation of a variety of functional polymers into molecular brush frameworks, and precise control over the macromolecular architecture, by controlling the lengths and structures of backbones and side chains independently.

Driven by our interest in developing facile synthetic methodologies to achieve increasingly sophisticated macromolecules, herein, we report the novel synthesis of triblock dumbbell-shaped molecular brushes *via* ROMP by sequential additions of macromonomers in a one-pot "grafting-through" manner. Although macromolecules with backbone multi-block structures, or even dumbbell/pom-pom shapes have been constructed by combining various controlled polymerizations,[132,238,246,247] this work represents an advance in synthetic techniques to allow for the facile preparation of brush polymers with densely-grafted side chains along the entire backbone with three different block segments, as ABA or asymmetric ABC triblock copolymer nanostructures.

4.2. Results and Discussion

Three poly(DL-lactide) macromonomers having terminal norbornene groups, with degrees of polymerization (DP) of 15, 30, and 45 (NB-PLA_{15}, **1**; NB-PLA_{30}, **2**; NB-PLA_{45}, **3**), and low polydispersity indices (PDI) of 1.20, 1.11, and 1.10 (figure 4.2.), respectively, were synthesized by 1,8-diazabicyclo[5.4.0]-undec-7-ene (DBU)-catalyzed ring-opening polymerization (ROP) of DL-lactide in dichloromethane (DCM) at room temperature (figure 4.1).[67,145]

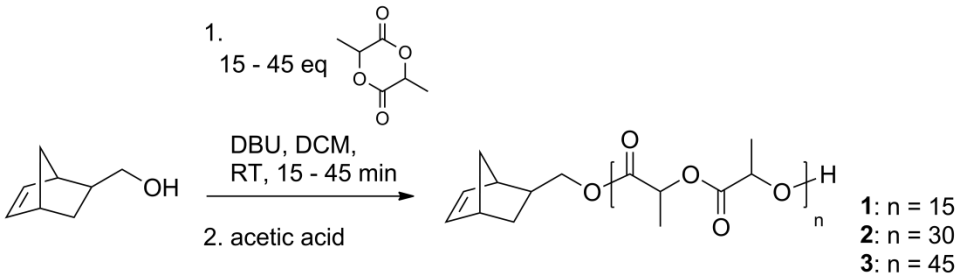

Figure 4.1. Syntheses of macromonomers, NB-PLA$_{15}$, **1**; NB-PLA$_{30}$, $_{2}$; NB-PLA$_{45}$, **3**.

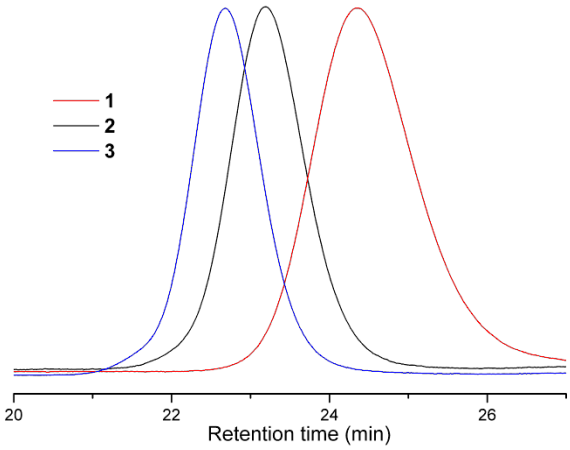

Figure 4.2. GPC traces of NB-PLA$_{15}$, **1**; NB-PLA$_{30}$, **2**; NB-PLA$_{45}$, **3**.

For this initial demonstration of dumbbell synthesis and characterization studies, the same composition, PLA, of side chains was chosen to avoid the potential differential segregation or aggregation of block brush copolymer components on the substrate during AFM characterization. In addition, PLA is a hydrolytically-degradable material, which is of interest as an environmentally- and biologically-benign building blocks. Convenient and precise control of the macromonomer lengths and chain ends were important to achieve well-defined side chains of the dumbbell-shaped brush copolymers.

The DBU-catalyzed ROP allowed for accurate tuning of the macromonomer structures, due to the high monomer conversion (>99%) and *ca.* quantitative initiation efficiency, as verified by agreement of DP values calculated from monomer conversion and chain end analysis by ^{1}H NMR spectroscopy, involving comparison of integration values of the NB group vinyl protons (6.05-6.10 ppm) and methine protons (5.09-5.25 ppm) of PLA (figure 4.3).

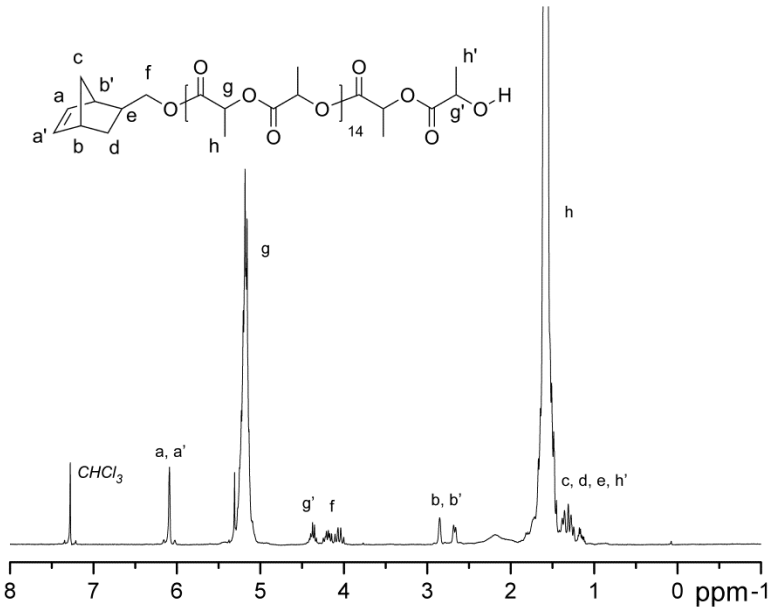

Figure 4.3. ^{1}H NMR (300 MHz, $CDCl_3$) spectrum of NB-PLA_{15}, **1**.

A preliminary study was then conducted to investigate the possibility of synthesizing triblock brush copolymers by three sequential additions of macromonomers to a solution of modified second generation Grubbs' catalyst $(H_2IMes)(pyr)_2(Cl)_2RuCHPh$ (**4**) as the initiator in DCM at room temperature (figure

4.4). Three portions of **2** (each portion with [**2**]/[**4**] = 25) were added sequentially with time intervals of 5, 10 and 20 min. The final macromonomer conversion was measured by gel permeation chromatography (GPC). It was shown that sequential additions of three portions of **2** could afford well-defined brush copolymer, **5**, with high overall macromonomer conversion (>90%) and low PDI (1.11), which demonstrated the living characteristics and high efficiency of ROMP of NB-terminated macromonomers. This approach towards triblock brush copolymers is attractive because the macromolecular architecture can be effectively controlled by adjusting the macromonomer sizes as well as the macromonomer to catalyst ratio, at each stage of the ROMP.

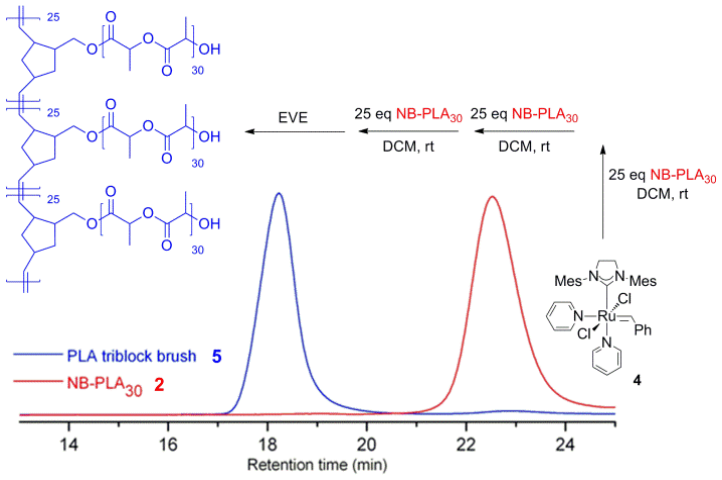

Figure 4.4. Preliminary study of synthesizing of triblock brush copolymer **5**.

Based on this result, we attempted the synthesis of dumbbell-shaped brush copolymer having the "balls" and "bar" composed of **3** and **1**, respectively, by sequential polymerization of **3**, **1**, and then **3** again, at stoichiometries relative to **4** that would give

DP(backbone) of 30, 100, and 30, respectively P(NB-*g*-PLA_{45})$_{30}$-*b*-P(NB-*g*-PLA_{15})$_{100}$-*b*-P(NB-PLA_{45})$_{30}$, **8** (figure 4.5). To achieve precise control of the structure and dimensions of the triblock brush copolymers, avoiding either mixtures of macromonomers being present or delays that may result in chain termination events, each portion of macromonomer solution must be added immediately after the consumption of the previous one. Therefore, a series of experiments was performed to determine the time required for each stage of ROMP for macromonomers **3** and **1**. ROMP was initiated by adding catalyst stock solution into macromonomer solution (*ca.* 100 mg/mL in toluene), and the molecular weights, PDIs and macromonomer conversions were measured by GPC. These kinetics studies revealed that the reactions of building up the first block (P(NB-*g*-PLA_{45})$_{30}$, **6**, [**3**]/[**4**] = 30:1) and the second block (P(NB-*g*-PLA_{45})$_{30}$-*b*-P(NB-*g*-PLA_{15})$_{100}$, **7**, [**3**]/[**4**]/[**1**] = 30:1:100) finished in *ca.* 7 min with 91% macromonomer conversion, and *ca.* 10 min with overall 91% macromonomer conversion, respectively. The chain extensions were verified by GPC analyses with observation of the consumption of macromonomer(s) and the shifts of the GPC traces from retention times of the macromonomers to the brush copolymer, **6**, and the diblock brush copolymer **7**, at increasingly shorter retention times, with less than 10% unreacted macromonomers remaining (figure 4.6). With the extents of macromonomer conversion being quite similar, we had suspected that residual macromonomers may lack the polymerizable NB α-chain terminus. However, MALDI-tof mass spectrometry confirmed that >98% of the PLA macromonomers possessed the NB group. We, therefore, attribute the *ca*. 90% macromonomer conversion to a combination of the *ca*.

2% lacking NB groups and *ca*. 5% NB groups being of the *endo* isomer, which is substantially less reactive toward ROMP. The molecular weights of the first block (M_n^{GPC} = 230 kDa) and second block (M_n^{GPC} = 400 kDa) measured by GPC equipped with a dynamic light scattering detector were close to the theoretical M_n values (first block: $M_n^{theo.}$ = 177 kDa; second block: $M_n^{theo.}$ = 373 kDa) (table 4.1). Moreover, the molecular weight distribution of the diblock brush copolymer remained monomodal and narrow. Next, with the polymerization times required to complete ROMP growth of the first (7 min) and second (10 min) blocks determined, we applied those time periods and investigated the synthesis of dumbbell-shaped brush copolymer by adding a third block macromonomer solution quickly into the polymerization mixture after the second block was constructed, without monitoring the reaction progress of each stage. After stirring at room temperature for 1 h, the third block was successfully chain extended to give **8**, as verified by the GPC peak shift to shorter retention time compared to **7**, high consumption of macromonomers with 91% total conversion, and agreement of theoretical molecular weight ($M_n^{theo.}$ = 550 kDa) and that measured by GPC (M_n^{GPC} = 660 kDa). The monomodal molecular weight distribution and low PDI of 1.14 indicated a well-defined structure for the dumbbell-shaped brush copolymer **8** (figure 4.6).

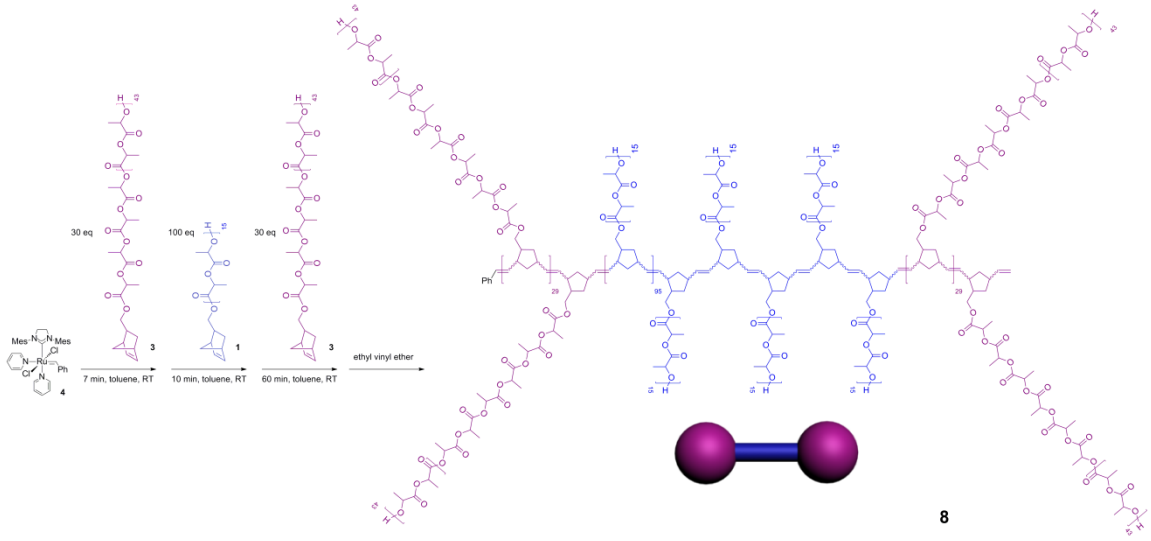

Figure 4.5. Synthesis of triblock molecular brush **8** by sequential addition of **3** and **1** *via* ROMP.

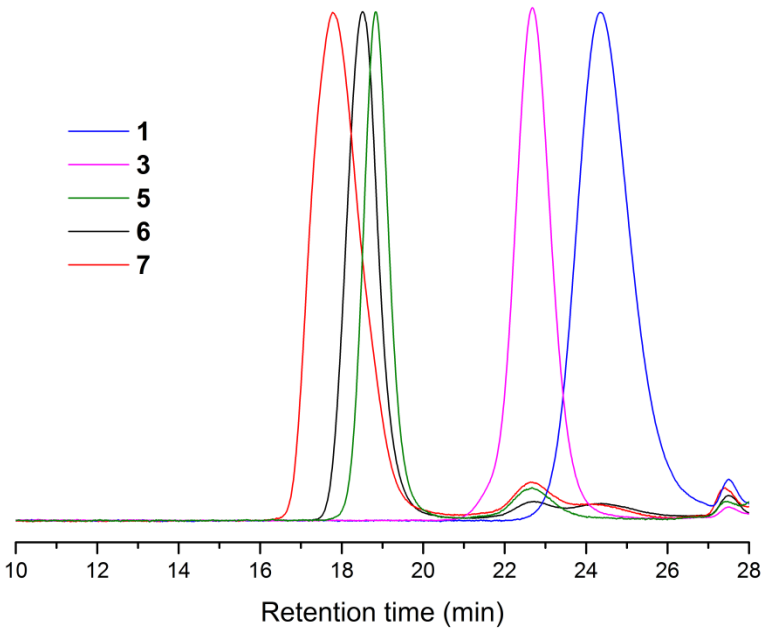

Figure 4.6. Representative GPC traces (RI detection) of macromonomers **1** and **3** after purification, and brush polymers **6**-**8** without purification.

To further demonstrate the versatility of making triblock brush copolymers by ROMP *via* macromonomer sequential additions, two more dumbbell-shaped brush copolymers: one with same size of "balls" but a shorter "bar" (P(NB-*g*-PLA_{45})$_{30}$-*b*-P(NB-*g*-PLA_{15})$_{60}$-*b*-P(NB-PLA_{45})$_{30}$, **9**), the other with same "bar" size but asymmetric "balls" (P(NB-*g*-PLA_{45})$_{30}$-*b*-P(NB-*g*-PLA_{15})$_{100}$-*b*-P(NB-PLA_{30})$_{30}$, **10**), were synthesized. The length of the backbone ("bar") was varied by alteration of the ratio of macromonomer to catalyst feed ([**1**]/[**4**]) during the second block growth, and the size of the "balls" was varied by alteration of the lengths of the macromonomers. These two triblock brush copolymers showed high macromonomer conversions, agreement of calculated and measured M_n values, and monomodal, narrow molecular weight distributions (table 4.1).

Table 4.1. Brush (block) copolymers **6**-**10**.

	Brush (co)polymers	[**3**]/[**4**]	[**1**]/[**4**]	[**3**]/[**4**]	[**2**]/[**4**]	conv[a]	M_n^{theo} (kDa)[b]	M_n^{GPC} (kDa)[c]	PDI
6	P(NB-*g*-PLA_{45})$_{30}$	30				91	177	230	1.04
7	P(NB-*g*-PLA_{45})$_{30}$-*b*-P(NB-*g*-PLA_{15})$_{100}$	30	100			91	373	400	1.08
8	P(NB-*g*-PLA_{45})$_{30}$-*b*-P(NB-*g*-PLA_{15})$_{100}$-*b*-P(NB-PLA_{45})$_{30}$	30	100	30		91	550	660	1.14
9	P(NB-*g*-PLA_{45})$_{30}$-*b*-P(NB-*g*-PLA_{15})$_{60}$-*b*-P(NB-PLA_{45})$_{30}$	30	60	30		91	471	583	1.10
10	P(NB-*g*-PLA_{45})$_{30}$-*b*-P(NB-*g*-PLA_{15})$_{100}$-*b*-P(NB-PLA_{30})$_{30}$	30	100		30	92	497	562	1.12

[a] Conversions of macromonomers were measured by comparing the peak areas of brush polymers and residual macromonomers of reaction mixture by GPC with RI detector. [b] Theoretical molecular weight, calculated from macromonomer to catalyst feed ratio × overall macromonomer conversion. [c] Determined by GPC using dual angle static light scattering detection.

Atomic force microscopy (AFM) is an effective characterization method to directly visualize molecular brushes. As shown in figure 4.7, AFM images of these three triblock brush copolymers revealed dumbbell-shaped macromolecular architectures with "balls" consisting of **2** or **3** and "bars" made of **1**. Specifically, for **8** (figure 4.7A, 4.7B), the width and length of the middle block were measured to be 18 $\pm$ 3 nm and 55 $\pm$ 9 nm, respectively, which are close to the calculated values (0.62 nm and 0.45 nm per monomeric unit for PNB backbone and PLA side chain, respectively), suggesting a fully extended conformation due to the densely-grafted side chains, as well as favorable interaction between the brush copolymers and mica substrate. The first and third blocks of **8** were of greater widths than was the central block. However, the measured widths, each of 34 $\pm$ 6 nm, were less than the theoretical value (*ca.* 41 nm) calculated for a fully extend conformation, which was attributed to less steric repulsion of side chains, as a result of a relatively small backbone DP value (DP = 30) compared to its side chains (DP = 45). For **9** (figure 4.7C), with decreased backbone DP value of the middle block, the "bar" had a length of 28 $\pm$ 6 nm with the "balls" sizes remaining similar to those of **8**. Moreover, for **10** (figure 4.7D), the third block, composed of **2**, had a width of 26 $\pm$ 3 nm, which correlated with the shorter PLA side chain length, compared to **3**.

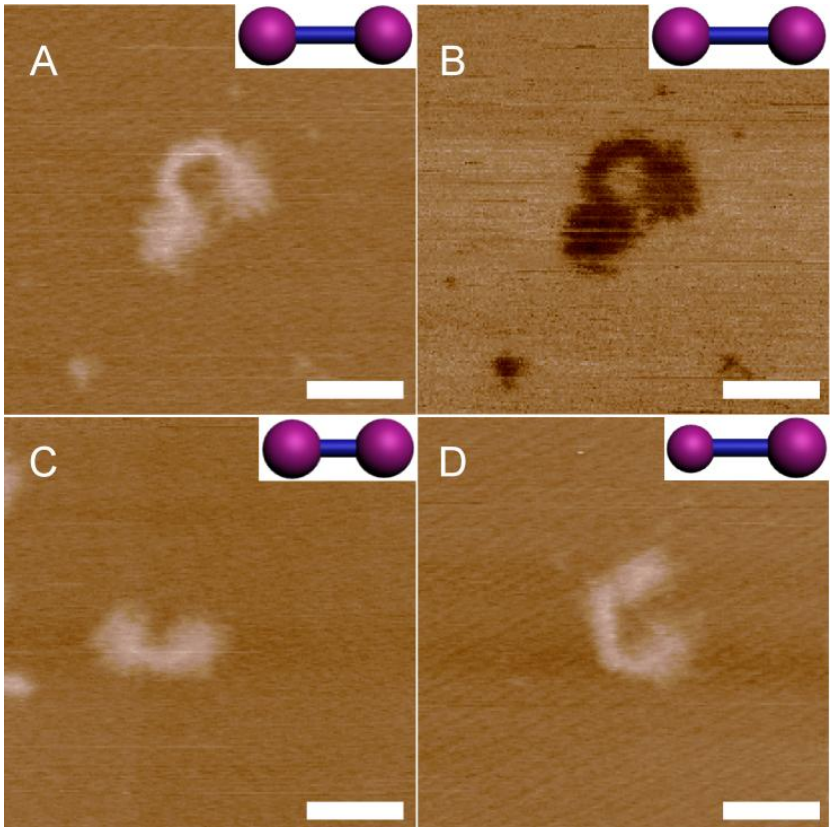

Figure 4.7. (A) AFM height image of **8**. (B) AFM phase image of **8**. (C) AFM height image of **9**. (D) AFM height image of **10**. (Samples were prepared by spin-casting dilute solutions onto freshly-cleaved mica, scale bar = 50 nm, z scale = 2 nm).

Partial dumbbell-shaped structures were also observed by AFM (figure 4.8 and figure 4.9). It was hypothesized that the partial dumbbells resulted from chain scission of the brush copolymer backbone, because fragments that could result only from breakage of the backbone were observed: single bars (figure 4.8) and broken dumbbells with pieces remaining in close proximity (figure 4.9). Chain scission could be caused by high bond tension generated from the repulsion of densely-grafted side chains on mica, a high surface energy substrate.[202,248] Although dense grafting and steric crowding along

vinylic polymer backbones has led to cleavage, chain scission has also been observed for cyclic brush copolymers having a polynorbornene backbone.[146] However, because there is overlap between the diblock and triblock brush chromatograms by GPC, we could not confirm that all of the partial dumbbells were the result of chain scissions. Having unevenly distributed side chains along the backbone, these dumbbell-shaped molecular brushes may be interesting materials to achieve structure-directed chain scission of grafted polymers on substrates or even in solution.

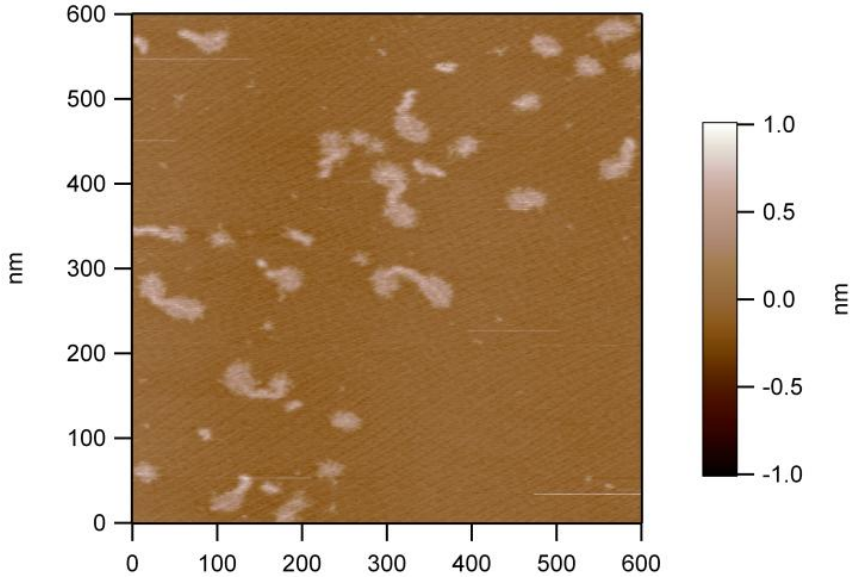

Figure 4.8. AFM height image of **8** showing coexistence of "intact" and "broken" dumbbells.

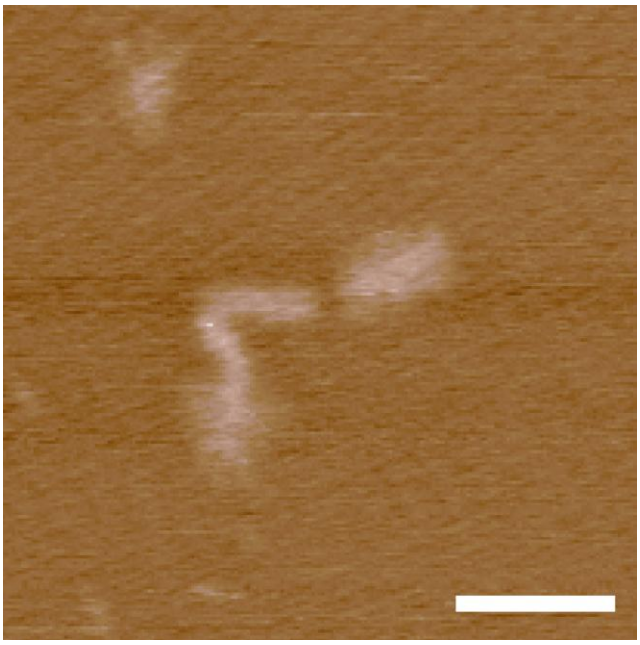

Figure 4.9. AFM height image of **8** showing chain scission occurred between first/third block and middle block. Scale bar = 50 nm.

4.3. Experimental Section

4.3.1. Materials

All Chemicals and reagents were purchased from Aldrich Chemical Co. and used as received, unless otherwise noted. DL-lactide was recrystallized twice from hexanes/ethyl acetate before use. Dichloromethane was distilled over CaH_2 and stored under N_2 before use. Toluene was purified by passage through solvent purification system (JC Meyer Solvent Systems) connected to a glove box without degassing before conducting ROMP. Modified 2nd generation Grubbs' catalyst ($(H_2IMes)(pyr)_2(Cl)_2RuCHPh$) was prepared according to reported method.[59]

4.3.2. Characterization methods

^{1}H NMR and ^{13}C NMR spectra were recorded on Varian Inova 300 MHz or Varian Mercury 300 MHz spectrometers interfaced to a UNIX computer using VnmrJ software. Chemical shifts were referred to the solvent resonance signals. IR spectra were recorded on an IR Prestige 21 system (Shimadzu Corp., Japan) and analyzed using IRsolution v. 1.40 software. Gel permeation chromatography (GPC) was performed on a Waters Chromatography, Inc., 1515 isocratic HPLC pump equipped with an inline degasser, a model PD2020 dual angle (15 ° and 90 °), static light scattering detector (Precision Detectors, Inc.), a model 2414 differential refractometer (Waters, Inc.), and four PL_{gel} polystyrene-*co*-divinylbenzene gel columns (Polymer Laboratories, Inc.) connected in series: 5 μm Guard (50 × 7.5 mm), 5 μm Mixed C (300 × 7.5 mm), 5 μm 10^4 (300 × 7.5 mm), and 5 μm 500 Å (300 × 7.5 mm) using the Breeze (version 3.30, Waters, Inc.) software. The instrument was operated at 35 °C with THF as eluent (flow rate set to 1.0 mL/min). Polymer solutions were prepared at a known concentration (*ca.* 3 mg/mL) and an injection volume of 200 μL was used. Data collection was performed with Precision Acquire 32 Acquisition program (Precision Detectors, Inc.) and analyses were carried out using Discovery32 software (Precision Detectors, Inc.) with a system calibration curve generated from plotting molecular weight as a function of retention time for a series of broad polydispersity poly(styrene) standards. Glass transition temperatures (T_g) were measured by differential scanning calorimetry on a Mettler-Toledo DSC822^e (Mettler-Toledo, Inc., Columbus, OH), with a heating rate of 10 °C /min. Measurements were analyzed using Mettler-Toledo Star^e v. 10.00 software. The

T_g was taken as the midpoint of the inflection tangent, upon the third heating scan. Thermogravimetric analysis was performed under N_2 atmosphere using a Mettler-Toledo model TGA/DSC 1, with a heating rate of 5 ℃/min. Measurements were analyzed using Mettler-Toledo Star^e v. 10.00 software. Atomic force microscopy (AFM) imaging was performed using a MFP-3D system (Asylum Research, Santa Barbara, CA) in tapping mode using standard silicon tips (SCANASYST-AIR, from Bruker, 115 μM, spring constant 0.4 N m^{-1}). Samples were prepared by spin casting dilute solutions (*ca.* 0.002 mg/mL) in chloroform onto freshly cleaved mica at 3000 rpm.

4.3.3. Representative procedure for the synthesis of NB-PLA macromonomers

A flame-dried 250-mL Schlenk flask equipped with a magnetic stir bar was charged with *exo*-5-norborene-2-methanol (1 eq.), DL-lactide (15-45 eq.), and dry dichloromethane (20 eq. to DL-lactide). The flask was sealed with a rubber septum and allowed to stir at room temperature for 20 min to ensure homogeneous mixing. Then, 1,8-diazabicyclo[5.4.0]-undec-7-ene (DBU, 1.2 eq.) was quickly added to the mixture to initiate the polymerization. After 15-45 min reaction time at room temperature, the reaction was quenched by adding several drops of acetic acid. The reaction was further stirred for 10 min before the reaction mixture was concentrated under vacuum. The polymer solution was precipitated from dichloromethane into cold methanol (3×) and dried under vacuum, overnight to yield a white solid. IR (cm^{-1}): 3495-3086, 3024-2916, 1743, 1450, 1365, 1265, 1188, 1080. ^{1}H NMR (300 MHz, $CDCl_3$, ppm) δ 6.09 (s, norbornenyl alkenyl protons), 5.25-5.06 (br, >C*H*CH_3 of PLA backbone), 4.14-3.96 (m, -C*H*$_2$OC(O)-) of NB group), 2.82 (s, 1H, allylic proton of NB group), 2.69 (s, 1H, allylic

proton of NB group), 1.67-1.45 (br, -CH_3 of PLA backbone), 1.40-1.13 (m, -C*H*< and >CHC*H*$_2$CH< of NB group). ^{13}C NMR (75 MHz, $CDCl_3$, ppm) δ 169.5, 136.9, 135.9, 68.9, 67.9, 66.7, 44.9, 43.4, 41.5, 37.9, 29.4, 16.5.

NB-PLA$_{15}$, 1. >99 % monomer conversion with 52 % isolation yield. $M_n^{theo.}$ = 2300 Da, M_n^{GPC} = 2000 Da, PDI = 1.20, T_g = 33 ℃, TGA in Ar: 220-360 ℃, 94% mass loss.

NB-PLA$_{30}$, 2. >99 % monomer conversion with 57 % isolation yield. $M_n^{theo.}$ = 4400 Da, M_n^{GPC} = 4700 Da, PDI = 1.11, T_g = 48 ℃, TGA in Ar: 260-390 ℃, 90% mass loss.

NB-PLA$_{45}$, 3. >99 % monomer conversion with 65 % isolation yield. $M_n^{theo.}$ = 6800 Da, M_n^{GPC} = 7000 Da, PDI = 1.10, T_g = 53 ℃, TGA in Ar: 270-390 ℃, 86% mass loss.

4.3.4. Representative procedure for the synthesis of triblock brush copolymers

In a glove box, toluene was added into vials containing pre-weighed macromonomer to yield solutions with macromonomer concentrations of *ca.* 100 mg/mL. A pre-determined amount of modified 2nd generation Grubbs' catalyst was added quickly into the vial of first block equipped with a stir bar. After *ca.* 7 min, the solution of second block was quickly added into the polymerization mixture, followed by the addition of solution of third block after 10 min. The reaction was allowed to stir for another 1 h, and quenched by adding several drops of ethyl vinyl ether (EVE). The brush polymer was precipitated into cold methanol twice and dried under vacuum overnight to yield a white powder. IR (cm^{-1}): 3510-3055, 3008-2924, 1751, 1450, 1357,

1180, 1080. ^{1}H NMR (300 MHz, CD_2Cl_2, ppm) δ 6.09 (s, norbornenyl alkenyl protons), 5.25-5.06 (br, >C*H*CH_3 of PLA backbone), 4.14-3.96 (m, -C*H*$_2$OC(O)-) of NB group), 2.82 (s, 1H, allylic proton of NB group), 2.69 (s, 1H, allylic proton of NB group), 1.67-1.45 (br, -CH_3 of PLA backbone), 1.40-1.13 (m, -C*H*$_3$ and >CHC*H*$_2$CH< of NB group). ^{13}C NMR (75 MHz, $CDCl_3$, ppm) δ 169.5, 136.9, 135.9, 68.9, 67.9, 66.7, 44.9, 43.4, 41.5, 37.9, 29.4, 16.5.

P(NB-*g*-PLA$_{45}$)$_{30}$-*b*-P(NB-*g*-PLA$_{15}$)$_{100}$-*b*-P(NB-PLA$_{45}$)$_{30}$, 8. 91 % macromonomer conversion with 77 % isolation yield. $M_n^{theo.}$ = 550 kDa, M_n^{GPC} = 660 kDa, PDI = 1.14, T_g = 52 ℃, TGA in Ar: 270-390 ℃, 73% mass loss, 390-450 ℃, 77% mass loss.

P(NB-*g*-PLA$_{45}$)$_{30}$-*b*-P(NB-*g*-PLA$_{15}$)$_{60}$-*b*-P(NB-PLA$_{45}$)$_{30}$, 9. 91 % macromonomer conversion with 76 % isolation yield. $M_n^{theo.}$ = 471 kDa, M_n^{GPC} = 583 kDa, PDI = 1.10, T_g = 53 ℃, TGA in Ar: 270-390 ℃, 75% mass loss, 390-450 ℃, 78% mass loss.

P(NB-*g*-PLA$_{45}$)$_{30}$-*b*-P(NB-*g*-PLA$_{15}$)$_{100}$-*b*-P(NB-PLA$_{30}$)$_{30}$, 10. 92 % macromonomer conversion with 75 % isolation yield. $M_n^{theo.}$ = 497 kDa, M_n^{GPC} = 562 kDa, PDI = 1.12, T_g = 52 ℃, TGA in Ar: 240-390 ℃, 71% mass loss, 390-450 ℃, 75% mass loss.

4.4. Conclusions

In summary, triblock dumbbell-shaped molecular brushes with well-defined structures were synthesized *via* "grafting-through" ROMP by sequential additions of macromonomers bearing terminal norbornene groups. The dimensions of both the

"balls" and the "bar" could be tuned, individually, by controlling the macromonomer sizes and the feeding ratios of side chains to catalyst, respectively. AFM characterization revealed the dumbbell-shaped architectures and allowed for direct measurements of the dimensions. With this strategy now demonstrated as a powerful methodology for the synthesis of multi-block brush copolymers, it can be applied to achieve various macromolecular architectures with tunable side chain compositions. In addition, by modification of the side chain termini, more advanced architectures can be derived. For instance, with the particular PLA materials employed here, their hydroxyl chain ends are easily modifiable to alter the surface of the molecular brushes, and their hydrolytic and enzymatic degradability could allow them to serve as bio-friendly materials or could be used as sacrificial domains to build up more complicated hollowed nanostructures, delivery vehicles, *etc*.

CHAPTER V

SYNTHESIS AND IN VIVO PHARMACOKINETIC EVALUATION OF DEGRADABLE SHELL CROSSLINKED POLYMER NANOPARTICLES WITH POLY(CARBOXYBETEINE) VS. POLY(ETHYLENE GLYCOL) SURFACE-GRAFTED COATINGS

5.1. Introduction

Over the past decade, nanoparticles have been increasingly employed as delivery vehicles for diagnostic and therapeutic applications, owing to the multifunctionality and multivalency.[152,153,249-254] For different biomedical applications, it is of paramount importance to control the pharmacokinetics and biodistribution of nanoparticles, which can be achieved through tuning their physicochemical properties, such as shapes, sizes, internal compositions, external surface charges and functionalities.[171,172,255-257] It's well known that nanoparticles are prone to be sequestrated by the mononuclear phagocyte system (MPS), which is triggered by the adsorption of plasma proteins onto nanoparticles.[170] Thus, "stealth" nanoparticles are needed to minimize the protein adsorption and avoid the MPS clearance. Currently, the most widely used strategy to empower nanoparticles with "stealthy" functions is grafting poly(ethylene glycol) (PEG), which is non-toxic, water-soluble and of low immunogenic response, onto the nanoparticle surface to prevent protein binding.[151,174,181] Although the mechanism is still controversial, studies suggested that it is the water barrier, created by strong hydrogen

bonding with water molecules from its ether groups that resists proteins from approaching the surface.

However, the PEG coating has been reported with disadvantages for *in vivo* applications, such as the lack of functional groups for post-modification, interference with cell uptake and endosome escape of nanoparticles, accelerated blood clearance after the second dose caused by immune responses, and the loss of biological activity of PEGylated therapeutic proteins.[177-179] Therefore, there have been continuous efforts to develop new materials, which are non-toxic, less immune-toxic, functionalizable and simple to synthesize, to outperform PEG. Among the many investigated materials, poly(zwitterions)s, especially poly(carboxybetaine)s (PCB) have attracted tremendous attention, due to its superior resistance to non-specific protein adsorption.[258-263] It was reported that PCB-grafted gold nanoparticles showed better *in vitro* stability than the PEGylated counterparts.[264] More importantly, the PCB coating could retain the bioactivity of the biomolecules, more effectively than could PEG, indicating the great potential of using PCB-modified nanoparticles for pre-clinical and translational research.[265-267]

Among various types of nanoparticles, shell crosslinked knedel-like (SCK) nanoparticles (SCK) have drawn particular attention, owing to the high loading capacity in the hydrophobic core and controlled payloads release from the hydrophilic shell, together with the unique attributes of stability and controlled shell transport that arise from the crosslinking.[160,268-272] Recently, we have developed a facile and efficient "pre-grafting" methodology to incorporate mPEG and (DOTA) chelator with quantitatively-

controlled densities onto SCKs for tunable *in vivo* pharmacokinetics and radiolabeling specific activities,[273,274] which therefore was employed in this study for PCB and PEG conjugation onto SCKs.

In the development of nanomaterials for personalized medicine, concerns have increased consistently on the *in vivo* fate, clearance, and toxicity of nanoparticles in nanomedicine health risk evaluation, which makes biodegradable polymeric nanoparticles the most attractive candidates for potential clinical applications. Poly(lactic acid) (PLA) is a commonly-used material for nanoparticle construction, largely because of its degradability *via* hydrolysis and biosafety of the degradation product, lactic acid.[275-277]

Driven by our interest in developing multivalent nanoparticles with controlled *in vivo* pharmacokinetics, while retaining high bioactivity for theranostic applications, a diblock amphiphilic copolymer poly(acrylic acid)-*b*-poly(lactide) (PAA-*b*-PLA) was grafted with PCB or PEG chains and sites for radiolabeling, assembled into micelles and shell crosslinked to prepare PLA-core degradable SCKs (dSCK). This robust "pre-grafting" strategy involved combinations of reversible addition-fragmentation chain transfer (RAFT) polymerization, ring-opening polymerization (ROP), supramolecular assembly and chemical conjugation. The degradability of dSCKs was analyzed with lactate assay. The *in vivo* biodistribution profiles of PCB- or PEG-conjugated dSCKs were tracked by ^{64}Cu radiolabeling through DOTA chelator conjugated within the PAA shell. Specifically, this work provides a new platform with tunable properties for nanoparticle translational research.

5.2. Results and Discussion

The amphiphilic diblock copolymer PAA_{75}-*b*-PLA_{33}, which served as the precursor to all of the dSCK materials, was obtained by sequential RAFT polymerization of *tert*-butyl acrylate (*t*BA) and ROP of lactide (LA), followed by acidolysis upon the treatment of trifluoroacetic acid (TFA). The order of two polymerizations was chosen to enable fine tuning of the hydrophobic PLA chain length, while maintaining the length of PAA segment constant. This combined RAFT polymerization and ROP required a bifunctional RAFT chain transfer agent (CTA) **1**, having a trithiocarbonate for RAFT polymerization and a terminal hydroxyl group that can facilitate ROP. The CTA was synthesized *via* esterification of 2-(dodecylthiocarbonothioylthio)-2-methylpropionic acid and 1,5-pentanediol, as shown in figure 5.1. Proton NMR spectroscopy of **1** showed a series of characteristic chemical shifts, including those of methylene protons adjacent to the ester group at 4.10 ppm, methylene protons next to the hydroxyl group at 3.63 ppm, and the methyl group from C12 chain of the CTA at 0.88 ppm, and the integration intensity ratios agreed with the theoretical values (see experimental section for details). The poly(*tert*-butyl acrylate) with a terminal hydroxyl group ($PtBA_{75}$-OH, **2**) was then afforded by RAFT polymerization of *t*BA by using **1** as the chain transfer agent, 2,2'-azobis(isobutyronitrile) (AIBN, 10 mol %) as the thermal radical initiator and 2-butanone (50 vol %) as the solvent at 56 °C, with the feed ratio of [*t*BA]:[**1**] = 100:1. The polymerization was quenched after 4.5 h when the monomer conversion was measured to be 75% by ^{1}H NMR spectroscopy. The well-defined structure of **2** was verified by gel permeation chromatography (GPC) analysis, with a monomodal

molecular weight distribution (MWD), a polydispersity index (PDI) of 1.12, and a number-average molecular weight (M_n^{GPC}) of 11000 Da, which is close to the theoretical molecular weight ($M_n^{theo.}$ = 10050 Da) calculated by ^{1}H NMR spectroscopy. The diblock copolymer, P*t*BA$_{75}$-*b*-PLA$_{33}$ (**3**) was afforded by chain extension of LA from macroinitiator **2** *via* 1,8-diazabicyclo[5.4.0]undec-7-ene (DBU)-catalyzed ROP in dichloromethane ([**2**]:[LA]:[DBU] = 1:38:1.2). The organo-catalyzed ROP was chosen to construct the PLA second block is due to the high initiation and polymerization efficiency at room temperature, as well as the absence of any metal contamination that might cause problems for ^{64}Cu radiolabeling (*vide infra*).[67,77] The polymerization was quenched after 1 h by adding several drops of acetic acid when monomer conversion was determined to be 85 % by ^{1}H NMR spectroscopy. The successful growth of the second block was verified by the observation of a complete shift of the GPC traces from the retention time of the first block **2**, to the diblock copolymer **3** at shorter retention time. The well-defined structure of the diblock copolymer was also confirmed by the good agreement between molecular weight determined by GPC to the theoretical value ($M_n^{theo.}$ = 14400 Da, M_n^{GPC} = 16200 Da), and a monomodal MWD and narrow PDI of 1.08. ^{1}H NMR spectroscopy further demonstrated the construction of the PLA block by comparing the integration ratio between methylene protons (2.36-2.13 ppm) from P*t*BA and methine protons (5.23-5.10 ppm) from PLA. Complete removal of the *tert*-butyl groups of **3** was achieved by TFA treatment for 2 h at room temperature, affording the amphiphilic diblock copolymer PAA$_{75}$-*b*-PLA$_{33}$, **4**.

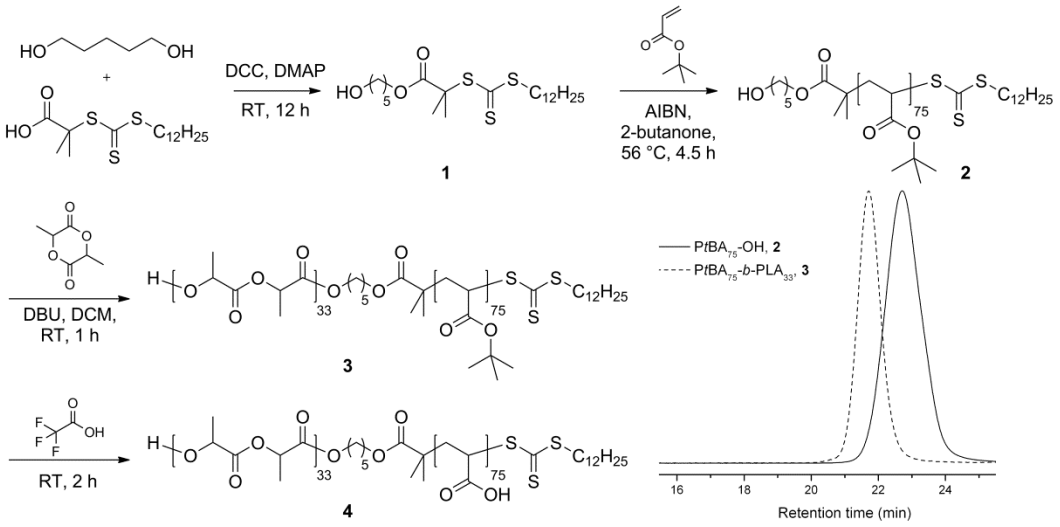

Figure 5.1. Synthetic scheme for the preparation of amphiphilic diblock copolymer PAA_{75}-*b*-PLA_{33}, **4**, and GPC traces of intermediates P*t*BA_{75}-OH, **2**, and P*t*BA_{75}-*b*-PLA_{33}, **3**.

By simple amidation, polymer grafts as well as small molecule moieties with primary amine groups can be incorporated onto PAA. In order to prepare dSCKs with comparable molecular weight PEGs and PCBs as polymer grafts, monoamine-functionalized PCB samples having molecular weights (MW) of 2 kDa and 5 kDa, equivalent MW to commercially-available monoamine-functionalized, methoxy-terminated poly(ethylene glycol) (2 kDa and 5 kDa), were synthesized by RAFT polymerizations. A similar PCB polymer with a terminal amine group was reported by Jiang *et al.* by applying atom transfer radical polymerization (ATRP) of 2-*tert*-butoxy-*N*-(2-(methacryloxy)ethyl)-*N,N'*-dimethyl-2-oxoethanaminium bromide (CB-*t*Bu monomer) with 2-aminoethyl 2-bromoisobutyrate trifluoroacetate as the initiator, and 1,1,4,7,10,10-hexamethyltriethylenetetramine (HMTETA)/CuBr as the catalyst.[262] However, in our study, any trace amount of copper salt impurities might cause

inefficient radiolabeling of ^{64}Cu, thus, in order to overcome the potential issue of metal contamination, we chose RAFT polymerization to construct PCB grafts with terminal amine groups to be used as polymer grafts. Our initial model study showed that RAFT polymerization of *N*-(2-(acryloyloxy)ethyl)-2-(*tert*-butoxy)-*N,N*-dimethyl-2-oxoethanaminium bromide with **1** as the chain transfer agent, AIBN as the initiator, *N,N*-dimethylformamide (DMF) as the solvent at 70 °C could afford well-defined PCB polymers with controllable MWs, however conjugation of the hydroxyl group-terminated PCB grafts onto PAA-*b*-PLA copolymer was not successful, due to the relatively low reaction efficiency of esterification compared to amidation. To introduce terminal primary amine groups into PCBs, we designed and synthesized a functionalized RAFT chain transfer agent, 2-aminoethyl-2-(dodecylthiocarbonothioylthio)-2-methylpropanoate trifluoroacetate (**5**), by esterification between 2-(dodecylthiocarbonothioylthio)-2-methylpropionic acid and *N*-(*tert*-butoxycarbonyl) ethanolamine, followed by TFA treatment (figure 5.2). The structure was confirmed by ^{1}H NMR, ^{13}C NMR, and IR spectroscopies, and high-resolution mass spectrometry. The RAFT polymerizations were conducted under optimized conditions, [**5**]:[monomer] = 1:20, in DMF at 70 °C. The polymerizations were quenched after 0.7 h and 3 h, after monomer conversions had reached 40 % and 90 %, respectively. The well-defined structures of PCBs (**6**: 2 kDa PCB; **7**: 5 kDa PCB) were confirmed by GPC analyses showing monomodal MWDs and narrow PDIs of 1.16 for **6** and 1.08 for **7**, respectively (figure 5.2). The well-controlled characteristic was also confirmed by the agreement of the degree of polymerization (DP) values that were calculated from monomer conversion

and chain end analysis integration ratio of the methyl protons resonating at 0.88 ppm from the C12 chain of the CTA unit *vs.* the acrylate methylene protons α- to the ammonium group (-$CH_2N(CH_3)_2C\boldsymbol{H_2}CH_2OOC$-) observed at 4.20-3.87 ppm by ^{1}H NMR spectroscopy.

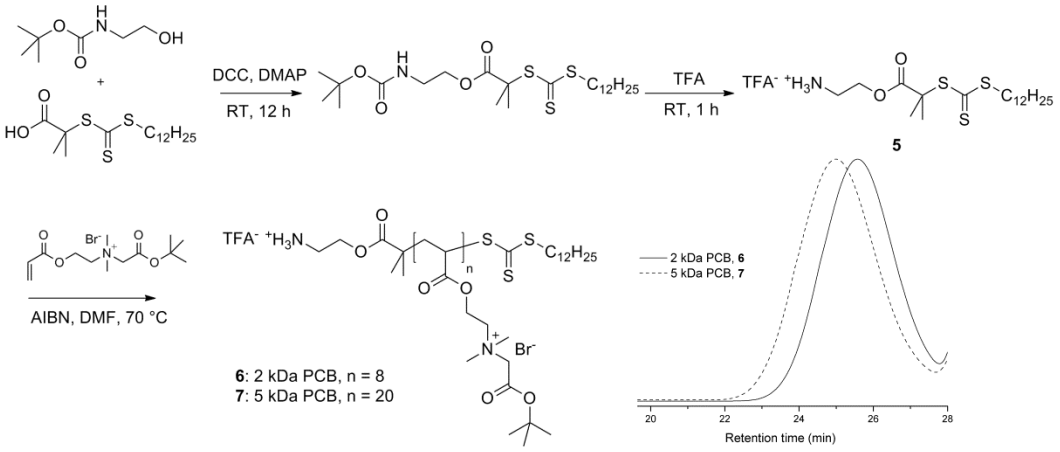

Figure 5.2. Synthetic scheme and GPC traces of poly(carboxybetaine) (PCB) grafts, **6** and **7**.

To minimize the water exposure time, which may cause premature hydrolysis of the PLA segment, conjugations of 2-aminoethyl-mono-amide-DOTA-tris(*t*-Bu ester), tyramine, mPEG-NH_2 (2 kDa and 5 kDa) or PCB-NH_2 (**6** and **7**) were conducted in a one-step manner by standard amidation chemistry in DMF at room temperature, as shown in figure 5.3. DOTA was selected as the chelator for ^{64}Cu because of its FDA approval and broad applications in clinical trials,[278] and tyramine is well-known to be labeled effectively by radioactive halogens.[279,280] The amounts of functional moieties were controlled by adjusting the stoichiometry of each molecule relative to **4**. The actual

incorporation of each unit was determined by ^{1}H NMR spectroscopy, by calculating from the integrals corresponding to characteristic protons from each unit. It should be noted, however, that the conjugates of **4** with PCB grafts exhibited poor solubility in DMF, DMSO and water, probably due to strong electrostatic interactions between PAA carboxylic acid groups and the PCB quaternary ammonium groups, thus no characterization was performed before the following deprotection step. The *tert*-butyl groups of the DOTA units and PCB grafts were subsequently removed by acidolysis, upon treatment with TFA. The polymers after deprotection were purified by dialysis against nanopure water followed by lyophilization, affording PEG-grafted block terpolymers **8**, **9**, and **10**, with five PEG of 2 kDa MW (5 PEG2k), five PEG grafts of PEG 5 kDa (5 PEG5k), and ten PEG grafts of 5 kDa (10 PEG5k), respectively, and PCB-grafted block terpolymers **11** and **12**, with five PCB grafts of 2 kDa and 5 kDa (5 PCB2k and 5 PCB5k), respectively.

The overall strategy for the preparation of the series of dSCKs, having variable lengths and densities of PEG or PCB surface grafts is illustrated in figure 5.4. A rapid, direct dissolution method was applied to prepare micelles from the grafted block terpolymer precursors, **8**-**12**, to avoid hydrolysis of PLA, as may occur during the conventional solvent displacement method that involves relatively long water exposure times. To facilitate radiolabeling, 1.0 mg/mL micelle solutions were prepared by directly dissolving each polymer precursor (**8**-**12**) into nanopure water, followed by extensive stirring for 2 h. Then, the dSCKs were obtained by crosslinking of the hydrophilic shell domain through amidation of approximately 20% of the hydrophilic

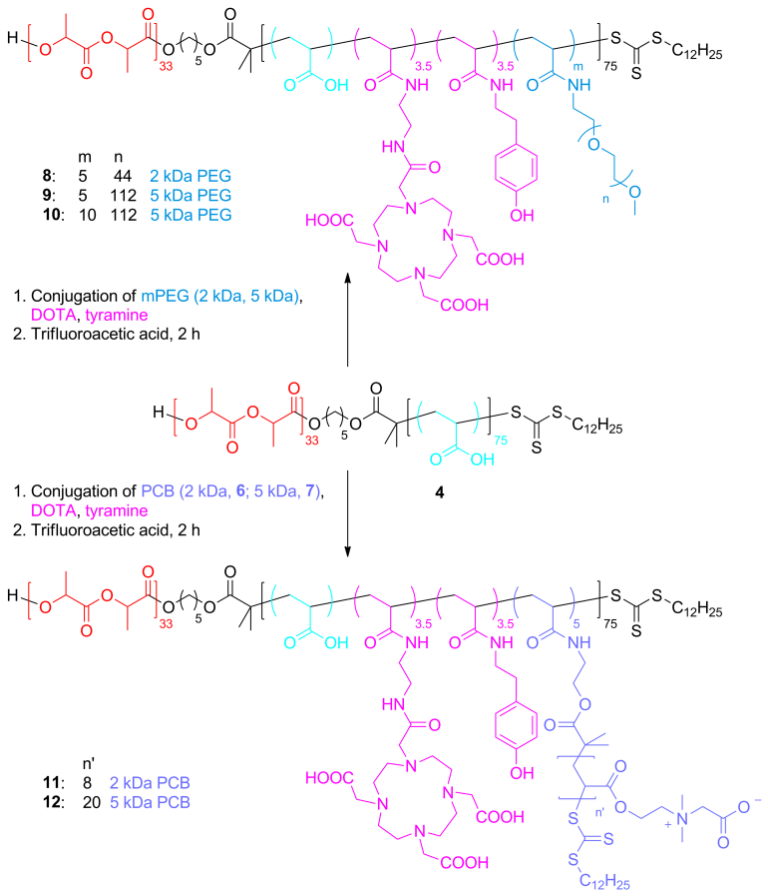

Figure 5.3. Synthetic scheme of grafted polymers **8-12**.

shell domain through amidation of approximately 20% of the carboxylic acid groups by reaction with crosslinker 2,2'-(ethylenedioxy) bis(ethylamine) (EDDA), followed by purification by dialysis overnight. The dSCKs were characterized by transmission electron microscopy (TEM), dynamic light scattering (DLS) and zeta potential (ζ-potential) measurements. As shown in table 5.1, each **dSCK1-5** displayed < 100 nm size, as measured in the dry state by TEM and in aqueous solution by DLS (number average) (figure 5.5). Moreover, with increased PEG chain length from 2 kDa (**dSCK1**) to 5 kDa (**dSCK2**) the ζ-potential increased from -41 mV to -28 mV, and with further

increased density of 5 kDa PEG to 10 per polymer chain (**dSCK3**), the ζ-potential slightly increased to -25 mV. This trend indicated that increasing the length and density of the PEG grafts, more effectively shielded the negative charge character of the PAA shell, driving the ζ-potential of the dSCK nanoparticles closer to neutral. In contrast to the shielding effects from PEG, zwitterionic PCB grafts provided the dSCKs (**dSCK4** and **dSCK5**) with strong negatively-charged characteristic, which is in agreement with reported results.[262]

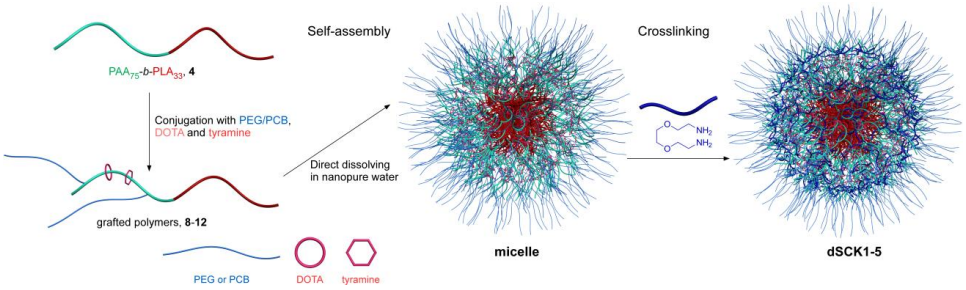

Figure 5.4. A schematic illustration for the overall strategy for the preparation of degradable SCK (dSCK) by self assembly of multifunctional block graft polymers **8-12** into micelles, followed by crosslinking to afford **dSCK1-5**, having different lengths and number of PEG *vs.* PCB grafts per block copolymer chain to afford different PEG *vs.* PCB surface coverage of the dSCKs.

Table 5.1. Physicochemical properties, ^{64}Cu radiolabeling specific activity of **dSCK1-5.**

Polymer precursor	**dSCK1** **8**	**dSCK2** **9**	**dSCK3** **10**	**dSCK4** **11**	**dSCK5** **12**
Polymer grafts	5 × PEG2k	5 × PEG5k	10 × PEG5k	5 × PCB2k	5 × PCB5k
D_h (nm)[a]	40 ± 2	30 ± 9	32 ± 9	29 ± 8	65 ± 19
Diameter (nm)[b]	18 ± 3	15 ± 4	14 ± 4	16 ± 4	32 ± 6
Zeta potential (mV)	-41 ± 4	-28 ± 3	-25 ± 4	-50 ± 5	-58 ± 4
^{64}Cu Specific Activity (μCi/μg)	105.5	154.9	79.2	81.8	139.0

[a] measured by DLS, number average, [b] measured by TEM.

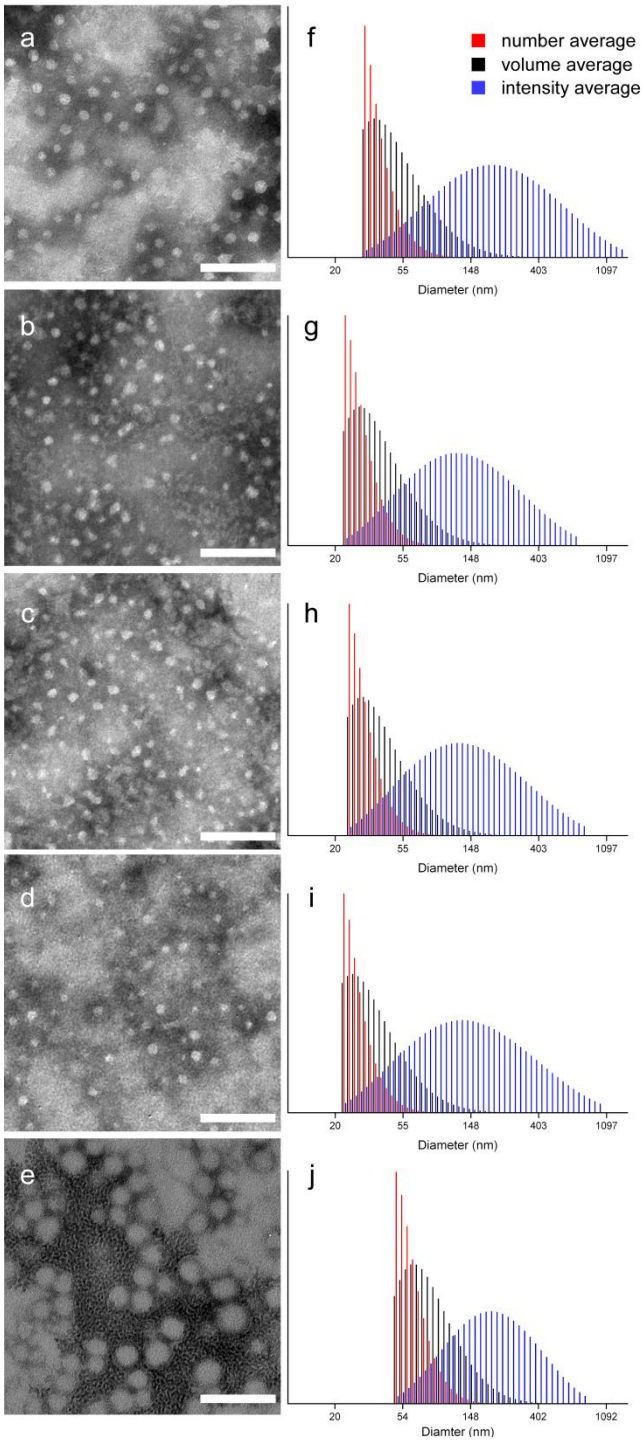

Figure 5.5. Left column: TEM images of (a) **dSCK1**; (b) **dSCK2**; (c) **dSCK3**; (d) **dSCK4**; (e) **dSCK5**. Right column: DLS histograms of (f) **dSCK1**; (g) **dSCK2**; (h) **dSCK3**, (i) **dSCK4**; (j) **dSCK5**. Scale bar = 100 nm.

Nanoparticle stability in serum is an important criterion for their *in vivo* biomedical applications. By monitoring the hydrodynamic diameter changes for the dSCKs over time in the presence of 10% bovine serum albumin (BSA), we investigated the stabilities of **dSCK1-5** with PEG or PCB grafts in 10 % BSA solution at 37 °C. As shown in figure 5.6, all of the dSCKs were stable over 12 h with only slight changes of their sizes, except for **dSCK5**, which exhibited *ca.* 15 % size increase. The subtle instability behavior of the nanoparticle presenting the longer PCB chains is under further investigation to determine the potential causes and biological effects *in vitro* and *in vivo*. Overall, the results are consistent with a previous study that found that both the presence of PEG and PCB could inhibit protein adsorption onto nanoparticles, which can potentially extend the blood circulation time.

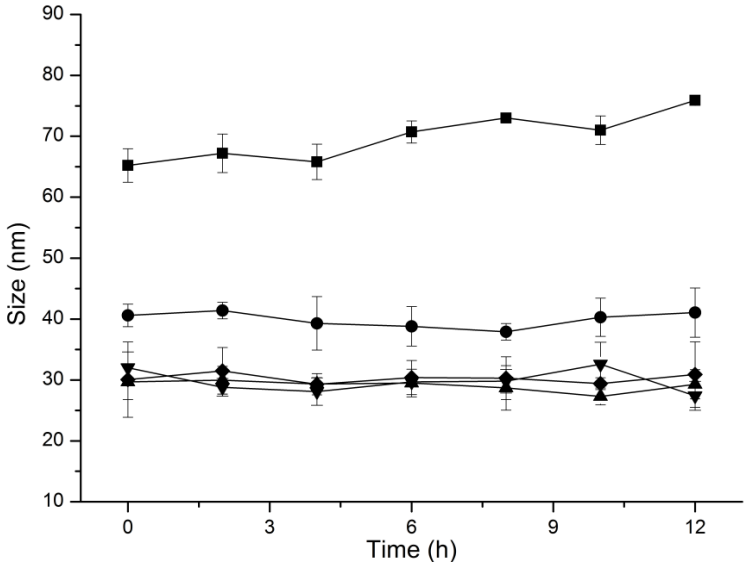

Figure 5.6. **dSCK1-5** *in vitro* size stability measured by DLS in triplicate in 10 % bovine serum albumin (BSA) solution at 37 ℃. (●) **dSCK1**; (♦) **dSCK2**; (▲) **dSCK3**; (▼) **dSCK4**; (■) **dSCK5**.

To evaluate the degradability of dSCKs, we studied the degradation of the dSCKs at 37 °C in pH 7.4 and pH 5.0 PBS, which represent physiological pH and endosomal/lysosomal or tumor tissue pH, respectively. The degradation was measured by the production of lactic acid, which is the final degradation molecule resulting from the hydrolysis of PLA, using a commercially-available lactate assay tool kit. As shown in figure 5.7, after 15 days both PEG-grafted and PCB-grafted dSCKs showed certain extents of LA production, with PCB-grafted dSCKs having faster degradation than the PEG-grafted dSCKs. More specifically, at pH 7.4, **dSCK1** and **dSCK4** having 5 PEG2k and 5 PCB2k per polymer chain, underwent 10% and 19% LA release; with 5 PEG5k grafted **dSCK2** and 5 PCB5k grafted **dSCK5**, 14% and 22% LA release was observed, respectively. We propose that the differences in degradation rates originated from the nature of PEG and PCB. PEG obtains its water solubility from the ability of binding water molecules by hydrogen bonding of its ether groups, while zwitterionic PCB, bearing both positive and negative charges, gains the non-fouling property by strong ionic structuring of water molecules, which may transfer water-soluble molecules, such as lactic acid and oligo-PLA faster than PEG, resulting in faster degradation of the PLA core or the release of the degradation product out of the dSCKs. In addition, dSCKs with longer polymer grafts (**dSCK2** *vs*. **dSCK1**; **dSCK5** *vs*. **dSCK4**) or higher density of polymer grafts on the shell (**dSCK3** *vs*. **dSCK2**) showed more LA release over 15 days. With similar trend of degradation profiles at pH 7.4, the LA release in PBS 5.0 buffer was slower, which was probably due to a combination of factors, such as slower release of oligo-PLA from the core through the crosslinked PAA-based shell barrier and

slower hydrolysis of PLA inside/outside the core region. Slower rates of PLA hydrolysis within the pH range of *ca*. 5 have been reported for hydrophobic PLA bulk samples and surface grafts.[281-284] In addition, the extents of swelling under pH 7.4 and pH 5.0 might be another factor, which accounts for the different rates in core PLA hydrolysis.[285] The differences in degradation rates for these core-shell dSCK nanoparticles having PCB *vs*. PEG surface grafts and under physiological *vs*. acidic pH may be utilized to control the release of imaging or therapeutic payloads.

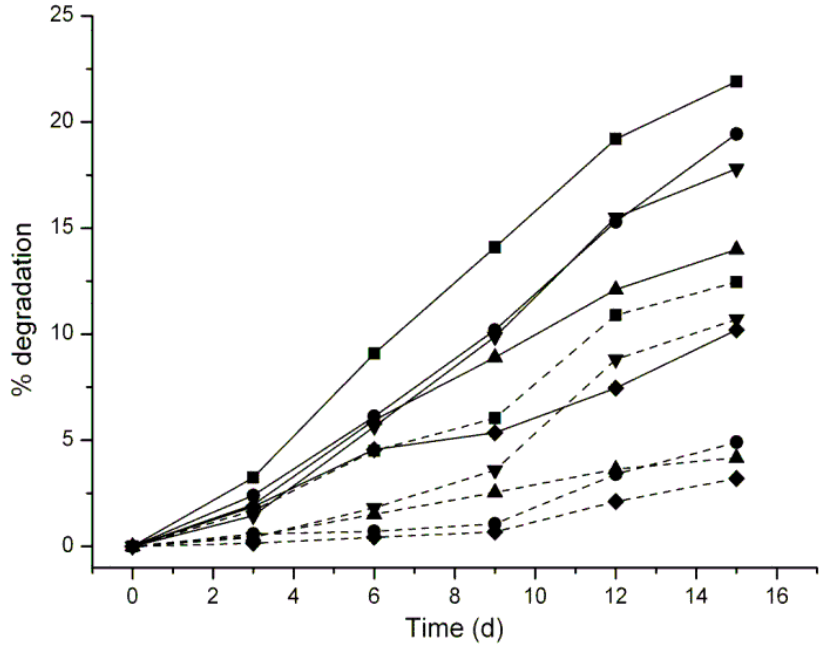

Figure 5.7. *In vitro* degradation of dSCKs in PBS pH = 7.4 buffer (solid lines) and PBS pH = 5.0 buffer (dashed lines) measured by lactate assay. (♦) **dSCK1**; (▲) **dSCK2**; (▼) **dSCK3**; (●) **dSCK4**; (■) **dSCK5**

We next studied the ^{64}Cu radiolabeling efficiency of dSCKs. All the dSCKs could be labeled with high specific activity through the DOTA chelator on the PAA shell (table 5.1). Serum stability studies showed that after size exclusion column purification, **dSCK1-5** had high (> 95%) radiochemical purity. During the 24 h incubation with mouse serum, there was almost no decrease of radiochemical purity for each individual dSCK. All the radiochemical purities of the ^{64}Cu-dSCKs were still more than 93%, as shown in figure 5.8.

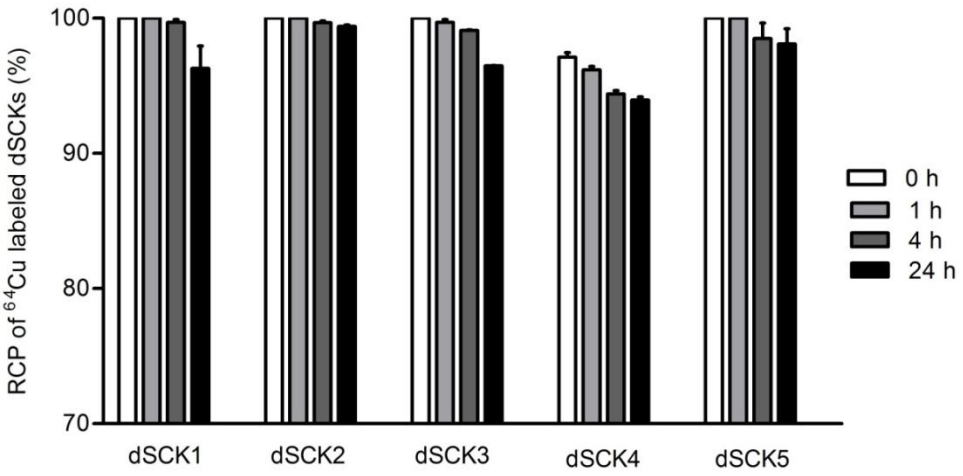

Figure 5.8. The radiochemical stability of ^{64}Cu-dSCKs in mouse serum at 45 ℃.

The effect of PEG chain length grafted to dSCKs on their *in vivo* pharmacokinetics is clearly depicted in figure 5.9. With the increasing MW of PEG from 2 kDa to 5 kDa, the blood retention of **dSCK2** was significantly ($p<0.05$, $n=4$) enhanced at each individual time point in contrast to **dSCK1** (3 fold at 1 h, 6 fold at 4 h and 24 h). The hepatic and splenic accumulations were both greatly reduced, while the

kidney clearance was increased at the same time. Interestingly, the bone and gastrointestinal (GI) tract (stomach and intestine) uptakes of **dSCK2** were also elevated during the study, reasonably due to the increased blood retention. However, the further increase of number of 5 kDa PEG from 5 to 10 per dSCK polymer precursor chain did not enhance the blood retention proportionally. As shown in figure 5.8, the biodistribution of **dSCK3** was very similar to that of **dSCK2**, with a slightly better renal clearance.

Although **dSCK1** (2 kDa PEG) and **dSCK4** (2 kDa PCB) had different surface coatings, they had similar physicochemical properties, including size and surface charge. The pharmacokinetic evaluation displayed similar initial blood retention with about 10%ID/g at 1 h post injection in C57BL/6 mice (figure 5.10). However, the 2 kDa PEG grafted **dSCK1** had a faster clearance, leading to a quick drop of blood retention to less than half of that obtained with 2 kDa PCB conjugated **dSCK4** at 4 h p.i. Also, the MPS accumulations (liver and spleen) of **dSCK1** were all significantly ($p<0.05$, $n=4$) higher than those acquired with **dSCK4**, although both particles maintained constant MPS uptakes during the 24 h study. Interestingly, in contrast to the main hepatic and splenic clearance of **dSCK1**, the major excretion pathway for **dSCK4** was through kidney (>16% ID/g at 24 h). Further, both particles had similar distributions in other organs, including bone and gastrointestinal (GI) tract (figure 5.10).

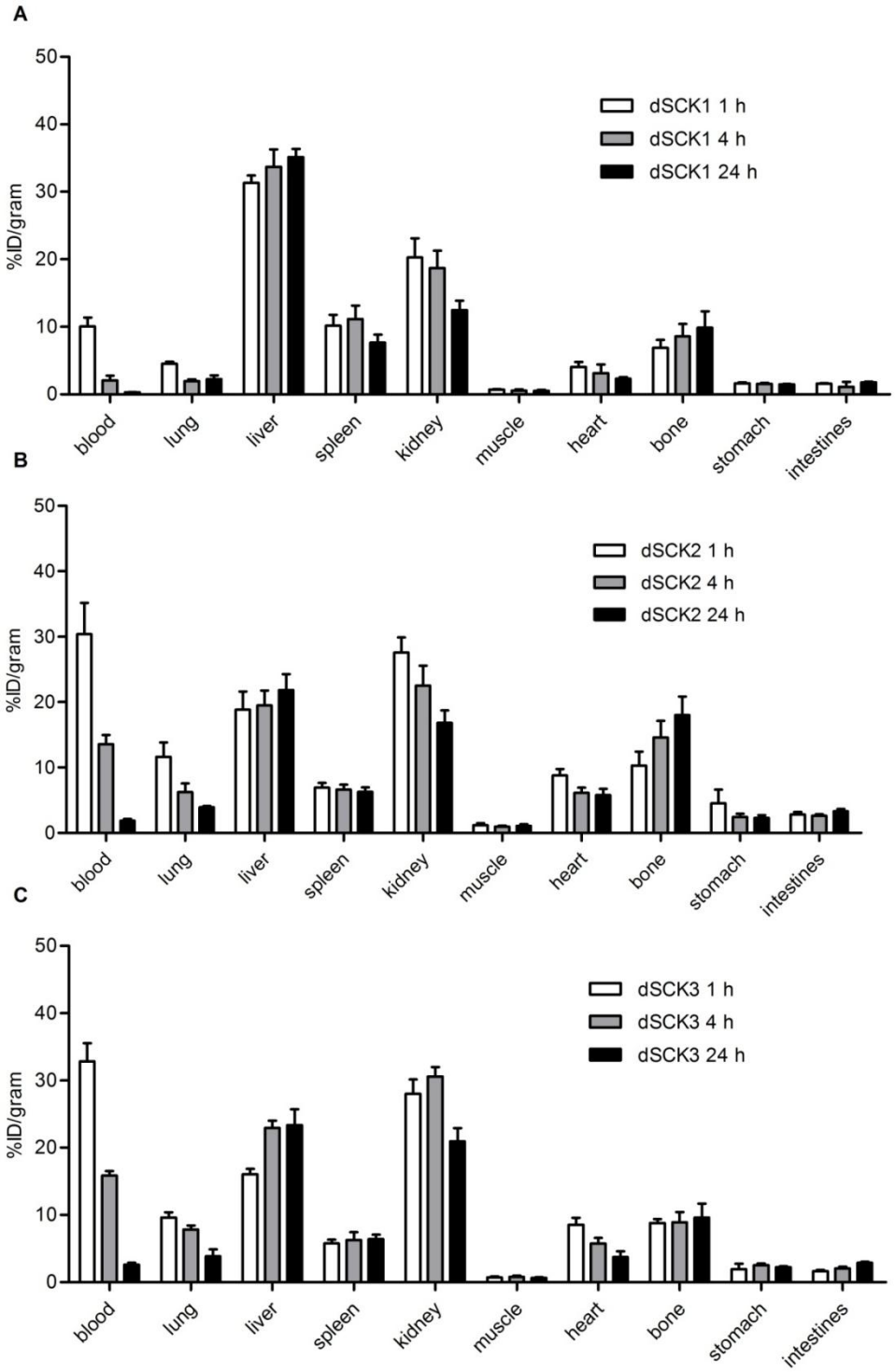

Figure 5.9. Biodistributions of (A) **dSCK1**, (B) **dSCK2**, and (C) **dSCK3**.

In contrast to **dSCK4**, the 5 kDa PCB grafted **dSCK5** showed greatly improved blood retention at 1 h although its size was about twice big as **dSCK4**. However, it rapidly dropped to a level similar to **dSCK4** at later time points (4 h and 24 h). The liver accumulations were slightly higher, while the spleen uptakes were very similar. Also, the kidney clearance was significantly ($p<0.05$, $n=4$) decreased during the 24 h period, reasonably owing to the size effect.

Compared to **dSCK5**, **dSCK2** had extended blood pool retention including blood, lung and heart, comparable liver and spleen accumulations, but enhanced kidney clearance. Again, this could be due to the effect of **dSCK5**'s size. Interestingly, consistent with the comparison between **dSCK1** and **dSCK4**, the bone uptake for **dSCK2** increased over time and was significantly ($p<0.05$, $n=4$) higher than that acquired with **dSCK4** at 4 h and 24 h p.i.

5.3. Experimental Section

5.3.1. Instrumentation

^{1}H NMR and ^{13}C NMR spectra were recorded on Varian Inova 300 MHz or Varian Mercury 300 MHz spectrometers interfaced to a UNIX computer using VnmrJ software. Chemical shifts were referred to the solvent resonance signals. IR spectra were recorded on an IR Prestige 21 system (Shimadzu Corp., Japan) and analyzed using IRsolution v. 1.40 software.

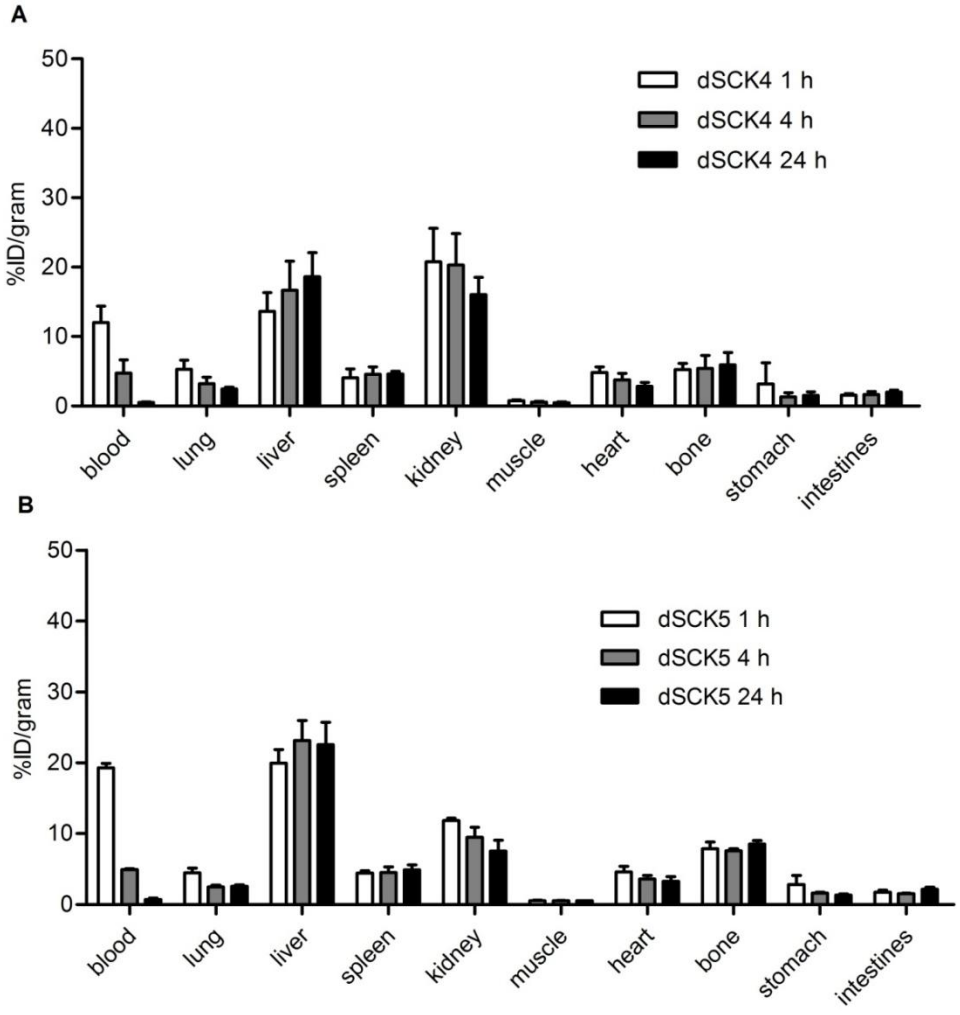

Figure 5.10. Biodistributions of (A) **dSCK4** and (B) **dSCK5**.

Tetrahydrofuran (THF) Gel permeation chromatography (GPC) was performed on a Waters Chromatography, Inc., 1515 isocratic HPLC pump equipped with an inline degasser, a model 2414 differential refractometer (Waters, Inc.), and four PLgel polystyrene-*co*-divinylbenzene gel columns (Polymer Laboratories, Inc.) connected in series: 5 μm Guard (50 × 7.5 mm), 5 μm Mixed C (300 × 7.5 mm), 5 μm 10^4 (300 × 7.5 mm), and 5 μm 500 Å (300 × 7.5 mm) using the Breeze (version 3.30, Waters, Inc.)

software. The instrument was operated at 35 °C with THF as eluent (flow rate set to 1.0 mL/min). Polymer solutions were prepared at a concentration of *ca*. 3 mg/mL and an injection volume of 200 μL was used. The system was calibrated with polystyrene standards (Polymer Laboratories, Amherst, MA). The DMF gel permeation chromatography (GPC) was conducted on a Waters Chromatography, Inc. (Milford, MA) system equipped with an isocratic pump model 1515, a differential refractometer model 2414, and a four-column set of 5 μm Guard (50 × 7.5 mm), Styragel HR 4 5 μm DMF (300 × 7.5 mm), Styragel HR 4E 5 μm DMF (300 × 7.5 mm), and Styragel HR 2 5 μm DMF (300 × 7.5 mm). The system was equilibrated at 70 °C in prefiltered DMF containing 0.05 M LiBr, which served as polymer solvent and eluent (flow rate set to 1.00 mL/min). Polymer solutions were prepared at a concentration of *ca*. 3 mg/mL and an injection volume of 200 μL was used. Data collection and analysis were performed with Empower 2 v. 6.10.01.00 software (Waters, Inc.). The system was calibrated with poly(ethylene glycol) standards (Polymer Laboratories, Amherst, MA).

Glass transition temperatures (*T*g) were measured by differential scanning calorimetry on a Mettler-Toledo DSC822^e (Mettler-Toledo, Inc., Columbus, OH), with a heating rate of 10 ℃ /min. Measurements were analyzed using Mettler-Toledo Star^e v. 10.00 software. The T_g was taken as the midpoint of the inflection tangent, upon the third heating scan. Thermogravimetric analysis was performed under N_2 atmosphere using a Mettler-Toledo model TGA/DSC 1, with a heating rate of 5 °C/min. Measurements were analyzed using Mettler-Toledo Star^e v. 10.00 software.

TEM samples were prepared by depositing *ca.* 5 μL of sample to carbon coated copper grids. Excess sample was wicked off using filter paper and the grids were allowed to dry in air for 10 min. The grids were then stained with 5 μL of 1% phosphotungstic acid (PTA) and excess stain was wicked off using filter paper. Specimens were observed on a JEOL 1200EX transmission electron microscope operating at 100 kV and micrographs were recorded at calibrated magnifications using an SIA-15C CCD camera. The number-average particle diameters (D_{av}) and standard deviations were generated from the analysis of particles from at least two different micrographs.

Dynamic light scattering (DLS) measurements were conducted using Delsa Nano C from Beckman Coulter, Inc. (Fullerton, CA) equipped with a laser diode operating at 658 nm. Size measurements were made in water (n = 1.3329, η = 0.890 cP at 25 ± 1 °C; n = 1.3293, η = 0.547 cP at 50 ± 1 °C; n = 1.3255, η = 0.404 cP at 70 ± 1 °C). Scattered light was detected at 165° angle and analyzed using a log correlator over 70 accumulations. The photomultiplier aperture and the attenuator were automatically adjusted to obtain a photon counting rate of *ca.* 10 kcps. The calculations of the particle size distribution and distribution averages were performed using CONTIN particle size distribution analysis routines. The samples in the glass sizing cell were equilibrated at the desired temperature for 5 min before measurements were made. The peak average of histograms from intensity, volume, or number distributions out of 70 accumulations was reported as the average diameter of the particles. The particle zeta potentials were determined by a Delsa Nano C particle analyzer (Beckman Coulter. Fullerton, CA)

equipped with a 30 mW dual laser diode (658 nm). The zeta potential of the particles in suspension was obtained by measuring the electrophoretic movement of charged particles under an applied electric field. Scattered light was detected at a 30 ° angle at 25 ℃. The zeta potential was measured at five regions in the flow cell and a weighted mean was calculated. These five measurements were used to correct for electroosmotic flow that was induced in the cell due to the surface charge of the cell wall. All determinations were repeated 5 times.

5.3.2. Materials

All Chemicals and reagents were purchased from Aldrich Chemical Co. and used as received, unless otherwise noted. *Tert*-butyl acrylate was passed through a neutral alumina column to remove the inhibitor before use. *2,2′*-Azobis(isobutyronitrile) (AIBN) was recrystallized twice from methanol before use. Lactide was recrystallized twice from hexanes/ethyl acetate before use. Dichloromethane (CH_2Cl_2) was distilled over CaH_2 and stored under N_2 before use. The lactate colorimetric assay kit (ab65331) was purchased from Abcam®. 2-Aminoethyl-mono-amide-DOTA-tris(*t*-Bu ester) was purchased from Macrocyclics, Inc. Monoamine-functionalized, methoxy-terminated poly(ethylene glycol)s were purchased from Rapp Polymere. The Spectra/Por dialysis membrane tubes were purchased from Spectrum Medical Industries Inc. Nanopure water (18 MΩ·cm) was acquired by means of a Milli-Q water filtration system, Millipore Corp. (Bedford, MA).

5.3.3. 5-hydroxypentyl 2-(dodecylthiocarbonothioylthio)-2-methylpropanoate (1)

To a 250 mL RB flask equipped with a stir bar was placed 2-(dodecylthiocarbonothioylthio)-2-methylpropionic acid (3.08 g, 8.45 mmol), 1,5-pentanediol (4.28 g, 41.1 mmol) and 4-(dimethylamino)pyridine (0.205 g, 1.67 mmol). Dry THF (50 mL) was then added into the flask to dissolve all reagents followed by dropwise addition of a solution of *N,N′*-dicyclohexylcarbodiimide (2.05 g, 9.85 mmol) in THF. The reaction mixture was allowed to stir at room temperature for 12 h. The solid was removed by filtration, and the filtrate was concentrated under vacuum and purified by silica gel flash chromatography eluting with ethyl acetate/hexanes (1:2). The product was afforded as a yellow oil. Yield: 62%. IR (cm^{-1}): 3547-3180, 2921, 2848, 1728, 1458, 1381, 1258, 1157, 1126, 1064, 810. ^{1}H NMR (300 MHz, $CDCl_3$, δ, ppm) 4.10 (t, 2H, J = 6.3 Hz, C*H*$_2$OC(O)), 3.63 (t, 2H, J = 6.5 Hz, C*H*$_2$OH), 3.26 (t, 2H, J = 7.3 Hz, C*H*$_2$SC(S)), 1.72-1.58 (m, 12H, HOCH$_2$C*H*$_2$CH$_2$*CH*$_2$CH$_2$OC(O), (C*H*$_3$)$_2$C, C*H*$_2$CH$_2$S), 1.47-1.29 (m, 20H, HO(CH$_2$)$_2$C*H*$_2$(CH$_2$)$_2$OC(O), S(CH$_2$)$_2$(C*H*$_2$)$_9$CH$_3$), 0.88 (t, 3H, J = 6.6 Hz, C*H*$_3$CH$_2$). ^{13}C NMR (75 MHz, $CDCl_3$, δ, ppm) 221.6, 173.1, 66.1, 62.8, 56.1, 37.0, 32.4, 32.0, 29.8, 29.7, 29.6, 29.5, 29.2, 29.1, 28.3, 28.0, 25.5, 22.8, 22.4, 14.3. HRMS (m/z): calcd for $C_{22}H_{42}O_3S_3$, 450.2296; found, 451.2374 $[M + H]^+$.

5.3.4. Synthesis of PtBA$_{75}$-OH (2)

To a 25 mL Schlenk flask with a stir bar and sealed by a rubber septum was charged with *t*BA (8.52 g, 66.6 mmol), 5-hydroxypentyl 2-(dodecylthiocarbonothioylthio)-2-methylpropanoate (300 mg, 0.666 mmol), AIBN (10.9 mg, 0.0664 mmol, 10 mol %), and 10 mL of 2-butanone as the solvent. After three

cycles of freeze-pump-thaw, the flask was placed in an oil bath at 56 ℃. The polymerization was quenched after 4.5 h when the monomer conversion was measured to be 75% by ^{1}H NMR. The polymer solution was precipitated three times in methanol/H_2O (2:1). The product was collected and dried under vacuum for 24 h at room temperature to afford **2** as a yellow solid. Yield: 4.85 g (72%, based on 75% conversion of *t*BA). $M_n^{theo.}$ = 10050 Da, M_n^{GPC} = 11000 Da, M_w/M_n = 1.12. IR (cm^{-1}): 3070-2792, 1728, 1450, 1365, 1249, 1141, 840, 748. ^{1}H NMR (300 MHz, $CDCl_3$, ppm) δ 4.04 (t, -C*H*$_2$OC(O)), 3.65 (t, -C*H*$_2$OH), 3.32 (t, -C*H*$_2$SC(S)-), 2.36-2.13 (br, >C*H*C(O)- of polymer backbone), 1.92-1.09 (br, alkyl chain of CTA, >C(C*H*$_3$)$_2$ of CTA, HOCH$_2$C*H*$_2$C*H*$_2$C*H*$_2$CH$_2$O-, -C*H*$_2$- of polymer back bone, *tert*-butyl group of *t*BA units), 0.87 (t, -C*H*$_3$ of CTA chain end). ^{13}C NMR (75 MHz, $CDCl_3$, ppm) δ 174.4-173.9, 80.6-80.2, 42.6-41.8, 37.5-34.9, 28.3. T_g = 41 ℃. TGA in N_2: 195 – 215 ℃, 40% mass loss; 215 – 440 ℃, 40% mass loss.

5.3.5. Synthesis of PtBA$_{75}$-b-PLA$_{33}$ (3)

To a 250 mL Schlenk flask with a stir bar and sealed by a rubber septum was charged with P*t*BA$_{75}$-OH (**2**) (2.04 g, 0.203 mmol), D,L-lactide (1.15 g, 7.79 mmol), and 80 mL of dry dichloromethane as the solvent. The polymerization was initiated by adding DBU (36.4 mg, 0.239 mmol) stock solution *via* N_2-washed syringe. The polymerization was quenched after 1 h by adding several drops of acetic acid when the monomer conversion was measured to be 85% by ^{1}H NMR. The polymer solution was precipitated three times in methanol/H_2O (2:1). The product was collected and dried under vacuum for 24 h at room temperature to afford **3** as a yellow solid. Yield: 2.40 g

(80%, based on 85% conversion of D,L-LA). $M_n^{theo.}$ = 14400 Da, M_n^{GPC} = 16200 Da, M_w/M_n = 1.08. IR (cm^{-1}): 3055-2824, 1743, 1728, 1450, 1366, 1250, 1142, 1088, 849, 748. ^{1}H NMR (300 MHz, $CDCl_3$, ppm) δ 5.23-5.10 (m, >C*H*CH_3 of PLA), 4.20-4.01 (m, -C*H*$_2$OC(O)), 3.32 (t, -C*H*$_2$SC(S)-), 2.36-2.13 (br, >C*H*C(O)- of P*t*BA polymer backbone), 1.92-1.09 (br, alkyl chain of CTA, >C(C*H*$_3$)$_2$ of CTA, $HOCH_2CH_2CH_2CH_2CH_2O$-, -CH2- of polymer back bone, tert-butyl group of *t*BA units, -C*H*$_3$ of PLA), 0.87 (t, -C*H*$_3$ of CTA chain end). ^{13}C NMR (75 MHz, $CDCl_3$, ppm) δ 174.4-173.9, 169.8-169.4, 80.6-80.4, 69.3-67.0, 42.6-41.8, 37.6-36.0, 28.2, 16.9-16.8. $T_{g(PtBA)}$ = 40 ℃, $T_{g(PLA)}$ = 51 ℃. TGA in N_2: 200 – 240 ℃, 25% mass loss; 240 – 360 ℃, 40% mass loss.

5.3.6. Synthesis of PAA$_{75}$-b-PLA$_{33}$ (4)

To a 250 mL flamed-dried RB flask with a stir bar was charged with P*t*BA$_{75}$-b-PLA$_{30}$ (**3**) (2.00 g, 0.0694 mmol). Trifluoroacetic acid (TFA, 150 mL) was added to dissolve the polymer and the reaction was allowed to stir 2 h at room temperature, after which the TFA was removed under vacuum. The crude product was dissolved in 100 mL DMF and transferred to a pre-soaked dialysis tubing (MWCO 6-8 kDa), and dialysis against nanopure water for two days. The aqueous was lyophilized to yield yellow solid of **4**. Yield: 1.10 g, 78%. $M_n^{theo.}$ = 10200 Da. IR (cm^{-1}): 3579-2731, 1720, 1643, 1442, 1381, 1180, 1249, 1087, 918, 864, 802. ^{1}H NMR (300 MHz, DMSO-d_6, ppm) δ 12.42-12.10 (br, -COO*H*), 5.23-5.10 (m, >C*H*CH_3 of PLA), 4.20-4.07 (m, -C*H*$_2$OC(O)), 3.32 (t, -C*H*$_2$SC(S)-), 2.28-2.03 (br, >C*H*C(O)- of P*t*BA polymer backbone), 1.84-1.09 (br, alkyl chain of CTA, >C(C*H*$_3$)$_2$ of CTA, $HOCH_2CH_2CH_2CH_2CH_2O$-, -CH2- of polymer

back bone, -C*H*$_3$ of PLA), 0.81 (t, -C*H*$_3$ of CTA chain end). ^{13}C NMR (75 MHz, $CDCl_3$, ppm) δ 175.9-175.6, 169.3-169.0, 69.1-68.1, 16.5. $T_{g(PLA)}$ = 50 ℃, $T_{g(PAA)}$ = 120 ℃. TGA in N_2: 195 – 215 ℃, 40% mass loss; 215 – 370 ℃, 30% mass loss.

5.3.7. 2-(tert-butoxycarbonylamino)ethyl 2-(dodecylthiocarbonothioylthio)-2-methylpropanoate

To a 100 mL RB flask equipped with a stir bar was placed 2-(dodecylthiocarbonothioylthio)-2-methylpropionic acid (2.14 g, 5.87 mmol), *N*-(*tert*-butoxycarbonyl)ethanolamine (0.946 g, 5.87 mmol) and 4-(dimethylamino)pyridine (0.143 g, 1.17 mmol). Dry CH_2Cl_2 (30 mL) was then added into the flask to dissolve all reagents followed by dropwise addition of a solution of *N,N′*-dicyclohexylcarbodiimide (1.45 g, 7.03 mmol) in CH_2Cl_2. The reaction mixture was allowed to stir at room temperature for 12 h. The solid was removed by filtration, and the filtrate was concentrated under vacuum and purified by silica gel flash chromatography eluting with ethyl acetate/hexanes (1:8). The product was afforded as a yellow oil. Yield: 78%. IR (cm^{-1}): 3471-3279, 2924, 2854, 1712, 1504, 1458, 1365, 1250, 1157, 1064, 818. ^{1}H NMR (300 MHz, $CDCl_3$, δ, ppm) 4.73 (br, 1H, N*H*C(O)), 4.16 (t, 2H, J = 4.8 Hz, C*H*$_2$OC(O)), 3.36 (t, 2H, J = 4.8 Hz, C*H*$_2$NH), 3.26 (t, 2H, J = 7.5 Hz, C*H*$_2$SC(S)), 1.69 (s, 9H, (C*H*$_3$)$_3$C), 1.45-1.40 (m, 12H, HOCH$_2$C*H*$_2$CH$_2$*CH*$_2$CH$_2$OC(O), (C*H*$_3$)$_2$C, C*H*$_2$CH$_2$S), 1.32-1.17 (m, 18H, S(CH$_2$)$_2$(C*H*$_2$)$_9$CH$_3$), 0.88 (t, 3H, J = 6.6 Hz, C*H*$_3$CH$_2$). ^{13}C NMR (75 MHz, $CDCl_3$, δ, ppm) 222.3, 173.1, 155.9, 79.6, 65.5, 56.1, 39.7, 37.2, 32.1, 29.8, 29.6, 29.5, 29.3, 29.1, 28.6, 28.0, 25.6, 22.9, 14.3. HRMS (m/z): calcd for $C_{24}H_{45}NO_4S_3$, 507.2511; found, 530.2448 $[M + Na]^+$.

5.3.8. 2-aminoethyl 2-(dodecylthiocarbonothioylthio)-2-methyl-propanoate trifluoro-acetate (5)

At 0 °C, trifluoroacetic acid (8.10 mL, 105 mmol) was added to a solution of 2-(*tert*-butoxycarbonylamino)ethyl 2-(dodecylthiocarbonothioylthio)-2-methylpropanoate (525 mg, 1.034 mmol) in dry CH_2Cl_2 (5 mL) and the reaction mixture was stirred at this temperature for 30 min and at room temperature for another 30 min. The solvent and TFA were removed under vacuum and purified by silica gel flash chromatography eluting with MeOH/CH_2Cl_2 (1:5). The product was afforded as a yellow oil. Yield: 69%. IR (cm^{-1}): 2924, 2854, 2345, 1728, 1674, 1458, 1257, 1188, 1141, 1064, 817. ^{1}H NMR (300 MHz, $CDCl_3$, δ, ppm) 8.08 (br, 3H, $TFA^-\cdot N\mathit{H}_3^+CH_2$), 4.37 (t, 2H, J = 5.1 Hz, $C\mathit{H}_2OC(O)$), 3.35-3.17 (m, 4H, $C\mathit{H}_2SC(S)$, $TFA^-\cdot NH_3^+C\mathit{H}_2CH_2$), 1.72-1.61 (m, 8H, $(C\mathit{H}_3)_2C$, $C\mathit{H}_2CH_2S$), 1.38-1.21 (m, 18H, $S(CH_2)_2(C\mathit{H}_2)_9CH_3$), 0.88 (t, 3H, J = 6.6 Hz, $C\mathit{H}_3CH_2$). ^{13}C NMR (75 MHz, $CDCl_3$, δ, ppm) 222.7, 173.7, 165.2, 105.2, 62.4, 56.1, 39.4, 37.5, 32.1, 29.8, 29.7, 29.6, 29.5, 29.3, 29.2, 27.9, 25.2, 22.9, 14.3. HRMS (m/z): calcd for $C_{21}H_{38}F_3NO_4S_3$, 521.1915; found, 520.9540 $[M - H]^-$.

5.3.9. N-(2-(acryloyloxy)ethyl)-2-(tert-butoxy)-N,N-dimethyl-2-oxoethanaminium bromide

2-(dimethylamino)ethyl acrylate (10.0 g, 69.8 mmol), *tert*-butyl bromoacetate (19.7 g, 101 mmol) were reacted in 40 mL acetonitrile for 24 h at 50 °C under N_2. The product was yielded as white solid by slowly adding 500 mL ethyl ether to the reaction mixture. The solvent was removed under vacuum for 24 h at room temperature. Yield: 83%. IR (cm^{-1}): 3610-3255, 3008, 2924, 1720, 1635, 1458, 1396, 1242, 1188, 1141,

979, 918, 810. ^{1}H NMR (300 MHz, D_2O, δ, ppm) 6.48 (dd, 1H, J = 17 and 1.0 Hz, *cis* C*H*H=CHCO-), 6.22 (dd, 1H, J = 17 and 9.0 Hz, CH_2=C*H*CO-), 6.06 (dd, 1H, J = 9.0 and 1.0 Hz, CH*H*=CHCO-), 4.67 (t, 2H, J = 4.2 Hz, -$CH_2N(CH_3)_2CH_2CH_2$OOC-), 4.33 (s, 2H, -$CH_2N(CH_3)_2CH_2CH_2$OOC-), 4.04 (t, 2H, J = 4.2 Hz, -$CH_2N(CH_3)_2CH_2CH_2$OOC-), 3.37 (s, 6H, -$CH_2N(CH_3)_2CH_2CH_2$OOC-), 1.52 (s, 9H, $(CH_3)_3$C-). ^{13}C NMR (75 MHz, DMSO-d_6, δ, ppm) 164.7, 163.9, 132.4, 127.7, 84.0, 62.1, 61.4, 57.9, 51.7, 27.6. HRMS (m/z): calcd for $C_{13}H_{24}BrNO_4$, 337.0889; found, 336.0790 $[M - H]^-$.

5.3.10. Synthesis of 2 kDa PCB (6)

To a 25 mL Schlenk flask with a stir bar and sealed by a rubber septum was charged with 2-aminoethyl 2-(dodecylthiocarbonothioylthio)-2-methylpropanoate trifluoroacetate (CTA) (110 mg, 0.192 mmol), *N*-(2-(acryloyloxy)ethyl)-2-(*tert*-butoxy)-*N,N*-dimethyl-2-oxoethanaminium bromide (1.43 g, 4.23 mmol), AIBN (6.91 mg, 0.0421 mmol, 20 mol %), and 10 mL of DMF as the solvent. After three cycles of freeze-pump-thaw, the flask was placed in an oil bath at 70 °C. The polymerization was quenched after 40 min when the monomer conversion was measured to be 40 % by ^{1}H NMR. The polymer solution was precipitated three times in ethyl acetate. The product was collected and dried under vacuum for 24 h at room temperature to afford PCB-2K as a yellow solid. Yield: 0.35 g (61%, based on 40% conversion of monomer). $M_n^{theo.}$ = 3200 Da, M_w/M_n = 1.16. IR (cm^{-1}): 3672-3217, 2924, 1728, 1627, 1458, 1373, 1250, 1149, 987, 841. ^{1}H NMR (300 MHz, DMSO-d_6, ppm) δ 8.10 (br, $TFA^-\cdot N\mathit{H}_3^+CH_2$), 4.83-4.37(br, $TFA^-\cdot NH_3^+CH_2CH_2OC(O)$, -$CH_2N(CH_3)_2CH_2CH_2$OOC-), 4.20-3.87 (br, -

$CH_2N(CH_3)_2CH_2CH_2OOC$-), 3.56-3.24 (br, -$CH_2N(CH_3)_2CH_2CH_2OOC$-, $CH_2SC(S)$, $TFA^-\cdot NH_3^+CH_2CH_2$), 2.47-2.30 (br, >C*H*C(O)- of polymer backbone), 1.93-1.16 (m, alkyl chain of CTA, >$C(CH_3)_2$ of CTA, -CH_2- of polymer back bone, *tert*-butyl groups), 0.85 (t, -CH_3 of CTA chain end). ^{13}C NMR (75 MHz, MeOD, δ, ppm) 166.5, 165.4-164.9, 86.5, 64.8-64.0, 53.3, 37.1, 31.8-31.0, 28.5. T_g = 116 °C

5.3.11. Synthesis of 5 kDa PCB (7)

To a 25 mL Schlenk flask with a stir bar and sealed by a rubber septum was charged with 2-aminoethyl 2-(dodecylthiocarbonothioylthio)-2-methylpropanoate trifluoroacetate (CTA) (100 mg, 0.192 mmol), *N*-(2-(acryloyloxy)ethyl)-2-(*tert*-butoxy)-*N,N*-dimethyl-2-oxoethanaminium bromide (1.29 g, 3.81 mmol), AIBN (6.28 mg, 0.0383 mmol, 20 mol %), and 9 mL of DMF as the solvent. After three cycles of freeze-pump-thaw, the flask was placed in an oil bath at 70 °C. The polymerization was quenched after 3.0 h when the monomer conversion was measured to be 90 % by ^{1}H NMR. The polymer solution was precipitated three times in ethyl acetate. The product was collected and dried under vacuum for 24 h at room temperature to afford PCB-5K as a yellow solid. Yield: 0.47 g (40%, based on 90% conversion of *monomer*). $M_n^{theo.}$ = 6600 Da, M_w/M_n = 1.08. T_g = 130 °C.

5.3.12. Synthesis of PEG/PCB, DOTA, tyramine grafted PAA-b-PLA (8-12)

Grafting PEG/PCB, 2-aminoethyl-mono-amide-DOTA-tris(*t*-Bu ester), tyramine onto PAA_{75}-*b*-PLA_{33} (**4**) involved the following: to a anhydrous *N,N*-dimethylformamide (DMF) solution of **4**, 1-[3'-(dimethylamino)propyl]-3-ethylcarbodiimide methiodide (EDCI), and 1-hydroxylbenzotriazole (HOBt) were added.

The mixtures were allowed to stir for 1 h at room temperature, followed by the addition of mono amine PEGs or PCBs. After 30 min, DMF solution of the mixture of 2-aminoethyl-mono-amide-DOTA-tris(*t*-Bu ester), tyramine and *N,N*-diisopropylethylamine (DIPEA) was added, followed by further stirring for 30 h. The relative feed ratios of DOTA and tyramine to **4** were kept constant at 5:5:1, whereas the PEG/PCB to **4** feed ratios were 7:1 when targeting five grafts per polymer chain, and 20:1 when targeting ten grafts per polymer chain, respectively. The grafted polymers were purified by dialyzing against nanopure H_2O (18.2 MΩ-cm) for 3 d to remove organic solvent and byproducts. The aqueous solutions were then lyophilized to afford the products as white solid with yield of 60-80%. PCB grafted polymer were not characterized due to the poor solubility. ^{1}H NMR (300 MHz, DMSO-d_6, ppm) δ 7.05-6.87 (br, aromatic protons from tyramine), 6.73-6.59 (br, aromatic protons from tyramine), 5.24-5.11 (m, >C*H*CH_3 of PLA), 3.56-3.19 (br, -OCH_2CH_2O- from PEG backbone, -CH_2CO- from DOTA, -CH_2CH_2NH- from tyramine), 2.40-2.05 (br, >C*H*C(O)- of polymer backbone, >NCH_2CH_2N< from DOTA), 1.67-0.98 (br, alkyl chain of CTA, >C(CH_3)$_2$ of CTA, -CH_2- of polymer back bone, *tert*-butyl groups from DOTA, -CH_3 of PLA).

5.3.13. Graft polymer precursor for 8 with five 2 kDa PEG

PAA_{75}-*b*-PLA_{33} (30 mg, 2.9 μmol), EDCI (17 mg, 57 μmol), HOBt (7.9 mg, 58 μmol), tyramine (2.0 mg, 14 μmol), 2-aminoethyl-mono-amide-DOTA-tris(*t*-Bu ester) (10 mg, 14 μmol), $mPEG_{2000}$-NH_2 (41 mg, 20 μmol), DIPEA (19 mg, 0.15 mmol). Yield: 70%.

Graft polymer precursor for 9 with five 5 kDa PEG

PAA_{75}-*b*-PLA_{33} (30 mg, 2.9 μmol), EDCI (17 mg, 57 μmol), HOBt (7.9 mg, 58 μmol), tyramine (2.0 mg, 14 μmol), 2-aminoethyl-mono-amide-DOTA-tris(*t*-Bu ester) (10 mg, 14 μmol), $mPEG_{5000}$-NH_2 (103 mg, 20.6 μmol), DIPEA (19 mg, 0.15 mmol). Yield: 80%.

Graft polymer precursor for 10 with ten 5 kDa PEG

PAA_{75}-*b*-PLA_{33} (30 mg, 2.9 μmol), EDCI (17 mg, 57 μmol), HOBt (7.9 mg, 58 μmol), tyramine (2.0 mg, 14 μmol), 2-aminoethyl-mono-amide-DOTA-tris(*t*-Bu ester) (10 mg, 14 μmol), $mPEG_{5000}$-NH_2 (294 mg, 58.8 μmol), DIPEA (19 mg, 0.15 mmol). Yield: 73%.

Graft polymer precursor for 11 with five 2 kDa PCB

PAA_{75}-*b*-PLA_{33} (30 mg, 2.9 μmol), EDCI (17 mg, 57 μmol), HOBt (7.9 mg, 58 μmol), tyramine (2.0 mg, 14 μmol), 2-aminoethyl-mono-amide-DOTA-tris(*t*-Bu ester) (10 mg, 14 μmol), **6** (64 mg, 20.6 μmol), DIPEA (45 mg, 0.35 mmol).

Graft polymer precursor for 12 with five 5 kDa PCB

PAA_{75}-*b*-PLA_{33} (30 mg, 2.9 μmol), EDCI (17 mg, 57 μmol), HOBt (7.9 mg, 58 μmol), tyramine (2.0 mg, 14 μmol), 2-aminoethyl-mono-amide-DOTA-tris(*t*-Bu ester) (10 mg, 14 μmol), **7** (136 mg, 20.6 μmol), DIPEA (45 mg, 0.35 mmol).

5.3.14. Deprotection to afford polymer 8-12

Polymers and TFA (200 equiv. to *tert*-butyl groups) were allowed to stir for 2 h, followed by removal of TFA under vacuum, dialysis against nanopure H_2O and lyophilization to afford final polymer precursors as white solid with yield of 70-80%. ^1H

NMR of PEG-grafted polymers (300 MHz, DMSO-d_6, ppm) δ 7.05-6.87 (br, aromatic protons from tyramine), 6.73-6.59 (br, aromatic protons from tyramine), 5.41-5.26 (m, >C*H*CH_3 of PLA), 4.81-3.92 (br, -OCH_2CH_2O- from PEG backbone, -CH_2CO- from DOTA, -CH_2CH_2NH- from tyramine), 2.40-2.05 (br, >C*H*C(O)- of polymer backbone, >NCH_2CH_2N< from DOTA), 1.67-0.98 (br, alkyl chain of CTA, >C(CH_3)$_2$ of CTA, -CH_2- of polymer back bone). ^{1}H NMR of PCB-grafted polymers (300 MHz, TFA-d, ppm) δ 7.13-6.07 (br, aromatic protons from tyramine), 6.90-6.80 (br, aromatic protons from tyramine), 5.24-5.11 (m, >C*H*CH_3 of PLA), 3.56-3.19 (br, -$CH_2N(CH_3)_2$C$H_2$$CH_2$OOC-, -$CH_2N(CH_3)_2CH_2$$CH_2$OOC, -C$H_2$CO- from DOTA, -C$H_2CH_2$NH- from tyramine), 2.73-2.36 (br, >C*H*C(O)- of polymer backbone, >NCH_2CH_2N< from DOTA), 1.95-1.25 (m, alkyl chain of CTA, >C(CH_3)$_2$ of CTA, -CH_2- of polymer back bone, -CH_3 of PLA), 0.86-0.79 (br, -CH_3 of CTA chain end).

5.3.15. Preparation of dSCK1-5

The micelles were prepared by direct dissolving polymer precursors into nanopure H_2O with polymer concentration *ca.* 1 mg/mL. The SCKs were prepared by adding *2,2*'-(ethylenedioxy)-bis(ethylamine) (EDDA) in nanopure H_2O dropwise. The reaction was allowed to stir for 2 h at room temperature. EDCI in nanopure H_2O was then added to the solution dropwise. The stoichiometry applied to achieve 20% nominal crosslinking was 10:1:2.2 for carboxylic acid unites/EDCI/EDDA. The crosslinking reactions were further stir at room temperature for 12. The final SCKs were obtained after dialyzing against nanopure water overnight.

dSCK2 with five 5 kDa PEG

$(D_h)_n$(DLS) = 30 ± 9 nm, $(D_h)_v$(DLS) = 45 ± 27 nm, $(D_h)_i$(DLS) = 162 ± 125 nm; ζ-potential: -28 ± 1.5 mV.

dSCK1 with five 2 kDa PEG

$(D_h)_n$(DLS) = 40 ± 12 nm, $(D_h)_v$(DLS) = 61 ± 39 nm, $(D_h)_i$(DLS) = 279 ± 238 nm; ζ-potential: -41 ± 1.3 mV.

dSCK3 with ten 5 kDa PEG

$(D_h)_n$(DLS) = 32 ± 9 nm, $(D_h)_v$(DLS) = 47 ± 28 nm, $(D_h)_i$(DLS) = 175 ± 141 nm; ζ-potential: -25 ± 2.2 mV.

dSCK4 with five 2 kDa PCB

$(D_h)_n$(DLS) = 65 ± 19 nm, $(D_h)_v$(DLS) = 94 ± 49 nm, $(D_h)_i$(DLS) = 223 ± 143 nm; ζ-potential: -58 ± 4.8 mV.

dSCK5 with five 5 kDa PEG

$(D_h)_n$(DLS) = 29 ± 8 nm, $(D_h)_v$(DLS) = 43 ± 27 nm, $(D_h)_i$(DLS) = 195 ± 173 nm; ζ-potential: -50 ± 2.6 mV.

dSCK *in vitro* size stability study

dSCKs were incubated with 10 wt% BSA solution at 37 °C under gentle stirring. At each time point, an aliquot of SCK solution was collected to measure the size using dynamic light scattering (DLS).

5.3.16. dSCK in vitro degradation study

dSCK solutions in PBS 7.4 buffer and PBS 5.0 buffer were prepared by dissolving lyophilized dSCK powder by the buffer solution with concentrations of *ca.* 1

mg/mL. The solutions were incubated at 37 °C. At each time point, the lactic acid levels were measured by lactate assay kit (abcam®, ab65331), the degradation percentages were calculated using calibration curve with DL-lactic acid as the standard.

5.3.17. ^{64}Cu radiolabeling dSCKs

^{64}Cu (half-life = 12.7 h, β^+ = 17%, β^- = 40%) was produced on the Washington University Medical School CS-15 cyclotron by the ^{64}Ni (p,n) ^{64}Cu nuclear reaction at a specific activity of 50-200 mCi/mg at the end of bombardment.[286] Degradable **dSCK1-5** (~4.5 μg) were incubated with 18.5 MBq of ^{64}Cu in 100 μL of 0.1 M pH 5.5 ammonium acetate buffer at 45°C for 1 h (n = 3). After ethylene diamine tetraacetic acid (EDTA) challenge (10 mM in 50 mM, pH 7.4, phosphate buffer), the radiochemical purities of the radiolabeled nanoparticles were measured by radioactive thin-layer chromatography (Bioscan, Washington DC), followed by the purification with 7k Zeba spin desalting column (Piercenet, Rockford, IL).

5.3.18. Serum stability study

The radiochemical purities of ^{64}Cu radiolabeled dSCKs were measured before the addition of mouse serum with 1:1 volume ratio. The ^{64}Cu-dSCKs and serum mixture was incubated in microcentrifuge tubes at 45°C. At each time point (1 h, 4 h, and 24 h post injection, p.i.), 10 μL of the sample was removed and incubated at 45°C with 5 μL of EDTA (10 mM in 50 mM pH 7.4 phosphate buffer) for 5 min. The radiochemical purities of the samples (n=3 for each dSCK) were tested using radioactive thin-layer chromatography (Bioscan, Washington DC).

5.3.19. In vivo biodistribution study

All animal studies were performed in compliance with guidelines set forth by the NIH Office of Laboratory Animal Welfare and approved by the Washington University Animal Studies Committee. *In vivo* biodistribution studies were performed using 185 kBq of ^{64}Cu-dSCKs (32-63 ng/mouse) in 100 μL saline (APP pharmaceuticals, Schaumburg, IL) injected via the tail vein of C57BL/6 mice weighing 20-25 g (n=4/group) under inhaled isoflurane. The mice were euthanized by cervical dislocation at each time point (1 h, 4 h, and 24 h p.i.). Organs of interest were collected, weighed, and counted in a well gamma counter (Beckman 8000). Standards were prepared and measured along with the organs to calculate the average and standard deviation of the percentage of the injected dose per gram of tissue (%ID/g).[287]

5.4. Conclusions

In summary, a series of **dSCK1-5** nanoparticles was prepared through a "pre-grafting" strategy with controlled sizes and surface charges, by designing, synthesizing and coupling an amphiphilic diblock copolymer of acrylic acid and lactide, and complementary monoamino-terminated zwitterionic PCB polymer grafts of varying lengths or comparable commercially-available monoamino-PEG grafts. All dSCKs were radiolabeled with ^{64}Cu in high specific activities and showed extended serum stabilities. The *in vivo* pharmacokinetic evaluation indicated that the 2 kDa PCB-grafted **dSCK4** had a slightly better biodistribution profile than did the 2 kDa PEG-grafted analog **dSCK1**, while longer chain (5 kDa) PEG grafts imparted **dSCK2** with superior biodistribution to that of the corresponding 5 kDa PCB-grafted nanoparticles, **dSCK5**.

All the dSCKs demonstrated pH-dependent degradation kinetics *in vitro*, with the PCB-grafted nanoparticles undergoing faster hydrolysis. These results suggest that PCB, as a new type of functionalizable anti-protein adsorption material, demonstrates comparable effects in tuning degradable polymer nanoparticle biodistributions. Further studies will be performed to compare their immunotoxicities and also the targeting efficiency of PCB-grafted dSCKs *vs*. PEG-functionalized dSCKs with positron emission tomography. The outcome from these studies may lay the foundation for using PCB as a versatile platform to design degradable nanoparticles for *in vivo* theranostics.

CHAPTER VI

CONCLUSIONS

It is of great importance to develop robust synthetic methodologies to construct well-defined, complex nanoscale objects with functional units. Two efficient strategies of building nanoscopic structures include direct polymerization of macromonomers and assembling from block copolymer to form nanoparticles. "Grafting through" strategy allows for the efficient synthesis of well-defined brush polymers, with controllable dimensions and functional groups. On the other hand, shell crosslinked knedel-like nanoparticles (SCKs), originated from supramolecular assembly of amphiphilic block copolymers into micelles, and followed by shell crosslinking, provide a promising platform as carriers for therapeutic and diagnostic applications.

In an effort to develop linear reactive polymers with dense pendent functional groups by atom efficient routes, the selective ATRP and selective ROMP were investigated to achieve two distinct reactive well-defined polymers from one single monomer. By taking advantage of the orthogonal reactivities of methacrylate and norbornene group towards radical polymerization and olefin metathesis polymerization, and systematic optimizing of ATRP conditions, both selective polymerization were successful. Chain extension of norbornene-functionalized poly(methyl methacrylate) with methyl methacrylate was performed to demonstrate the living characteristic of the selective ATRP. This strategy provided a good example of constructing reactive polymers by direct polymerization of functional monomers. The norbornene group was

chosen due to its reactivity towards ROMP, however, other polymerizable groups with reactivity difference with methacrylate group, such a cycloalkene, and cyclic heteroatom-containing monomers can also be investigated to obtain a variety of reactive polymers.

To further utilize the orthogonal reactivity of the norbornene group and methacrylate group, we investigated the facile synthesis of well-defined molecular brush polymers in a one-pot strategy, without isolating or purifying any intermediates during the entire process. By selective RAFT polymerization, norbornene-terminated poly(methyl methacrylate)s were synthesized with controlled molecular weights and narrow molecular weight distributions. The control experiment demonstrated the ROMP could proceed with high macromonomer conversion in the presence of methacrylate group, but not with the acrylate group. By applying the optimized condition, two molecular brush polymers with different side chain lengths and close backbone lengths were prepared by one-pot tandem RAFT polymerization and ROMP, with precise control over each step. AFM characterizations were conducted to determine the sizes of two brush polymers. The study demonstrated a promising strategy to produce certain types of well-defined brush polymers, future work include other compatible monomers as the side chain compositions, as well as the preparation of functional brush polymers direct from functional monomers by this one-pot strategy.

To expand the macromolecular architectures, the construction of triblock brush polymers with dumbbell-shaped topology was studied. The poly(lactide)s were chosen as the side chain composition to reduce any side reactions from potential alkenes

contamination from radical polymerization. The preliminary study showed that triblock brush polymer could be efficiently afforded by sequential addition of three side chain macromolecules. By tuning the side chain and backbone lengths, the sizes of the "ball" and "bar" could be precisely controlled, which were verified by AFM. For the future work, the size-controlled multiblock brush polymers having different morphologies and region-controlled functionalities can be applied as useful templates to understand the *in vivo* behaviors of shaped nanoparticles and probe some biological processes.

Next, we demonstrated the preparation of both poly(carboxybetaine) (PCB)-grafted and poly(ethylene glycol) (PEG)-grafted degradable SCKs (dSCK) and the evaluation of their *in vivo* pharmacokinetics. Both DOTA and tyramine, sites for radiolabeling, were installed together with PCB/PEG onto an amphiphilic diblock copolymer, poly(acrylic acid)-*b*-poly(lactide). A series of grafted dSCKs with different numbers and lengths of grafts were prepared by direct dissolving graft polymer precursors into water to form micelles, followed by shell crosslinking. All dSCKs were radiolabeled with ^{64}Cu in high specific activities, which allows for *in vivo* evaluation and potential positron emission tomography (PET) imaging. The comparative *in vivo* studies showed that 2 kDa PCB-grafted dSCKS has superior biodistribution than the 2 kDa PEG-grafted analog, whereas, dSCKs with long grafts (5 kDa) showed reversed tend. The comparable *in vivo* pharmacokinetic result of PCB-dSCK to the PEG-dSCK suggested that PCB, as a promising novel non-fouling material, may be an excellent alternative to the conventional PEG materials. Moreover, due to the capability of PCB to stabilize proteins without sacrificing their biological activities, the future studies

include the comparative investigation of the targeting efficiency of PCB-grafted dSCK *vs*. PEG-grafted dSCK to develop long circulating nanoparticles with high targeting efficiency. In addition, the *in vitro* and *in vivo* immune-toxicity study is vital to evaluation of the possibility of PCB-grafted nanoparticles for clinical applications.

REFERENCES

(1) Lieber, C. M. *MRS Bull.* **2003**, *28*, 486.

(2) Whitesides, G. M. *Small* **2005**, *1*, 172.

(3) Kroto, H. W.; Heath, J. R.; Obrien, S. C.; Curl, R. F.; Smalley, R. E. *Nature* **1985**, *318*, 162.

(4) Binnig, G.; Rohrer, H. *IBM J. Res. Dev.* **1986**, *30*, 355.

(5) Xiang, J.; Lu, W.; Hu, Y. J.; Wu, Y.; Yan, H.; Lieber, C. M. *Nature* **2006**, *441*, 489.

(6) Scholes, G. D.; Rumbles, G. *Nature Mater.* **2006**, *5*, 683.

(7) Kay, E. R.; Leigh, D. A.; Zerbetto, F. *Angew. Chem. Int. Ed.* **2007**, *46*, 72.

(8) Balzani, V.; Clemente-Leon, M.; Credi, A.; Ferrer, B.; Venturi, M.; Flood, A. H.; Stoddart, J. F. *Proc. Natl. Acad. Sci. U.S.A.* **2006**, *103*, 1178.

(9) Boisselier, E.; Astruc, D. *Chem. Soc. Rev.* **2009**, *38*, 1759.

(10) Michalet, X.; Pinaud, F. F.; Bentolila, L. A.; Tsay, J. M.; Doose, S.; Li, J. J.; Sundaresan, G.; Wu, A. M.; Gambhir, S. S.; Weiss, S. *Science* **2005**, *307*, 538.

(11) Kakizawa, Y.; Kataoka, K. *Adv. Drug Deliv. Rev.* **2002**, *54*, 203.

(12) Bell, A. T. *Science* **2003**, *299*, 1688.

(13) Dai, L. M.; Chang, D. W.; Baek, J. B.; Lu, W. *Small* **2012**, *8*, 1130.

(14) Guo, K. W. *Int. J Energ. Res.* **2012**, *36*, 1.

(15) Kamat, P. V. *J. Phys. Chem. C* **2008**, *112*, 18737.

(16) Xia, Y. N.; Whitesides, G. M. *Annu. Rev. Mater. Res.* **1998**, *28*, 153.

(17) Chou, S. Y.; Krauss, P. R.; Renstrom, P. J. *Science* **1996**, *272*, 85.

(18) Zhang, S. G. *Nat. Biotechnol.* **2003**, *21*, 1171.

(19) Lu, W.; Lieber, C. M. *Nature Mater.* **2007**, *6*, 841.

(20) Ariga, K.; Hill, J. P.; Lee, M. V.; Vinu, A.; Charvet, R.; Acharya, S. *Sci. Technol. Adv. Mater.* **2008**, *9*.

(21) Ariga, K.; Hill, J. P.; Ji, Q. M. *Phys. Chem. Chem. Phys.* **2007**, *9*, 2319.

(22) Grimm, V.; Revilla, E.; Berger, U.; Jeltsch, F.; Mooij, W. M.; Railsback, S. F.; Thulke, H. H.; Weiner, J.; Wiegand, T.; DeAngelis, D. L. *Science* **2005**, *310*, 987.

(23) Rotello, V. M. *Abstr Pap Am Chem S* **2011**, *242*.

(24) Hawker, C. J.; Russell, T. P. *MRS Bull.* **2005**, *30*, 952.

(25) Discher, D. E.; Eisenberg, A. *Science* **2002**, *297*, 967.

(26) Kataoka, K.; Harada, A.; Nagasaki, Y. *Adv. Drug Deliv. Rev.* **2001**, *47*, 113.

(27) Braunecker, W. A.; Matyjaszewski, K. *Prog. Polym. Sci.* **2007**, *32*, 93.

(28) Forster, S.; Antonietti, M. *Adv. Mater.* **1998**, *10*, 195.

(29) Park, C.; Yoon, J.; Thomas, E. L. *Polymer* **2003**, *44*, 6725.

(30) Fasolka, M. J.; Mayes, A. M. *Annu. Rev. Mater. Res.* **2001**, *31*, 323.

(31) Zhao, D. Y.; Feng, J. L.; Huo, Q. S.; Melosh, N.; Fredrickson, G. H.; Chmelka, B. F.; Stucky, G. D. *Science* **1998**, *279*, 548.

(32) Hadjichristidis, N.; Pitsikalis, M.; Pispas, S.; Iatrou, H. *Chem. Rev.* **2001**, *101*, 3747.

(33) Hadjichristidis, N.; Pitsikalis, M.; Iatrou, H.; Pispas, S. *Macromol. Rapid Commun.* **2003**, *24*, 979.

(34) Matyjaszewski, K. *Science* **2011**, *333*, 1104.

(35) Hadjichristidis, N.; Iatrou, H.; Pitsikalis, M.; Mays, J. *Prog. Polym. Sci.* **2006**, *31*, 1068.

(36) Matyjaszewski, K.; Tsarevsky, N. V. *Nature Chem.* **2009**, *1*, 276.

(37) Hawker, C. J.; Bosman, A. W.; Harth, E. *Chem. Rev.* **2001**, *101*, 3661.

(38) Wang, J. S.; Matyjaszewski, K. *Macromolecules* **1995**, *28*, 7901.

(39) Chiefari, J.; Chong, Y. K.; Ercole, F.; Krstina, J.; Jeffery, J.; Le, T. P. T.; Mayadunne, R. T. A.; Meijs, G. F.; Moad, C. L.; Moad, G.; Rizzardo, E.; Thang, S. H. *Macromolecules* **1998**, *31*, 5559.

(40) Benoit, D.; Chaplinski, V.; Braslau, R.; Hawker, C. J. *J. Am. Chem. Soc.* **1999**, *121*, 3904.

(41) Ouchi, M.; Terashima, T.; Sawamoto, M. *Chem. Rev.* **2009**, *109*, 4963.

(42) Matyjaszewski, K.; Xia, J. H. *Chem. Rev.* **2001**, *101*, 2921.

(43) Kato, M.; Kamigaito, M.; Sawamoto, M.; Higashimura, T. *Macromolecules* **1995**, *28*, 1721.

(44) Wang, J. S.; Matyjaszewski, K. *J. Am. Chem. Soc.* **1995**, *117*, 5614.

(45) Jakubowski, W.; Min, K.; Matyjaszewski, K. *Macromolecules* **2006**, *39*, 39.

(46) Min, K.; Gao, H. F.; Matyjaszewski, K. *Macromolecules* **2007**, *40*, 1789.

(47) Pintauer, T.; Matyjaszewski, K. *Chem. Soc. Rev.* **2008**, *37*, 1087.

(48) Matyjaszewski, K.; Jakubowski, W.; Min, K.; Tang, W.; Huang, J. Y.; Braunecker, W. A.; Tsarevsky, N. V. *Proc. Natl. Acad. Sci. U.S.A.* **2006**, *103*, 15309.

(49) Magenau, A. J. D.; Strandwitz, N. C.; Gennaro, A.; Matyjaszewski, K. *Science* **2011**, *332*, 81.

(50) Bortolamei, N.; Isse, A. A.; Magenau, A. J. D.; Gennaro, A.; Matyjaszewski, K. *Angew. Chem. Int. Ed.* **2011**, *50*, 11391.

(51) Moad, G.; Rizzardo, E.; Thang, S. H. *Aust. J. Chem.* **2009**, *62*, 1402.

(52) Moad, G.; Rizzardo, E.; Thang, S. H. *Polymer* **2008**, *49*, 1079.

(53) Calderon, N.; Ofstead, E. A.; Ward, J. P.; Judy, W. A.; Scott, K. W. *J. Am. Chem. Soc.* **1968**, *90*, 4133.

(54) Calderon, N. *Acc. Chem. Res.* **1972**, *5*, 127.

(55) Katz, T. J. M., James *J. Am. Chem. Soc.* **1975**, *97*, 1592.

(56) Katz, T. J.; Lee, S. J.; Acton, N. *Tetrahedron Lett.* **1976**, 4247.

(57) Tebbe, F. N.; Parshall, G. W.; Reddy, G. S. *J. Am. Chem. Soc.* **1978**, *100*, 3611.

(58) Bielawski, C. W.; Grubbs, R. H. *Prog. Polym. Sci.* **2007**, *32*, 1.

(59) Love, J. A.; Morgan, J. P.; Trnka, T. M.; Grubbs, R. H. *Angew. Chem. Int. Ed.* **2002**, *41*, 4035.

(60) Matson, J. B.; Grubbs, R. H. *J. Am. Chem. Soc.* **2008**, *130*, 6731.

(61) Li, Z.; Zhang, K.; Ma, J.; Cheng, C.; Wooley, K. L. *J. Polym. Sci., Part A: Polym. Chem.* **2009**, *47*, 5557.

(62) Xia, Y.; Kornfield, J. A.; Grubbs, R. H. *Macromolecules* **2009**, *42*, 3761.

(63) Nederberg, F.; Connor, E. F.; Möller, M.; Glauser, T.; Hedrick, J. L. *Angew. Chem. Int. Ed.* **2001**, *40*, 2712.

(64) Kricheldorf, H. R.; Garaleh, M.; Schwarz, G. *J. Macromol. Sci., Pure Appl. Chem.* **2005**, *A42*, 139.

(65) Johnson, R. M.; Fraser, C. L. *Biomacromolecules* **2004**, *5*, 580.

(66) Feng, H.; Dong, C. M. *J. Polym. Sci., Part A: Polym. Chem.* **2006**, *44*, 5353.

(67) Lohmeijer, B. G. G.; Pratt, R. C.; Leibfarth, F.; Logan, J. W.; Long, D. A.; Dove, A. P.; Nederberg, F.; Choi, J.; Wade, C.; Waymouth, R. M.; Hedrick, J. L. *Macromolecules* **2006**, *39*, 8574.

(68) Lohmeijer, B. G. G.; Dubois, G.; Leibfarth, F.; Pratt, R. C.; Nederberg, F.; Nelson, A.; Waymouth, R. M.; Wade, C.; Hedrick, J. L. *Org. Lett.* **2006**, *8*, 4683.

(69) Nederberg, F.; Lohmeijer, B. G. G.; Leibfarth, F.; Pratt, R. C.; Choi, J.; Dove, A. P.; Waymouth, R. M.; Hedrick, J. L. *Biomacromolecules* **2007**, *8*, 153.

(70) Zhang, L.; Pratt, R. C.; Nederberg, F.; Horn, H. W.; Rice, J. E.; Waymouth, R. M.; Wade, C. G.; Hedrick, J. L. *Macromolecules* **2010**, *43*, 1660.

(71) Brignou, P.; Gil, M. P.; Casagrande, O.; Carpentier, J. F.; Guillaume, S. M. *Macromolecules* **2010**, *43*, 8007.

(72) Dove, A. P.; Pratt, R. C.; Lohmeijer, B. G. G.; Waymouth, R. M.; Hedrick, J. L. *J. Am. Chem. Soc.* **2005**, *127*, 13798.

(73) Pratt, R. C.; Lohmeijer, B. G. G.; Long, D. A.; Lundberg, P. N. P.; Dove, A. P.; Li, H. B.; Wade, C. G.; Waymouth, R. M.; Hedrick, J. L. *Macromolecules* **2006**, *39*, 7863.

(74) Myers, M.; Connor, E. F.; Glauser, T.; Mock, A.; Nyce, G.; Hedrick, J. L. *J. Polym. Sci., Part A: Polym. Chem.* **2002**, *40*, 844.

(75) Connor, E. F.; Nyce, G. W.; Myers, M.; Mock, A.; Hedrick, J. L. *J. Am. Chem. Soc.* **2002**, *124*, 914.

(76) Nyce, G. W.; Glauser, T.; Connor, E. F.; Mock, A.; Waymouth, R. M.; Hedrick, J. L. *J. Am. Chem. Soc.* **2003**, *125*, 3046.

(77) Kiesewetter, M. K.; Shin, E. J.; Hedrick, J. L.; Waymouth, R. M. *Macromolecules* **2010**, *43*, 2093.

(78) Iha, R. K.; Wooley, K. L.; Nystrom, A. M.; Burke, D. J.; Kade, M. J.; Hawker, C. J. *Chem. Rev.* **2009**, *109*, 5620.

(79) Coessens, V.; Pintauer, T.; Matyjaszewski, K. *Prog. Polym. Sci.* **2001**, *26*, 337.

(80) McCormack, C. L.; Lowe, A. B. *Acc. Chem. Res.* **2004**, *37*, 312.

(81) Gauthier, M. A.; Gibson, M. I.; Klok, H. A. *Angew. Chem. Int. Ed.* **2009**, *48*, 48.

(82) Theato, P. *J. Polym. Sci., Part A: Polym. Chem.* **2008**, *46*, 6677.

(83) Zhao, H.; Sterner, E. S.; Coughlin, E. B.; Theato, P. *Macromolecules* **2012**, *45*, 1723.

(84) Beck, J. B.; Killops, K. L.; Kang, T.; Sivanandan, K.; Bayles, A.; Mackay, M. E.; Wooley, K. L.; Hawker, C. J. *Macromolecules* **2009**, *42*, 5629.

(85) Flores, J. D.; Shin, J.; Hoyle, C. E.; McCormick, C. L. *Polym. Chem.* **2010**, *1*, 213.

(86) Ma, J.; Bartels, J. W.; Li, Z.; Zhang, K.; Cheng, C.; Wooley, K. L. *Aust. J. Chem.* **2010**, *63*, 1159.

(87) Ma, J.; Cheng, C.; Sun, G. R.; Wooley, K. L. *Macromolecules* **2008**, *41*, 9080.

(88) Campos, L. M.; Killops, K. L.; Sakai, R.; Paulusse, J. M. J.; Damiron, D.; Drockenmuller, E.; Messmore, B. W.; Hawker, C. J. *Macromolecules* **2008**, *41*, 7063.

(89) Moses, J. E.; Moorhouse, A. D. *Chem. Soc. Rev.* **2007**, *36*, 1249.

(90) O'Reilly, R. K.; Joralemon, M. J.; Hawker, C. J.; Wooley, K. L. *Chem. Eur. J.* **2006**, *12*, 6776.

(91) Binder, W. H.; Sachsenhofer, R. *Macromol. Rapid Commun.* **2007**, *28*, 15.

(92) Jiang, X. Z.; Zhang, J. Y.; Zhou, Y. M.; Xu, J.; Liu, S. Y. *J. Polym. Sci., Part A: Polym. Chem.* **2008**, *46*, 860.

(93) Yu, W. H.; Kang, E. T.; Neoh, K. G. *Langmuir* **2004**, *20*, 8294.

(94) Barbey, R.; Klok, H. A. *Langmuir* **2010**, *26*, 18219.

(95) Tsarevsky, N. V.; Bencherif, S. A.; Matyjaszewski, K. *Macromolecules* **2007**, *40*, 4439.

(96) Cheng, C.; Sun, G.; Khoshdel, E.; Wooley, K. L. *J. Am. Chem. Soc.* **2007**, *129*, 10086.

(97) Sun, G. R.; Cheng, C.; Wooley, K. L. *Macromolecules* **2007**, *40*, 793.

(98) Sun, G.; Fang, H. F.; Cheng, C.; Lu, P.; Zhang, K.; Walker, A. V.; Taylor, J. S. A.; Wooley, K. L. *Acs Nano* **2009**, *3*, 673.

(99) Doege, K. J.; Sasaki, M.; Kimura, T.; Yamada, Y. *J. Biol. Chem.* **1991**, *266*, 894.

(100) Muir, H. *Biochem. Soc. Trans.* **1983**, *11*, 613.

(101) Sheiko, S. S.; Sumerlin, B. S.; Matyjaszewski, K. *Prog. Polym. Sci.* **2008**, *33*, 759.

(102) Zhang, M. F.; Müller, A. H. E. *J. Polym. Sci., Part A: Polym. Chem.* **2005**, *43*, 3461.

(103) Jenekhe, S. A.; Chen, X. L. *Science* **1998**, *279*, 1903.

(104) Geng, Y.; Dalhaimer, P.; Cai, S. S.; Tsai, R.; Tewari, M.; Minko, T.; Discher, D. E. *Nature Nanotech.* **2007**, *2*, 249.

(105) Cui, H. G.; Chen, Z. Y.; Zhong, S.; Wooley, K. L.; Pochan, D. J. *Science* **2007**, *317*, 647.

(106) Hudson, S. D.; Jung, H. T.; Percec, V.; Cho, W. D.; Johansson, G.; Ungar, G.; Balagurusamy, V. S. K. *Science* **1997**, *278*, 449.

(107) Yuan, J. Y.; Xu, Y. Y.; Walther, A.; Bolisetty, S.; Schumacher, M.; Schmalz, H.; Ballauff, M.; Müller, A. H. E. *Nature Mater.* **2008**, *7*, 718.

(108) Neugebauer, D.; Zhang, Y.; Pakula, T.; Sheiko, S. S.; Matyjaszewski, K. *Macromolecules* **2003**, *36*, 6746.

(109) Pakula, T.; Zhang, Y.; Matyjaszewski, K.; Lee, H. I.; Boerner, H.; Qin, S. H.; Berry, G. C. *Polymer* **2006**, *47*, 7198.

(110) Tsukahara, Y.; Namba, S.; Iwasa, J.; Nakano, Y.; Kaeriyama, K.; Takahashi, M. *Macromolecules* **2001**, *34*, 2624.

(111) Xia, Y.; Olsen, B. D.; Kornfield, J. A.; Grubbs, R. H. *J. Am. Chem. Soc.* **2009**, *131*, 18525.

(112) Rzayev, J. *Macromolecules* **2009**, *42*, 2135.

(113) Bolton, J.; Bailey, T. S.; Rzayev, J. *Nano Lett.* **2011**, *11*, 998.

(114) Runge, M. B.; Bowden, N. B. *J. Am. Chem. Soc.* **2007**, *129*, 10551.

(115) Runge, M. B.; Dutta, S.; Bowden, N. B. *Macromolecules* **2006**, *39*, 498.

(116) Mullner, M.; Yuan, J. Y.; Weiss, S.; Walther, A.; Fortsch, M.; Drechsler, M.; Muller, A. H. E. *J. Am. Chem. Soc.* **2010**, *132*, 16587.

(117) Zhang, M. F.; Drechsler, M.; Muller, A. H. E. *Chem. of Mater.* **2004**, *16*, 537.

(118) Yuan, J. Y.; Lu, Y.; Schacher, F.; Lunkenbein, T.; Weiss, S.; Schmalz, H.; Muller, A. H. E. *Chem. of Mater.* **2009**, *21*, 4146.

(119) Zhang, M. F.; Estournes, C.; Bietsch, W.; Muller, A. H. E. *Adv. Funct. Mater.* **2004**, *14*, 871.

(120) Li, Y. X.; Nothnagel, J.; Kissel, T. *Polymer* **1997**, *38*, 6197.

(121) Du, J. Z.; Tang, L. Y.; Song, W. J.; Shi, Y.; Wang, J. *Biomacromolecules* **2009**, *10*, 2169.

(122) Johnson, J. A.; Lu, Y. Y.; Burts, A. O.; Xia, Y.; Durrell, A. C.; Tirrell, D. A.; Grubbs, R. H. *Macromolecules* **2010**, *43*, 10326.

(123) Johnson, J. A.; Lu, Y. Y.; Burts, A. O.; Lim, Y. H.; Finn, M. G.; Koberstein, J. T.; Turro, N. J.; Tirrell, D. A.; Grubbs, R. H. *J. Am. Chem. Soc.* **2011**, *133*, 559.

(124) Zou, J. O.; Jafr, G.; Themistou, E.; Yap, Y.; Wintrob, Z. A. P.; Alexandridis, P.; Ceacareanu, A. C.; Cheng, C. *Chem Commun* **2011**, *47*, 4493.

(125) Miki, K.; Kimura, A.; Oride, K.; Kuramochi, Y.; Matsuoka, H.; Harada, H.; Hiraoka, M.; Ohe, K. *Angew. Chem. Int. Ed.* **2011**, *50*, 6567.

(126) Schappacher, M.; Deffieux, A. *Science* **2008**, *319*, 1512.

(127) Deffieux, A.; Schappacher, M. *Macromolecules* **1999**, *32*, 1797.

(128) Gao, H.; Matyjaszewski, K. *J. Am. Chem. Soc.* **2007**, *129*, 6633.

(129) Cheng, G. L.; Boker, A.; Zhang, M. F.; Krausch, G.; Muller, A. H. E. *Macromolecules* **2001**, *34*, 6883.

(130) Borner, H. G.; Beers, K.; Matyjaszewski, K.; Sheiko, S. S.; Moller, M. *Macromolecules* **2001**, *34*, 4375.

(131) Zhang, M. F.; Breiner, T.; Mori, H.; Muller, A. H. E. *Polymer* **2003**, *44*, 1449.

(132) Qin, S. H.; Matyjaszewski, K.; Xu, H.; Sheiko, S. S. *Macromolecules* **2003**, *36*, 605.

(133) Matyjaszewski, K.; Qin, S. H.; Boyce, J. R.; Shirvanyants, D.; Sheiko, S. S. *Macromolecules* **2003**, *36*, 1843.

(134) Lee, H. I.; Matyjaszewski, K.; Yu-Su, S.; Sheiko, S. S. *Macromolecules* **2008**, *41*, 6073.

(135) Lee, H. I.; Matyjaszewski, K.; Yu, S.; Sheiko, S. S. *Macromolecules* **2005**, *38*, 8264.

(136) Deng, G. H.; Chen, Y. M. *J. Polym. Sci., Part A: Polym. Chem.* **2009**, *47*, 5527.

(137) Zhu, H.; Deng, G. H.; Chen, Y. M. *Polymer* **2008**, *49*, 405.

(138) Huang, K.; Canterbury, D. P.; Rzayev, J. *Macromolecules* **2010**, *43*, 6632.

(139) Dziezok, P.; Sheiko, S. S.; Fischer, K.; Schmidt, M.; Moller, M. *Angew. Chem. Int. Ed.* **1997**, *36*, 2812.

(140) Tsukahara, Y.; Mizuno, K.; Segawa, A.; Yamashita, Y. *Macromolecules* **1989**, *22*, 1546.

(141) Vogt, A. P.; Sumerlin, B. S. *Macromolecules* **2006**, *39*, 5286.

(142) Ohno, S.; Matyjaszewski, K. *J. Polym. Sci., Part A: Polym. Chem.* **2006**, *44*, 5454.

(143) Cheng, C.; Khoshdel, E.; Wooley, K. L. *Macromolecules* **2005**, *38*, 9455.

(144) Patton, D. L.; Advincula, R. C. *Macromolecules* **2006**, *39*, 8674.

(145) Barker, I. A.; Hall, D. J.; Hansell, C. F.; Du Prez, F. E.; O'Reilly, R. K.; Dove, A. P. *Macromol. Rapid Commun.* **2011**, *32*, 1362.

(146) Xia, Y.; Boydston, A. J.; Grubbs, R. H. *Angew. Chem. Int. Ed.* **2011**, *50*, 5882.

(147) Coessens, V.; Matyjaszewski, K. *J. Macromol. Sci., Pure Appl. Chem.* **1999**, *A36*, 667.

(148) Duncan, R. *Nat. Rev. Drug Discovery* **2003**, *2*, 347.

(149) Paul, D. R.; Robeson, L. M. *Polymer* **2008**, *49*, 3187.

(150) Rodriguez-Hernandez, J.; Checot, F.; Gnanou, Y.; Lecommandoux, S. *Prog. Polym. Sci.* **2005**, *30*, 691.

(151) Moghimi, S. M.; Hunter, A. C.; Murray, J. C. *FASEB J.* **2005**, *19*, 311.

(152) Torchilin, V. P. *Adv. Drug Deliv. Rev.* **2006**, *58*, 1532.

(153) Gref, R.; Minamitake, Y.; Peracchia, M. T.; Trubetskoy, V.; Torchilin, V.; Langer, R. *Science* **1994**, *263*, 1600.

(154) Jeong, B.; Bae, Y. H.; Lee, D. S.; Kim, S. W. *Nature* **1997**, *388*, 860.

(155) Alexandridis, P.; Holzwarth, J. F.; Hatton, T. A. *Macromolecules* **1994**, *27*, 2414.

(156) Riess, G. *Prog. Polym. Sci.* **2003**, *28*, 1107.

(157) Allen, C.; Maysinger, D.; Eisenberg, A. *Colloids Surf., B* **1999**, *16*, 3.

(158) Thurmond, K. B.; Kowalewski, T.; Wooley, K. L. *J. Am. Chem. Soc.* **1996**, *118*, 7239.

(159) Zhang, Q.; Remsen, E. E.; Wooley, K. L. *J. Am. Chem. Soc.* **2000**, *122*, 3642.

(160) Thurmond, K. B.; Kowalewski, T.; Wooley, K. L. *J. Am. Chem. Soc.* **1997**, *119*, 6656.

(161) O'Reilly, R. K.; Hawker, C. J.; Wooley, K. L. *Chem. Soc. Rev.* **2006**, *35*, 1068.

(162) Wooley, K. L. *J. Polym. Sci., Part A: Polym. Chem.* **2000**, *38*, 1397.

(163) Joralemon, M. J.; O'Reilly, R. K.; Hawker, C. J.; Wooley, K. L. *J. Am. Chem. Soc.* **2005**, *127*, 16892.

(164) Li, Y. L.; Du, W. J.; Sun, G. R.; Wooley, K. L. *Macromolecules* **2008**, *41*, 6605.

(165) Lee, N. S.; Sun, G. R.; Lin, L. Y.; Neumann, W. L.; Freskos, J. N.; Karwa, A.; Shieh, J. J.; Dorshow, R. B.; Wooley, K. L. *J. Mater. Chem.* **2011**, *21*, 14193.

(166) Sorrells, J. L.; Shrestha, R.; Neumann, W. L.; Wooley, K. L. *J. Mater. Chem.* **2011**, *21*, 8983.

(167) Sun, G. R.; Berezin, M. Y.; Fan, J. D.; Lee, H.; Ma, J.; Zhang, K.; Wooley, K. L.; Achilefu, S. *Nanoscale* **2010**, *2*, 548.

(168) Alexis, F.; Pridgen, E.; Molnar, L. K.; Farokhzad, O. C. *Mol. Pharmaceutics* **2008**, *5*, 505.

(169) Dobrovolskaia, M. A.; Aggarwal, P.; Hall, J. B.; McNeil, S. E. *Mol. Pharmaceutics* **2008**, *5*, 487.

(170) Hume, D. A. *Curr. Opin. Immunol.* **2006**, *18*, 49.

(171) Owens, D. E.; Peppas, N. A. *Int J Pharm* **2006**, *307*, 93.

(172) Li, S. D.; Huang, L. *Mol. Pharmaceutics* **2008**, *5*, 496.

(173) Gref, R.; Luck, M.; Quellec, P.; Marchand, M.; Dellacherie, E.; Harnisch, S.; Blunk, T.; Muller, R. H. *Colloids Surf., B* **2000**, *18*, 301.

(174) Peracchia, M. T.; Vauthier, C.; Desmaele, D.; Gulik, A.; Dedieu, J. C.; Demoy, M.; d'Angelo, J.; Couvreur, P. *Pharmaceut Res* **1998**, *15*, 550.

(175) Storm, G.; Belliot, S. O.; Daemen, T.; Lasic, D. D. *Adv. Drug Deliv. Rev.* **1995**, *17*, 31.

(176) Vermette, P.; Meagher, L. *Colloids Surf., B* **2003**, *28*, 153.

(177) Emanuele Ostuni; Robert G. Chapman; R. Erik Holmlin; Shuichi Takayama; Whitesides, G. M. *Langmuir* **2001**, *17*, 5605.

(178) Gaberc-Porekar, V.; Zore, I.; Podobnik, B.; Menart, V. *Curr Opin Drug Disc* **2008**, *11*, 242.

(179) Herold, D. A.; Keil, K.; Bruns, D. E. *Biochem. Pharmacol.* **1989**, *38*, 73.

(180) Reboucas, J. D.; Esparza, I.; Ferrer, M.; Sanz, M. L.; Irache, J. M.; Gamazo, C. *J. Biomed. Biotechnol.* **2012**.

(181) Veronese, F. M.; Mero, A. *Biodrugs* **2008**, *22*, 315.

(182) Beil, J. B.; Zimmerman, S. C. *Macromolecules* **2004**, *37*, 778.

(183) Ma, J.; Cheng, C.; Sun, G. R.; Wooley, K. L. *J. Polym. Sci., Part A: Polym. Chem.* **2008**, *46*, 3488.

(184) Parrish, B.; Emrick, T. *Macromolecules* **2004**, *37*, 5863.

(185) Ma, J.; Cheng, C.; Wooley, K. L. *Macromolecules* **2009**, *42*, 1565.

(186) Jing, F.; Hillmyer, M. A. *J. Am. Chem. Soc.* **2008**, *130*, 13826.

(187) Chen, L.; Phillip, W. A.; Cussler, E. L.; Hillmyer, M. A. *J. Am. Chem. Soc.* **2007**, *129*, 13786.

(188) O'Reilly, R. K.; Joralemon, M. J.; Hawker, C. J.; Wooley, K. L. *New J. Chem.* **2007**, *31*, 718.

(189) O'Reilly, R. K.; Joralemon, M. J.; Hawker, C. J.; Wooley, K. L. *J. Polym. Sci., Part A: Polym. Chem.* **2006**, *44*, 5203.

(190) Aimi, J.; McCullough, L. A.; Matyjaszewski, K. *Macromolecules* **2008**, *41*, 9522.

(191) Schitter, R. M. E.; Jocham, D.; Stelzer, F.; Moszner, N.; Volkel, T. *J. Appl. Polym. Sci.* **2000**, *78*, 47.

(192) Preishuber-Pflugl, P.; Podolan, R.; Stelzer, F. *J. Mol. Catal. A: Chem.* **2000**, *160*, 53.

(193) Maughon, B. R.; Grubbs, R. H. *Macromolecules* **1996**, *29*, 5765.

(194) Liaw, D. J.; Huang, C. C.; Hong, S. M. *J. Polym. Sci., Part A: Polym. Chem.* **2006**, *44*, 6287.

(195) Kumar, A.; Jang, S. Y.; Padilla, J.; Otero, T. F.; Sotzing, G. A. *Polymer* **2008**, *49*, 3686.

(196) Dong, Z. M.; Liu, X. H.; Tang, X. L.; Li, Y. S. *Macromolecules* **2009**, *42*, 4596.

(197) Odian, G. *Principles of Polymerization*; 4th ed.; Wiley: Hoboken, NJ, 2004.

(198) Xia, J. H.; Matyjaszewski, K. *Macromolecules* **1997**, *30*, 7697.

(199) Killops, K. L.; Campos, L. M.; Hawker, C. J. *J. Am. Chem. Soc.* **2008**, *130*, 5062.

(200) Percec, V.; Ahn, C. H.; Ungar, G.; Yeardley, D. J. P.; Möller, M.; Sheiko, S. S. *Nature* **1998**, *391*, 161.

(201) Sheiko, S. S.; Möller, M. *Chem. Rev.* **2001**, *101*, 4099.

(202) Sheiko, S. S.; Sun, F. C.; Randall, A.; Shirvanyants, D.; Rubinstein, M.; Lee, H. I.; Matyjaszewski, K. *Nature* **2006**, *440*, 191.

(203) Yuan, J. Y.; Xu, Y. Y.; Müller, A. H. E. *Chem. Soc. Rev.* **2011**, *40*, 640.

(204) Zou, J.; Jafr, G.; Themistou, E.; Yap, Y.; Wintrob, Z. A.; Alexandridis, P.; Ceacareanu, A. C.; Cheng, C. *Chem Commun* **2011**, *47*, 4493.

(205) Yuan, W. Z.; Zhao, Z. D.; Gu, S. Y.; Ren, J. *J. Polym. Sci., Part A: Polym. Chem.* **2010**, *48*, 3476.

(206) Yu, Y.; Zou, J.; Yu, L.; Jo, W.; Li, Y. K.; Law, W. C.; Cheng, C. *Macromolecules* **2011**, *44*, 4793.

(207) Cheng, C.; Qi, K.; Khoshdel, E.; Wooley, K. L. *J. Am. Chem. Soc.* **2006**, *128*, 6808.

(208) Chen, X. P.; Ayres, N. *J. Polym. Sci., Part A: Polym. Chem.* **2011**, *49*, 3030.

(209) Zhao, J. P.; Zhang, G. Z.; Pispas, S. *J. Polym. Sci., Part A: Polym. Chem.* **2010**, *48*, 2320.

(210) Dag, A.; Sahin, H.; Durmaz, H.; Hizal, G.; Tunca, U. *J. Polym. Sci., Part A: Polym. Chem.* **2011**, *49*, 886.

(211) Sun, J. P.; Hu, J. W.; Liu, G. J.; Xiao, D. S.; He, G. P.; Lu, R. F. *J. Polym. Sci., Part A: Polym. Chem.* **2011**, *49*, 1282.

(212) Morandi, G.; Montembault, W.; Pascual, S.; Legoupy, S.; Fontaine, L. *Macromolecules* **2006**, *39*, 2732.

(213) Li, Z.; Ma, J.; Lee, N. S.; Wooley, K. L. *J. Am. Chem. Soc.* **2011**, *133*, 1228.

(214) Grogna, M.; Cloots, R.; Luxen, A.; Jerome, C.; Passirani, C.; Lautram, N.; Desreux, J. F.; Detrembleur, C. *J. Polym. Sci., Part A: Polym. Chem.* **2011**, *49*, 3700.

(215) Sumerlin, B. S.; Neugebauer, D.; Matyjaszewski, K. *Macromolecules* **2005**, *38*, 702.

(216) Cheng, C.; Khoshdel, E.; Wooley, K. L. *Macromolecules* **2007**, *40*, 2289.

(217) Choi, T. L.; Grubbs, R. H. *Angew. Chem. Int. Ed.* **2003**, *42*, 1743.

(218) Li, Z.; Ma, J.; Cheng, C.; Zhang, K.; Wooley, K. L. *Macromolecules* **2010**, *43*, 1182.

(219) Li, A.; Li, Z.; Zhang, S. Y.; Sun, G. R.; Policarpio, D. M.; Wooley, K. L. *Acs Macro Lett.* **2012**, *1*, 241.

(220) Boydston, A. J.; Holcombe, T. W.; Unruh, D. A.; Fréchet, J. M. J.; Grubbs, R. H. *J. Am. Chem. Soc.* **2009**, *131*, 5388.

(221) Kang, E. H.; Lee, I. S.; Choi, T. L. *J. Am. Chem. Soc.* **2011**, *133*, 11904.

(222) Cheng, C.; Khoshdel, E.; Wooley, K. L. *Nano Lett.* **2006**, *6*, 1741.

(223) Lu, H.; Wang, J.; Lin, Y.; Cheng, J. J. *J. Am. Chem. Soc.* **2009**, *131*, 13582.

(224) Stamenović, M. M.; Espeel, P.; Van Camp, W.; Du Prez, F. E. *Macromolecules* **2011**, *44*, 5619.

(225) Hansell, C. F.; Espeel, P.; Stamenović, M. M.; Barker, I. A.; Dove, A. P.; Du Prez, F. E.; O'Reilly, R. K. *J. Am. Chem. Soc.* **2011**, *133*, 13828.

(226) Li, A.; Ma, J.; Wooley, K. L. *Macromolecules* **2009**, *42*, 5433.

(227) Bielawski, C. W.; Louie, J.; Grubbs, R. H. *J. Am. Chem. Soc.* **2000**, *122*, 12872.

(228) Rule, J. D.; Moore, J. S. *Macromolecules* **2002**, *35*, 7878.

(229) Pollino, J. M.; Stubbs, L. P.; Weck, M. *Macromolecules* **2003**, *36*, 2230.

(230) Maynard, H. D.; Okada, S. Y.; Grubbs, R. H. *Macromolecules* **2000**, *33*, 6239.

(231) Asrar, J. *Macromolecules* **1992**, *25*, 5150.

(232) Chatterjee, A. K.; Choi, T. L.; Sanders, D. P.; Grubbs, R. H. *J. Am. Chem. Soc.* **2003**, *125*, 11360.

(233) Lexer, C.; Saf, R.; Slugovc, C. *J. Polym. Sci., Part A: Polym. Chem.* **2009**, *47*, 299.

(234) Djalali, R.; Li, S. Y.; Schmidt, M. *Macromolecules* **2002**, *35*, 4282.

(235) Huang, K.; Jacobs, A.; Rzayev, J. *Biomacromolecules* **2011**, *12*, 2327.

(236) Zhang, K.; Lackey, M. A.; Wu, Y.; Tew, G. N. *J. Am. Chem. Soc.* **2011**, *133*, 6906.

(237) Huang, K.; Rzayev, J. *J. Am. Chem. Soc.* **2009**, *131*, 6880.

(238) Miura, Y.; Satoh, K.; Kamigaito, M.; Okamoto, Y.; Kaneko, T.; Jinnai, H.; Kobukata, S. *Macromolecules* **2007**, *40*, 465.

(239) Rajaram, S.; Choi, T. L.; Rolandi, M.; Fréchet, J. M. J. *J. Am. Chem. Soc.* **2007**, *129*, 9619.

(240) Lord, S. J.; Sheiko, S. S.; LaRue, I.; Lee, H. I.; Matyjaszewski, K. *Macromolecules* **2004**, *37*, 4235.

(241) Fu, G. D.; Phua, S. J.; Kang, E. T.; Neoh, K. G. *Macromolecules* **2005**, *38*, 2612.

(242) Boyce, J. R.; Shirvanyants, D.; Sheiko, S. S.; Ivanov, D. A.; Qin, S. H.; Börner, H.; Matjaszewski, K. *Langmuir* **2004**, *20*, 6005.

(243) Tsoukatos, T.; Pispas, S.; Hajichristidis, N. *Macromolecules* **2000**, *33*, 9504.

(244) Lanson, D.; Schappacher, M.; Borsali, R.; Deffieux, A. *Macromolecules* **2007**, *40*, 5559.

(245) Runge, M. B.; Lipscomb, C. E.; Ditzler, L. R.; Mahanthappa, M. K.; Tivanski, A. V.; Bowden, N. B. *Macromolecules* **2008**, *41*, 7687.

(246) Gitsov, I.; Fréchet, J. M. J. *Macromolecules* **1994**, *27*, 7309.

(247) Bayer, U.; Stadler, R. *Macromol. Chem. Phys.* **1994**, *195*, 2709.

(248) Panyukov, S. V.; Sheiko, S. S.; Rubinstein, M. *Phys. Rev. Lett.* **2009**, *102*, 148301.

(249) Wang, A. Z.; Langer, R.; Farokhzad, O. C. *Annu. Rev. Med.* **2012**, *63*, 185.

(250) Schober, O.; Rahbar, K.; Riemann, B. *Eur. J. Nucl. Med. Mol. Imaging* **2009**, *36*, 302.

(251) Nyström, A. M.; Wooley, K. L. *Acc. Chem. Res.* **2011**, *44*, 969.

(252) Liu, Y.; Welch, M. J. *Bioconjug Chem.* **2012**, *23*, 671.

(253) Elsabahy, M.; Wooley, K. L. *Chem. Soc. Rev.* **2012**, *41*, 2545.

(254) Brigger, I.; Dubernet, C.; Couvreur, P. *Adv. Drug Deliv. Rev.* **2002**, *54*, 631.

(255) Venkataraman, S.; Hedrick, J. L.; Ong, Z. Y.; Yang, C.; Ee, P. L. R.; Hammond, P. T.; Yang, Y. Y. *Adv. Drug Deliv. Rev.* **2011**, *63*, 1228.

(256) Khlebtsov, N.; Dykman, L. *Chem. Soc. Rev.* **2011**, *40*, 1647.

(257) Elsabahy, M.; Wooley, K. L. *J. Polym. Sci., Part A: Polym. Chem.* **2012**, *50*, 1869.

(258) Zhang, Z.; Chen, S. F.; Jiang, S. Y. *Biomacromolecules* **2006**, *7*, 3311.

(259) Vaisocherova, H.; Yang, W.; Zhang, Z.; Cao, Z. Q.; Cheng, G.; Piliarik, M.; Homola, J.; Jiang, S. Y. *Anal. Chem.* **2008**, *80*, 7894.

(260) Jiang, S.; Cao, Z. *Adv. Mater.* **2010**, *22*, 920.

(261) Carr, L. R.; Zhou, Y.; Krause, J. E.; Xue, H.; Jiang, S. *Biomaterials* **2011**, *32*, 6893.

(262) Cao, Z.; Yu, Q.; Xue, H.; Cheng, G.; Jiang, S. *Angew. Chem. Int. Ed.* **2010**, *49*, 3771.

(263) Abraham, S.; So, A.; Unsworth, L. D. *Biomacromolecules* **2011**, *12*, 3567.

(264) Yang, W.; Zhang, L.; Wang, S.; White, A. D.; Jiang, S. *Biomaterials* **2009**, *30*, 5617.

(265) Veronese, F. M.; Pasut, G. *Drug Discov. Today* **2005**, *10*, 1451.

(266) Keefe, A. J.; Jiang, S. Y. *Nature Chem.* **2012**, *4*, 60.

(267) Bailon, P.; Palleroni, A.; Schaffer, C. A.; Spence, C. L.; Fung, W. J.; Porter, J. E.; Ehrlich, G. K.; Pan, W.; Xu, Z. X.; Modi, M. W.; Farid, A.; Berthold, W. *Bioconjugate Chem.* **2001**, *12*, 195.

(268) Zhang, S. Y.; Li, Z.; Samarajeewa, S.; Sun, G. R.; Yang, C.; Wooley, K. L. *J. Am. Chem. Soc.* **2011**, *133*, 11046.

(269) Zhang, L.; Gu, F. X.; Chan, J. M.; Wang, A. Z.; Langer, R. S.; Farokhzad, O. C. *Clin. Pharmacol. Ther.* **2008**, *83*, 761.

(270) Torchilin, V. P. *Adv. Drug Deliv. Rev.* **2002**, *54*, 235.

(271) Samarajeewa, S.; Shrestha, R.; Li, Y. L.; Wooley, K. L. *J. Am. Chem. Soc.* **2012**, *134*, 1235.

(272) Lin, L. Y.; Lee, N. S.; Zhu, J. H.; Nyström, A. M.; Pochan, D. J.; Dorshow, R. B.; Wooley, K. L. *J. Controlled Release* **2011**, *152*, 37.

(273) Sun, X. K.; Rossin, R.; Turner, J. L.; Becker, M. L.; Joralemon, M. J.; Welch, M. J.; Wooley, K. L. *Biomacromolecules* **2005**, *6*, 2541.

(274) Sun, G.; Hagooly, A.; Xu, J.; Nyström, A. M.; Li, Z.; Rossin, R.; Moore, D. A.; Wooley, K. L.; Welch, M. J. *Biomacromolecules* **2008**, *9*, 1997.

(275) Tian, H. Y.; Tang, Z. H.; Zhuang, X. L.; Chen, X. S.; Jing, X. B. *Prog. Polym. Sci.* **2012**, *37*, 237.

(276) Middleton, J. C.; Tipton, A. J. *Biomaterials* **2000**, *21*, 2335.

(277) Anderson, J. M.; Shive, M. S. *Adv. Drug Deliv. Rev.* **1997**, *28*, 5.

(278) http://clinicaltrials.gov/ct2/results?term=dota.

(279) Almutairi, A.; Rossin, R.; Shokeen, M.; Hagooly, A.; Ananth, A.; Capoccia, B.; Guillaudeu, S.; Abendschein, D.; Anderson, C. J.; Welch, M. J.; Fréchet, J. M. J. *Proc. Natl. Acad. Sci. U.S.A.* **2009**, *106*, 685.

(280) Adam, M. J.; Wilbur, D. S. *Chem. Soc. Rev.* **2005**, *34*, 153.

(281) Xu, L. B.; Crawford, K.; Gorman, C. B. *Macromolecules* **2011**, *44*, 4777.

(282) Makino, K.; Arakawa, M.; Kondo, T. *Chem. Pharm. Bull.* **1985**, *33*, 1195.

(283) Jung, J. H.; Ree, M.; Kim, H. *Catal. Today* **2006**, *115*, 283.

(284) Belbella, A.; Vauthier, C.; Fessi, H.; Devissaguet, J. P.; Puisieux, F. *Int J Pharm* **1996**, *129*, 95.

(285) Hoare, T.; Pelton, R. *J. Phys. Chem. B* **2007**, *111*, 11895.

(286) McCarthy, D. W.; Shefer, R. E.; Klinkowstein, R. E.; Bass, L. A.; Margeneau, W. H.; Cutler, C. S.; Anderson, C. J.; Welch, M. J. *Nucl. Med. Biol.* **1997**, *24*, 35.

(287) Liu, Y. J.; Ibricevic, A.; Cohen, J. A.; Cohen, J. L.; Gunsten, S. P.; Fréchet, J. M. J.; Walter, M. J.; Welch, M. J.; Brody, S. L. *Mol. Pharmaceutics* **2009**, *6*, 1891.